1985

Single-crystal polarized electronic spectra of the compounds dichlorotetrakis ([mu]-pivalato)dirhenium(III),tetra-n-butylammonium octachlorodirhenate(III), tetra-n-butylammonium octabromodirhenate(III), dimolybdenum(II)tetrapivalate, and the X-ray diffraction cyrstal structures of tetra-n-butylammonium octobromodirhenate(III) and two polymorphs of dimolybdenum(II) tetrapivalate

Hai-Wei Huang
Iowa State University

Huang, Hai-Wei

SINGLE-CRYSTAL POLARIZED ELECTRONIC SPECTRA OF THE COMPOUNDS DICHLOROTETRAKIS(MU-PIVALATO)DIRHENIUM(III), TETRA-N-BUTYLAMMONIUM OCTACHLORODIRHENATE(III), TETRA-N-BUTYLAMMONIUM OCTABROMODIRHENATE(III), DIMOLYBDENUM(II) TETRAPIVALATE, AND THE X-RAY DIFFRACTION CRYSTAL STRUCTURES OF TETRA-N-BUTYLAMMONIUM OCTABROMODIRHENATE(III) AND TWO POLYMORPHS OF DIMOLYBDENUM(II) TETRAPIVALATE

Iowa State University PH.D. 1985

PLEASE NOTE:

In all cases this material has been filmed in the best possible way from the available copy. Problems encountered with this document have been identified here with a check mark __✓__.

1. Glossy photographs or pages _____
2. Colored illustrations, paper or print _____
3. Photographs with dark background ✓
4. Illustrations are poor copy _____
5. Pages with black marks, not original copy ✓
6. Print shows through as there is text on both sides of page _____
7. Indistinct, broken or small print on several pages ✓
8. Print exceeds margin requirements _____
9. Tightly bound copy with print lost in spine _____
10. Computer printout pages with indistinct print _____
11. Page(s) _____ lacking when material received, and not available from school or author.
12. Page(s) _____ seem to be missing in numbering only as text follows.
13. Two pages numbered _____. Text follows.
14. Curling and wrinkled pages _____
15. Dissertation contains pages with print at a slant, filmed as received _____
16. Other _____

_____

_____

Single-crystal polarized electronic spectra of the compounds dichlorotetrakis(μ-pivalato)dirhenium(III), tetra-n-butylammonium octachlorodirhenate(III), tetra-n-butylammonium octabromodirhenate(III), dimolybdenum(II) tetrapivalate, and the X-ray diffraction crystal structures of tetra-n-butylammonium octabromodirhenate(III) and two polymorphs of dimolybdenum(II) tetrapivalate

by

Hai-Wei Huang

A Dissertation Submitted to the
Graduate Faculty in Partial Fulfillment of the
Requirements for the Degree of
DOCTOR OF PHILOSOPHY

Department: Chemistry

Major: Inorganic Chemistry

Approved:

Signature was redacted for privacy.

In Charge of Major Work

Signature was redacted for privacy.

For the Major Department

Signature was redacted for privacy.

For the Graduate College

Members of the committee:

Signature was redacted for privacy.

Iowa State University
Ames, Iowa

1985

TABLE OF CONTENTS

INTRODUCTION

The chemistry of compounds containing multiple bonds between transition metal atoms has developed rapidly since the initial recognition, in the early 1960s, of the first metal-metal double bond (1), the first triple bond (2) and the first quadruple bond (3). Several of the elements, particularly molybdenum and rhenium, have a consistent tendency to form such bonds. In these cases, the Mo_2^{4+} and Re_2^{6+} central units appear to be structurally rigid, and the observed variation in metal-metal distance is relatively slight for different compounds. Thus, the Mo-Mo quadruple bond lengths span a range from 2.088(1) in $Mo_2(O_2CCMe_3)_4$ (4) to 2.183(2) A in $Mo_2(C_3H_5)_4$ (5), and the known range of Re-Re quadruple bond lengths is from 2.178(1) in $Re_2Me_8^{2-}$ ion (6) to about 2.24 A in several compounds (7), e.g., $Re_2Cl_8^{2-}$ salts.

In this research, spectra and crystal structures of $[N(n\text{-}C_4H_9)_4]_2Re_2Br_8$, i.e., $(TBA)_2Re_2Br_8$, and polymorphs of $Mo_2[O_2CC(CH_3)_3]_4$, i.e., $Mo_2(piv)_4$, are presented and discussed. Also, the details of the electronic spectra of $Re_2[O_2CC(CH_3)_3]_4Cl_2$ and $[N(n\text{-}C_4H_9)_4]_2Re_2Cl_8$, i.e., $(TBA)_2Re_2Cl_8$, are discussed. In all of these compounds, dimeric complexes possess the quadruple bond between two transition metal atoms and have effectively a local D_{4h}

symmetry.

A quadruple bond occurs only with transition metal dimers which possess d^8 electronic configuration. The quadruple bond is composed of a σ bond, a degenerate pair of π bonds, and a δ bond. Using the basic Hückel concept, namely, that MO energies are proportional to overlap integrals for similar types of orbitals, and noting that these overlaps must increase in the order $\delta << \pi < \sigma$, it is expected that the orbitals be ordered in energy as follows, beginning with the most stable:

$$\sigma < \pi << \delta < \delta^* << \pi^* < \sigma^*$$

Hence, the $\delta \rightarrow \delta^*$ transition requires the least excitation energy. Later, it was quickly recognized that the $\delta \rightarrow \delta^*$ transition will be dipole allowed for light polarized along the metal-metal bond, whereas the $\pi \rightarrow \delta^*$ or $\delta^* \rightarrow \pi$ transitions are forbidden. Polarized spectroscopy therefore might serve to identify this $\delta \rightarrow \delta^*$ transition.

Cowman and Gray (8) reported polarized single crystal spectra for tetrabutylammonium octachlorodirhenium(III). They found that the integrated intensity of the 14,183 cm^{-1} band definitely does not decrease on cooling from 300 to 5 K, eliminating transition assignments which require vibronic intensity-giving mechanisms. Also, they observed no A term in the MCD spectrum in this region of absorption. Therefore, they suggested that an allowed transition to a

nondegenerate excited state is responsible for the 14,183 cm^{-1} band. They supported the assignment of the low energy absorption system in quadruply bonded, binuclear Re(III) complexes to the $\delta \rightarrow \delta^*$ ($^1A_{1g} \rightarrow {}^1A_{2u}$) transition by the fact that the first band in the crystal spectra of $Re_2Cl_6[P(C_2H_5)_3]_2$ possessed a z-polarized transition.

In a subsequent crystal structure determination of $(TBA)_2Re_2Cl_8$, Cotton et al. (9) found a disordered structure. Because the two square planar $ReCl_4$ units have an eclipsed configuration, the eight chloride ligands occupy the corners of a nearly perfect cube. The crystals of $(TBA)_2Re_2Cl_8$ possess a subtle form of disorder, so that 73.89% of the Re-Re units are aligned in one direction, while 26.11% are aligned in a direction perpendicular to this. The common midpoint of the two Re-Re lines is a crystallographic center of inversion. Cotton showed that a z-polarized transition for the two types of anions accounted quite well for the overall relative intensities of the two polarizations in Cowman and Gray's spectra (8).

This type of disorder in $M_2X_8^{n-}$ ions was first observed some years ago in $K_4Mo_2Cl_8 \cdot 2H_2O$ (10), where 7% of the $Mo_2Cl_8^{4-}$ ions are in a perpendicular orientation. There also is a disorder in $Re_2Cl_4(PEt_3)_4$ which attains the limit of randomness; i.e., three equivalent, mutually perpendicular orientations are equally populated. It should be noted that

even though a second orientation of the M_2 unit might be enthalpically less favorable than the main one, the disordering makes a favorable entropic contribution to the free energy. It is the sign of the combination, $\Delta H - T\Delta S$, that determines the extent of disordering compatible with minimizing the free energy of the crystal.

Soon after the recognition of the quadruple bond in the $[Re_2Cl_8]^{2-}$ ion, the correct structure of $Mo_2(O_2CCH_3)_4$ was proposed by Lawton and Mason (11). The fact that Mo^{2+} and Re^{3+} are isoelectronic implies that $Mo_2(O_2CCH_3)_4$ should also contain a quadruple bond. The structure was later accurately determined to give an Mo-Mo distance of 2.093(1) A (12). The molecule of $Mo_2(O_2CCH_3)_4$ was found to consist of four carboxylate groups bridging the two metal atoms as illustrated in Figure 1, M = Mo. The molecules are arranged to form infinite chains in which there is weak axial coordination of each metal of every molecule by oxygen atoms of its neighbors.

The molybdenum(II) carboxylates $Mo_2(O_2CR)_4$ might well be considered as the most important class of compounds to contain a Mo-Mo quadruple bond because they have traditionally been the starting point for the synthesis of almost all other derivatives of the quadruply bonded Mo_2^{4+} core. Formation of the compound $Mo_2(O_2CCH_3)_4$ from $Mo(CO)_6$ provided an important and convenient synthesis route for a

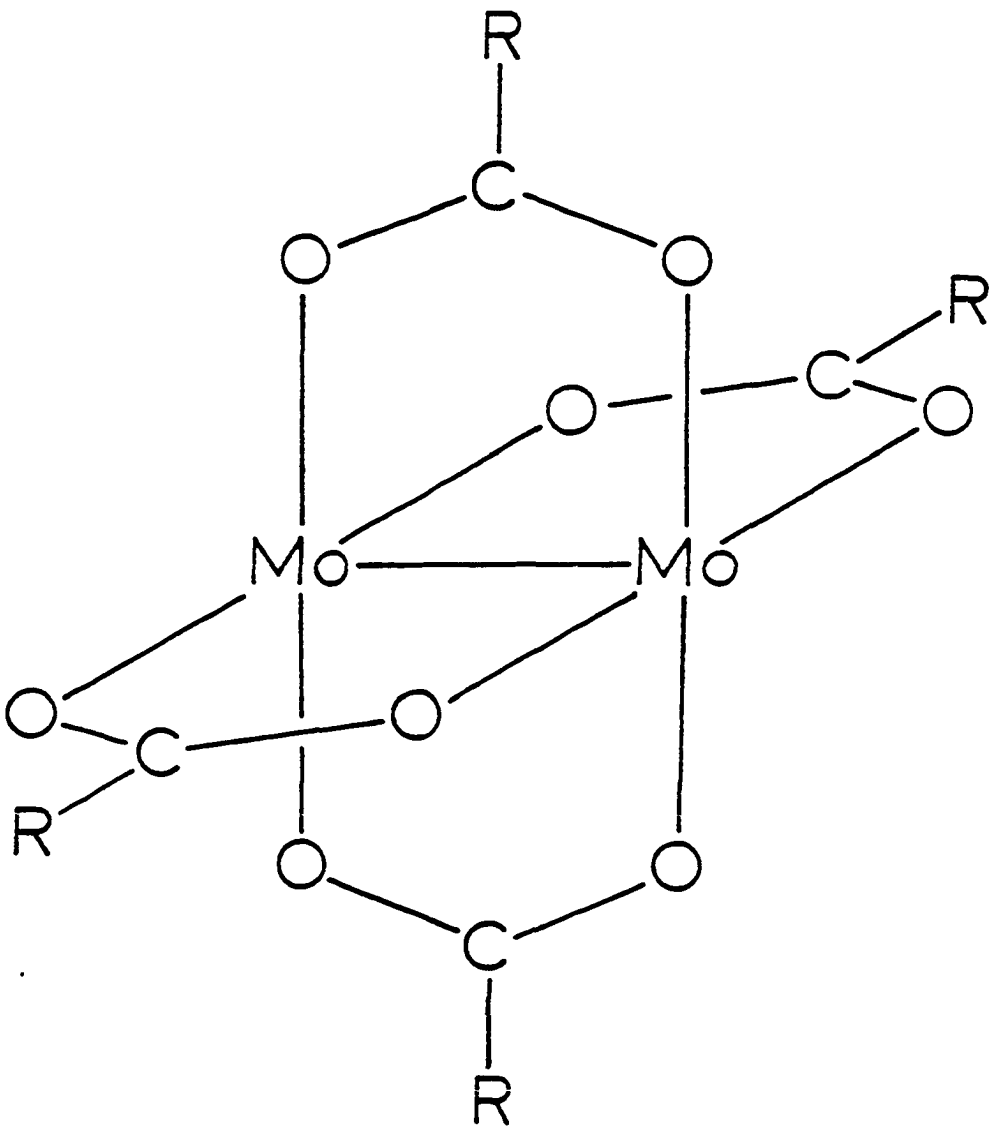

Figure 1. General structure of dimolybdenum tetra-carboxylate complexes

molybdenum(II) carboxylate (13-15). This reaction proceeds in a very low yield (15-20%) when pure acetic acid or a mixture of the acid and its anhydride are used (16). The remaining molybdenum is converted to one or more trinuclear species of the type $[Mo_3X_2(O_2CCH_3)_6(H_2O)_3]^{n+}$, where the Mo_3X_2 unit is a trigonal bipyramid in which the axial or capping units X are either μ_3-O or μ_3-CCH_3, or one of each. There are Mo-Mo bonds in these clusters, but not multiple ones (17).

The first Mo dimer complex to be investigated by means of polarized absorption spectroscopy was the quadruply-bonded glycine complex in tetra-μ-glycine-dimolybdenum(II) sulfate tetrahydrate, $Mo_2(O_2CCH_2NH_3)_4(SO_4)_2 \cdot 4H_2O$. This compound crystallizes in space group $I\bar{4}$. In the primitive cell, there is only one Mo_2^{4+} unit. The Mo-Mo bond, which establishes the molecular z axis, is aligned with the crystallographic c axis. The single crystal spectra were recorded in the region 20,000-25,000 cm^{-1} at 15 K for c(z) and a(x, y) polarizations. In z polarization, two progressions are observed. A weak one begins at 20,570 cm^{-1} and consists of four lines with a mean separation of 343 $\pm$10 cm^{-1}. In x, y polarization, there are also two progressions. Each is an order of magnitude more intense than the weak progression in z polarization. The first progression in x, y begins at 21,790 cm^{-1} and consists of

seven lines with an average separation of 342 ± 11 cm^{-1} while the second begins at 21,930 cm^{-1} and six lines can be discerned with an average separation of 344 ± 8 cm^{-1}. Cotton et al. (18) attributed the first, weak progression in z polarization to an electronic transition, forbidden in D_{4h} symmetry but allowed in the S_4 symmetry of the crystal field. Since the deviation from D_{4h} is small, this progression was supposed to be weak. The peak at 20,570cm^{-1} was taken as the 0-0 line of the $\delta \rightarrow \delta^*$ transition. The other progression in z polarization and the progressions in x, y polarization were attributed to vibronic components involving the same electronic excitation with asymmetric vibrations under D_{4h}, with frequencies in the excited electronic state of 940, 1220, and 1360 cm^{-1}, respectively. The vibrational spacings of the progressions, averaging 340-345 cm^{-1}, were attributed to that normal mode which consists chiefly of Mo-Mo stretching. This mode has a frequency of 393 cm^{-1} in the ground state. The transition presumably involves an electronic excitation from an Mo-Mo bonding orbital into an Mo-Mo antibonding orbital. The important point is that the observations reported seemed inconsistent with an assignment of this absorption band to the $\delta \rightarrow \delta^*$ transition which would be electric dipole allowed under D_{4h} symmetry.

Polarized crystal spectra (19) for $K_4Mo_2(SO_4)_4 \cdot 2H_2O$, in which the $Mo_2(SO_4)_4^{4-}$ ion has four bridging sulfates, have indicated a band at 19,400 cm^{-1} with a polarization consistent with a $\delta \rightarrow \delta^*$ assignment. Also, for $K_3Mo_2(SO_4)_4 \cdot 3.5\ H_2O$, in which one electron from the quadruple bond has been lost by oxidation, the first band with an origin at about 6,300 cm^{-1} has the polarization predicted for the $\delta \rightarrow \delta^*$ assignment (20). Nevertheless, a group of tetra-μ-carboxylato-dimolybdenum(II) complexes have presented a conflicting situation. These complexes are also generally considered under the D_{4h} point group about the metal-metal bond. The spectra for several of these carboxylato complexes have possessed vibrational structure with much greater resolvable detail than any of the other dimers, except for possibly $K_3Mo_2(SO_4)_4 \cdot 3H_2O$; and it has been possible to observe crystal polarizations for a number of individual vibrational lines. Unlike the tetragonal crystals of tetrakis(μ-glycine)dimolybdenum(II) sulfate tetrahydrate, where z- and x,y-polarized lines were indicated unambiguously, the molecular polarization of individual lines was not clearly indicated. The presence of lines in both polarizations of comparable intensity originally led to the conclusion that this band should not be assigned as a $\delta \rightarrow \delta^*$ transition (18). This conclusion was apparently supported by the spectra recorded for

tetrakis(μ-formato)dimolybdenum(II), where the polarization ratio for the lowest observed line in the spectra was opposite to that expected for a z-polarized transition (19). In addition, Trogler et al. (21) reported single-crystal spectra for tetrakis(μ-acetato)dimolybdenum(II) and a multicrystal unpolarized spectrum for tetrakis(μ-trifluoroacetato)dimolybdenum(II). They assigned the observed band as $\delta \rightarrow \pi^*$ ($^1A_{1g} \rightarrow {}^1E_g$). However, Martin et al. (22) were able to measure polarization ratios for the sharp line at the longest wavelength for two different crystal faces of $Mo_2(O_2CCH_3)_4$, which was the origin of the most intense Franck-Condon progression. From this information, the orientation of the transition moment for this line could be determined. It was found to be 34^o away from the metal-metal bond or the molecular z axis. The rotation of the transition moment was attributed to crystal field perturbation. Also, the observed hot bands implied that this first line was electric dipole allowed rather than being of vibronic (Herzberg-Teller) origin and was therefore the 0-0 line of the $\delta \rightarrow \delta^*$ transition. It was concluded that the band was an electric-dipole-allowed transition with an unusually low transition moment so the vibronic lines were not orders of magnitude weaker as is the normal case for allowed transitions. A second dominant progression was attributed to degenerate pairs of transitions with x,y-polarization.

In 1978, Cotton, Extine, and Gage (4) reported the crystal structure of $Mo_2[O_2CC(CH_3)_3]_4$. This complex crystallized in the triclinic space group $P\bar{1}$ with a = 11.793(3) A, b = 12.154(4) A, c = 10.403(4) A, α = 90.07(3)^0, β = 104.61(3)^0, γ = 71.33(2)^0, V = 1361.8(7) A^3, and Z = 2. The $Mo_2(O_2CCMe_3)_4$ molecules are arranged in chains with one oxygen atom on each end of the molecule lying approximately along the direction for axial coordination to a neighboring molecule. The Mo-Mo distance of 2.088(1) A was found in the molecules. The mean intramolecular Mo-O distances lie in the range 2.098 to 2.135 A and the mean axial intermolecular contacts are 2.870(5) and 2.926(5) A. Their structure was refined to R = 0.060, and R_w = 0.085. Apparently, the chain packing for this triclinic crystal is different from any other known $Mo_2(O_2CR)_4$ compounds. All the others had similar intermolecular geometry.

The $Re_2(O_2CR)_4X_2$ systems have not yet been intensively investigated. During the study in which the preparative route to the $[Re_2Cl_8]^{2-}$ and $[Re_2Br_8]^{2-}$ anions were first established (23), it was shown that the $(Bu_4N)_2Re_2Cl_8$ salt could be converted to the orange carboxylate-bridged dimers $Re_2(O_2CR)_4Cl_2$ (R = CH_3 or C_2H_5) upon reaction with a mixture of the appropriate carboxylic acid and its anhydride. Furthermore, in the case of $Re_2(O_2CC_2H_5)_4Cl_2$, this reaction

could be reversed by reacting the carboxylate with concentrated hydrochloric acid. These two reactions provided the first direct evidence for a close structural and electronic relationship between $[Re_2X_8]^{2-}$ and $Re_2(O_2CR)_4X_2$. The carboxylate complexes of the type $Re_2(O_2CR)_4X_2$ represent the maximum extent to which substitution of the halide ligands of the parent $[Re_2X_8]^{2-}$ anions may occur. Mechanistic studies of halide substitution in complexes containing the Re_2^{6+} core are rare, but one such investigation by Webb and Espenson (24) has established that the reaction

$$Re_2(O_2CC_2H_5)_4Cl_2 + Br^- \rightarrow Re_2(O_2CC_2H_5)_4ClBr + Cl^-$$

in acetonitrile proceeds by a two-step mechanism involving loss of Cl^- prior to coordination of Br^-. Neutral donors such as DMF, water, and so on, have been indicated to stabilize $[Re_2(O_2CC_2H_5)_4Cl]^+$ species.

Collins et al. further studied the tetrakis(pivalato)-dihalides (25). They found the compounds $Re_2(O_2CCMe_3)_4Cl_2$ and $Re_2(O_2CCMe_3)_4Br_2$ are isomorphous, crystallizing in the space group I4/m with Z = 2. The molecules have crystallographically imposed 4/m (C_{4h}) symmetry, and neglecting the rotational orientations of the CMe_3 groups, very nearly D_{4h} symmetry. The XReReX groups are perfectly linear and parallel to the crystal c axis. Adjacent

nonbonded Cl···Cl and Br···Br contacts are at distances of 3.543(3) and 3.714(3) A, respectively. These may be compared with the commonly accepted van der Waals radii which are 3.60/2 and 3.90/2 A for Cl and Br. The Re-Cl and Re-Br bonds are relatively weak (see Table 1) since their lengths are greater than those in species such as $Re_2Cl_8^{2-}$ (ca. 2.32 A) (9) and $Re_2Br_8^{2-}$ (ca. 2.48 A) (26). The long distances are consistent with the low Re-Cl stretching frequencies (27), 199 and 223 cm^{-1} in the Raman and infrared, respectively, for $Re_2(O_2CCH_3)Cl_2$, as compared to frequencies of ca. 360 cm^{-1} for $Re_2Cl_8^{2-}$ (18, 21). Table 1 shows the important molecular dimensions.

The discovery of multiple bonds between transition metal atoms posed a new challenge to the theory of molecular electronic structure. The first encouraging developments began in the early 1970s with the modifications of certain theoretical techniques. This work, pioneered by Slater and Johnson (28), resulted in what is commonly called the SCF-Xα-SW method; the abbreviation indicates self-consistent field Xα scattered wave. This method treats a molecule as a group of touching or slightly overlapping spherical atoms, assigns potentials within each atomic sphere and in the interstices, and solves the wave equation subject to the appropriate boundary conditions where these regions meet. It is the treatment of this problem in terms of the meeting

Table 1. Interatomic distances and angles and their estimated standard deviations[a] for $Re_2[O_2CC(CH_3)_3]_4Cl_2$ and $Re_2[O_2CC(CH_3)_3]_4Br_2$

	Distances, A	
Atoms	Chloride	Bromide
Re-Re	2.236(1)	2.234(1)
Re-Cl(Br)	2.477(3)	2.603(1)
Re-O	2.025(4)	2.029(5)

	Angles, degrees	
	Chloride	Bromide
Re-Re-Cl(Br)	180.00[b]	180.00[b]
Re-Re-O	89.82(9)	89.54(10)

[a]Figures in parentheses are esd's occurring in the least significant figure listed.

[b]Fixed by symmetry.

of wave (eigenfunctions) from separate origins that gives rise to the scattered wave (SW) description. The term Xα refers to an approximate way of evaluating the mean exchange energy. It can be proved that the differences of eigenvalues of the Xα method are more accurate than Hartree-Fock energy values, in that they take account of the modification or relaxation of the orbitals in transition from the initial to the final states.

The first quantitative calculations for quadruple bond were performed by the SCF-Xα-SW method on the $[Mo_2Cl_8]^{4-}$ ion (29, 30) and the $[Re_2Cl_8]^{2-}$ ion (31, 32). These calculations provided detailed description of the ground state electronic structures of these ions that are in agreement with the original qualitative description (33) of a quadruple bond based on orbital overlap considerations. By 1975, SCF-Xα-SW calculations for octochloro-dimolybdate(II), $Mo_2Cl_8^{4-}$, and dimolybdenum tetraformate, $Mo_2(O_2CH)_4$, had been reported by Norman and Kolari (29, 34). An improved calculation for the formate and calculations for Mo_2 and Mo_2^{4+} were reported by Norman et al. in 1977 (35). The energy level diagram for $Mo_2(O_2CH)_4$ is completely analogous to that for $Mo_2Cl_8^{4-}$ in the occupation and ordering of the metal-metal bonding and antibonding orbitals. The splitting between the bonding and antibonding pair is greater for $Mo_2(O_2CH)_4$, reflecting the stronger bond (2.09 A

in $Mo_2(O_2CH)_4$, 2.14 A in $Mo_2Cl_8^{4-}$). A smaller effective positive charge on the Mo_2^{4+} unit causes expansion of the electron density into formate orbitals and thus increases the effectiveness of metal-metal bonding. Later on, the ground-state electronic structures of the anions $Tc_2Cl_8^{3-}$ and $W_2Cl_8^{4-}$ were calculated using the SCF-Xα-SW method (36) by Cotton and Kalbacher. They found the results of calculations for $Tc_2Cl_8^{3-}$, $Mo_2Cl_8^{4-}$, $W_2Cl_8^{4-}$, and $Re_2Cl_8^{2-}$ are comparable with one another. In all four cases, the pictures of the electronic structure obtained are qualitatively similar. They found the pattern of orbitals in descending order of energy $\delta^*(2b_{1u}) > \delta(2b_{2g}) > \pi(5e_u)$. Thus, the first electronic band which was predicted by Xα-scattered wave calculations (29, 31) to be the $\delta \rightarrow \delta^*$ transition, although the calculated energies for the transitions have been generally much lower than the observed values.

The $[Re_2Cl_8]^{2-}$ ion and the $[Re_2Br_8]^{2-}$ ion have been studied extensively. The spectra of $Re_2Cl_8^{2-}$ and $Re_2Br_8^{2-}$ have absorption bands that peak about 14,000cm^{-1}, and which are the lowest observed electronic transitions. Mortola et al. have performed theoretical calculations on $Re_2Cl_8^{2-}$, using the Xα-scattered wave method (31); and they also examined the polarized electronic spectra of a crystal of $[(n\text{-}C_4H_9)_4N]_2[Re_2Cl_8]$ at 5 K. They suggested the following

transition assignments for the complex: 14,180 cm^{-1}, b_{2g} $\delta \rightarrow b_{1u}$ δ^*; 30,870 cm^{-1}, $e_g \rightarrow b_{1u}$ δ^* (e_g referred to an e_g orbital of $Re_2Cl_8^{2-}$ which is mainly chloride-based); 39,215 cm^{-1}, e_u $\pi \rightarrow e_g$ π^*. Bursten et al. reported calculations (37) which gave results in essential agreement with the calculation of Mortola et al.; but their inclusion of a correction for inner-shell and valence relativistic effects did cause some appreciable shifts. Figure 2 shows the results of their SCF-Xα-SW calculations for both relativistic and non-relativistic treatment. They also reported the calculated singlet and triplet transitions which are listed in Table 2.

By 1979, Noodleman and Norman developed an Xα-VB model (38), and applied the treatment to the $\delta \rightarrow \delta^*$ transition in $Mo_2Cl_4^{4-}$. This method yielded an excitation energy closer to experiment than previous theoretical values. Under the simplifying assumption that the δ-type VB orbitals are completely localized, the predicted $^1A_{1g} \rightarrow {}^1A_{2u}$ ($\delta \rightarrow \delta^*$) energy is 15.2 kcm^{-1}, compared with the experimental value of 18.8 kcm^{-1} (29). Their preliminary Xα-VB predictions for the lowest triplet ($^3A_{2u}$) and lowest singlet ($^1A_{2u}$) excited states of $Mo_2Cl_8^{4-}$ are 10.1 and 25.2 kcm^{-1}, respectively. They proposed that the Xα-VB theory should be applicable to any molecule which can be viewed as formed from molecular

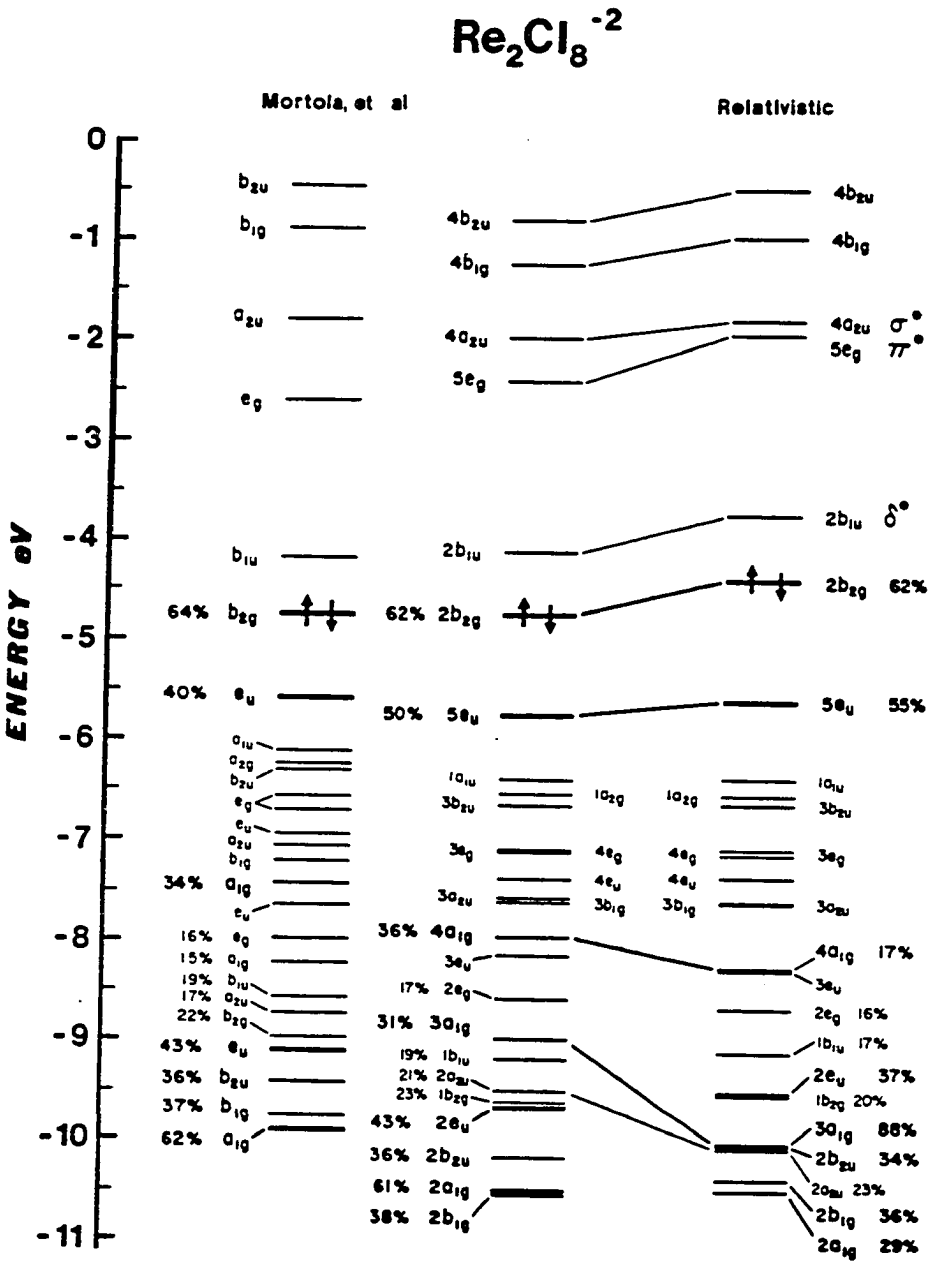

Figure 2. Results of SCF-Xα-SW calculations, both relativistic and nonrelativistic

Table 2. Calculated Energies for the Singlet and Triplet Electronic Transitions of $[Re_2Cl_8]^{2-}$ below 30000cm^{-1}[a]

Transition	type	state[b]	singlet	triplet
$2b_{2g} \rightarrow 2b_{1u}$	$\delta \rightarrow \delta^*$	A_{2u}	7040	3650
$5e_u \rightarrow 2b_{1u}$	$\pi \rightarrow \delta^*$	E_g	16730	14020
$2b_{2g} \rightarrow 5e_g$	$\delta \rightarrow \pi^*$	E_g	22120	18130
$1a_{1u} \rightarrow 2b_{1u}$	LMCT	B_{1g}	24050	23280
$1a_{2g} \rightarrow 2b_{1u}$	LMCT	B_{2u}	(25330)	(24540)
$3b_{2u} \rightarrow 2b_{1u}$	LMCT	A_{2g}	(26030)	(25330)
$4e_g \rightarrow 2b_{1u}$	LMCT	E_u	29500	28770
$3e_g \rightarrow 2b_{1u}$	LMCT	E_u	(29960)	(29230)
$5e_u \rightarrow 5e_g$	$\pi \rightarrow \pi^*$	A_{2u}	31470	28550

[a]Values in parentheses are estimated from shifts of similar transitions. All other transition energies are calculated using Slater's transition state formalism.

[b]The ground state is $^1A_{1g}$. Orbitally allowed transitions are singlet A_{2u} and singlet E_u states.

Table 3. $\bar{\nu}$(M-M) frequencies for quadruply bonded dimetal species[a]

Compound	$\bar{\nu}$(M-M), cm^{-1}
$K_4[Mo_2Cl_8]$	345
$Mo_2(O_2CCH_3)_4$	406
$Mo_2(O_2CCH_3)_4 \cdot 2py$	363
$Mo_2(O_2CCF_3)_4$	397
$Mo_2(O_2CCF_3)_4 \cdot 2py$	367
$Mo_2(mhp)_4$	425
$Re_2(O_2CR)_4Cl_2$[b]	288-295
$Re_2(O_2CR)_4Br_2$[b]	277-284
$(Bu^n_4N)_2[Re_2Cl_8]$	272-275
$(Bu^n_4N)_2[Re_2Br_8]$	275-278
$(Bu^n_4N)_2[Re_2I_8]$	259

[a]Reference 39.

[b]R may be CH_3, C_2H_5, C_3H_7, C_6H_{11}, or C_6H_5.

fragments having net spin, and an Xα-VB theory for atoms can be developed by breaking spherical symmetry in the atom and allowing anisotropic potentials for up and down spin, analogous to the GVB description of carbon (40).

An interesting feature of the vibrational spectra of the multiple-bonded dinuclear species is the vibration that corresponds mainly to M-M stretching, ν(M-M). In most cases, this vibration (which is always of the totally symmetric type) is active in the Raman spectrum only. Table 3 lists the reported ν(M-M) frequencies for Mo_2^{4+} and Re_2^{6+} complexes. The two groups differ somewhat, since the ν(Mo-Mo) values vary over a considerable range (363-425 cm^{-1}), while the ν(Re-Re) values are all within narrower limits (259-295 cm^{-1}). Actually, the force constants are proportional to frequencies squared; it means that the variability of force constants is greater for Mo-Mo bonds than for Re-Re bonds. Also, it is noted that the frequencies of ν(M-M) are usually fairly constant when ligands are changed from Cl to Br. This feature indicates that at least in some cases the localization of the mode in the M-M bond is fairly complete.

Because of the question about whether the observed spectral transitions are electric dipole allowed or forbidden, it is important to consider the selection rules. The intensity of an electronic transition depends on the

transition moment integral

$$\hat{\mu} = \langle \psi_{el}' | (\hat{M}_x + \hat{M}_y + \hat{M}_z) | \psi_{el}^{\,0} \rangle$$

The ground and excited state electronic wavefunctions are represented by $\psi_{el}^{\,0}$ and ψ_{el}', respectively, and $\hat{M}_x$, $\hat{M}_y$, and $\hat{M}_z$ are components of the electric dipole operator $\hat{M}$. For example, $\hat{M}_x = \Sigma e\hat{X}_i$, where e is the charge on the electron and $\hat{X}_i$ is the x component of the vector position of the i^{th} electron relative to the center of mass. The sum is taken over all the electrons. For a non-vanishing integral, group theory requires that the symmetry product of all functions and the operator involved in the integral contain the totally symmetric representation, i.e., the triple direct product $\Gamma(\psi_{el}') \times \Gamma(op) \times \Gamma(\psi_{el}^{\,0})$ must contain the totally symmetric irreducible representation of the point group of the molecule. The $\Gamma(op)$ represents the irreducible representation of $\hat{M}_x$, $\hat{M}_y$, or $\hat{M}_z$, and the $\Gamma(\psi)$s are the symmetry representations of the wavefunctions. Under D_{4h} symmetry, $\hat{M}_z$ transforms as A_{2u}, and $\hat{M}_x$ and $\hat{M}_y$ form a degenerate pair transforming as E_u. If such a product involving $\hat{M}_z$ gives A_{1g}, then the transition is electric dipole-allowed for light plane-polarized in the $\hat{z}$ direction. Similarly, an A_{1g} product resulting from $\hat{M}_x$ and $\hat{M}_y$ indicates the transition is electric dipole-allowed with x, y polarization.

When transitions are electric dipole-forbidden, there is yet another mechanism which may allow certain transitions. This is the vibronic, or Hertzberg-Teller mechanism, producing transitions which are, normally, much lower in intensity than electric dipole-allowed transitions. In the consideration of the transition moment integral, it was assumed that the electronic and vibrational wavefunctions could be completely separated (although it was not stated). This was a mathematical simplication which does not strictly apply to the physical realm. In polyatomic molecules, vibrations with appropriate symmetries will produce mixing of wavefunctions with various symmetries. The transition moment integral is expressed as

$$\hat{\mu} = \langle \psi_{el}' \psi_{vib}' | (\hat{M}_x + \hat{M}_y + \hat{M}_z) | \psi_{el}^0 \psi_{vib}^0 \rangle$$

using the vibronic (vibrational-electronic) wavefunction $\psi_{el}\psi_{vib}$ in place of ψ_{el} used previously. The same requirement for a non-vanishing integral applies here, except that the symmetry representation of ψ_{vib}^0 and ψ_{vib}' must be included in the product. For room temperature and cryogenic measurements of spectra, the v = 0 vibrational level is the most populated level in ψ_{vib}^0 and has A_{1g} symmetry. With this in the treatment, the product $\Gamma(\psi_{el}') \times \Gamma(\psi_{el}^0) \times \Gamma(\psi_{vib}')$ contains A_{2u} for z polarization, and $\Gamma(\psi_{el}') \times \Gamma(\psi_{el}^0) \times \Gamma(\psi_{vib}')$ contains E_u for x, y polarization.

These selection rules are valid only for spin-allowed transitions. Spin-forbidden transition may be observed if there is significant spin-orbit coupling. In this case, the ground and excited state wavefunctions must each include the mixed spin states. To account for the symmetry of the spin functions, the double rotational group is required. The magnetic dipole or electric quadrupole mechanisms for electronic transitions are considered too weak to be considered.

EXPERIMENTAL

Preparation

$[(n\text{-}C_4H_9)_4N]_2[Re_2Cl_8]$ and $[(n\text{-}C_4H_9)_4N]_2[Re_2Br_8]$ were prepared according to the procedure of Cotton et al. (41). Potassium perrhenate, 2.0 g., was heated in 40 ml. of 50% aqueous hypophosphorous acid for 10 hours at about 90°. To the resulting dark solution was added 4.0 g. of tetra-n-butylammonium bromide in 75 ml. of 6 N HCl, and heating was continued for 12 hours. The hot solution was then filtered, yielding the crude blue product which was washed with 20 ml. of 6 N HCl and then three 20-ml. portions of ethanol. After drying under vacuum for 4 hours, the blue product was recrystallized by dissolving it in 200 ml. of methanol, filtering, adding 50 ml. of 12 N HCl, and evaporating the methanol on a steam bath to form the compound $(TBA)_2Re_2Cl_8$.

Among the dark blue crystals of $(TBA)_2Re_2Cl_8$ were a number of very thin platelets that were ideal for spectroscopy. The platelets under a polarizing microscope appeared blue green at both extinctions with a distinct difference in the intensities of the absorption. Indices of refraction for Na-D light, indicated by the Becke line method, were found to be 1.546(4) for the high-absorption extinction and 1.580(4) for the low-absorption one.

Olive-green crystals of $(TBA)_2Re_2Br_8$ were produced by the addition 50 ml. of concentrated HBr into the solution of 1.5 g. of $(TBA)_2Re_2Cl_8$ in 200 ml. of methanol. Evaporation of the methanol on a steam bath yielded the product. A majority of the bromide-salt crystals were clearly dichroic with a yellow-green absorption for one extinction and a tan for the other. The Na-D indices of refraction were 1.585(4) for the green extinction and 1.632(4) for the tan extinction. However, among the crystals were a very small fraction which appeared tan in both polarizations. These were apparently the type of crystal faces observed in a few instances by Cowman and Gray (8) and upon which in part they based their original assignment for a z-polarized transition for the band (42).

The compound $Re_2[O_2C(CCH_3)_3]_4Cl_2$ was prepared by allowing $(TBA)_2Re_2Cl_8$ (0.5 g) to react with pivalic acid (0.5 g) at ca. 150 ^{0}C for 48 hours. The residue, when washed with 30 ml. of n-hexane and 10 ml. of acetone, yielded red crystals (25). An examination of the crystals indicated they were mostly small square prisms. Faces containing the prism needle axis were distinctly dichroic, appearing red-orange for light polarized along the needle axis and yellowish for light polarized perpendicular to the axis. Indices of refraction for the 100 face were determined to be n_c = 1.674 and n_a = 1.572 by means of the Becke line method (43).

The compound $Mo_2(O_2CC(CH_3)_3)_4$ was prepared according to the procedure of McCarley et al. (44) by reacting $Mo(CO)_6$ with the calculated amount of pivalic acid in refluxing o-dichlorobenzene. The solution was heated at ca. 150 ^oC under low N_2 flow for 3 days. The compound crystallized as slender yellow needles when the reaction mixture was cooled to room temperature. The yellow crystalline product was filtered, washed with benzene and cyclohexane, and dried under vacuum for one day. This preparation of $Mo_2(piv)_4$ was somewhat different from Cotton et al.'s procedure. Their crystals of $Mo_2(piv)_4$ were grown by sublimation of a small sample in an evacuated sealed glass tube at ca. 100^oC. Microscopic examination showed two types of faces among the specimens in this research. The extinction was observed along the needle axis in one type. The extinction was observed 18^o away needle axis in another type. The crystals with different types of faces were sorted out from the preparation for X-ray diffraction comparison.

Crystal Optics and Spectra

Light energy is generally considered to travel by means of a transverse wave motion in which the vibration of the electromagnetic field is usually perpendicular to the direction of travel of the energy. Those materials or devices that convert ordinary light to plane-polarized light

are generally called polarizers. The electric field of light emergent from a polarizer has been made to vibrate parallel to one particular direction which is called, for convenience, the "privileged direction" of the polarizer. When plane-polarized light is incident on the face of anisotropic crystal it can be transmitted only in two mutually perpendicular privileged directions for that crystal face. If the plane of polarization of incident light is not aligned with either privileged direction, then the light is split into two components polarized along these directions. An absorption spectrum for one crystal polarization is obtained by using incident radiation which is polarized along that one of these two particular polarization directions. Any observed absorption must be at either a maximum or minimum along these directions.

The optical indicatrix illustrates how the refractive index of a transparent material varies according to the vibration direction of the light wave in the material (monochromatic light assumed). Consider an infinite number of vectors radiating outward in all directions from a common point within the crystal. Each vector is drawn proportional in length to the crystal's refractive index for light vibrating parallel to that vector direction. The indicatrix is a surface connecting the tips of these vectors. The indicatrix is purely a method of rationalizing optical

phenomena. In isotropic media, by definition, the index of refraction does not change with the vibration direction of the light. Consequently, all the vectors relating the refractive index to vibration direction are of equal length, and therefore all isotropic indicatrixes are perfect spheres. Cubic crystals, transparent glasses, and liquids are characterized by such indicatrixes. In anisotropic media, the index of refraction actually varies according to the vibration direction of the light in the crystal. Consequently, the optical indicatrix for anisotropic media is not a sphere but an ellipsoid. There are two types of anisotropic optical indicatrixes, the uniaxial and biaxial indicatrix.

The uniaxial indicatrix will be discussed first. Crystals of the hexagonal and tetragonal systems exhibit, for monochromatic light vibrating parallel to the c axis, a unique index of refraction customarily symbolized as ε. In Figure 3, a vector proportional in length to the value of ε has been drawn parallel to the c axis to indicate this (45). On the other hand, for all vibration directions at 90 degrees to the c axis, the crystal's refractive indices all equal a common value, symbolized as ω. By constructing vectors proportional in length to ω along these vibration directions, a circle of radius ω is defined; this circular section is always perpendicular to the c axis.

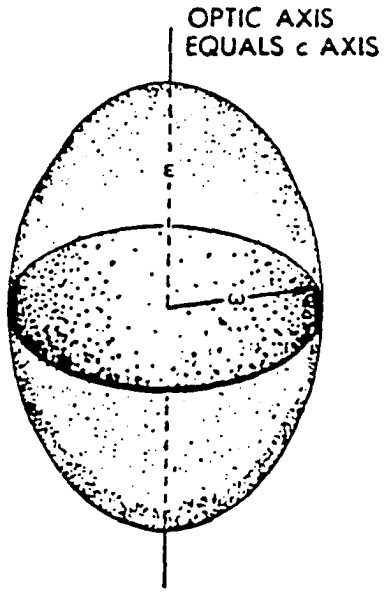

Figure 3. The uniaxial indicatrix for the crystal

The direction in the uniaxial indicatrix that coincides with the crystal's c axis is called the optical axis. With reference to it, three types of sections may be cut through the indicatrix center: (a) a principal section (that is, one which contains the optic axis and therefore intersects the indicatrixes in an ellipse whose semiaxes are equal to ε and ω); (b) the circular section (that is, a section cut normal to the optic axis); and (c) a random section (that is, the intersection of the indicatrix with a plane cut at random angle (θ) to the optic axis). A random section always intersects the indicatrix in an ellipse whose semiaxes are ω and ε'. These are illustrated in Figure 4.

A biaxial crystal belongs to the orthorhombic, monoclinic, or triclinic system and possesses three significant indices of refraction, commonly symbolized as α, β, and γ. Of these, α and γ represent, respectively, the smallest and largest refractive indices exhibited by the crystal; β is intermediate in value between them. The shape of the biaxial indicatrix is a three-dimensional ellipsoid, all central sections of which are ellipses except for two circular sections. The radius of these circular sections is β. The two normals to these sections are called the optical axes. These are illustrated in Figure 5.

With the center of an indicatrix on a crystal face, the major and minor axes of the intersection ellipses of the

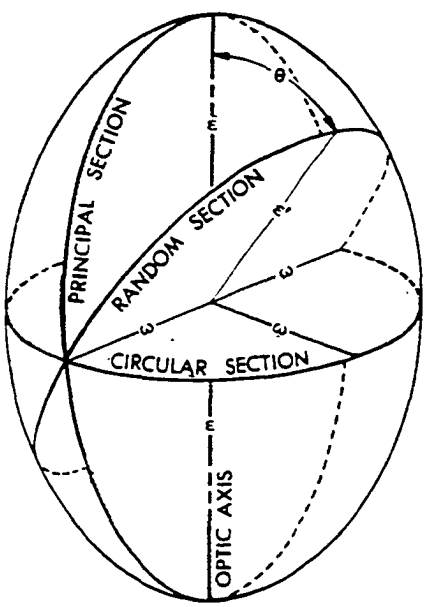

Figure 4. Illustration of the three types of central sections through a uniaxial indicatrix

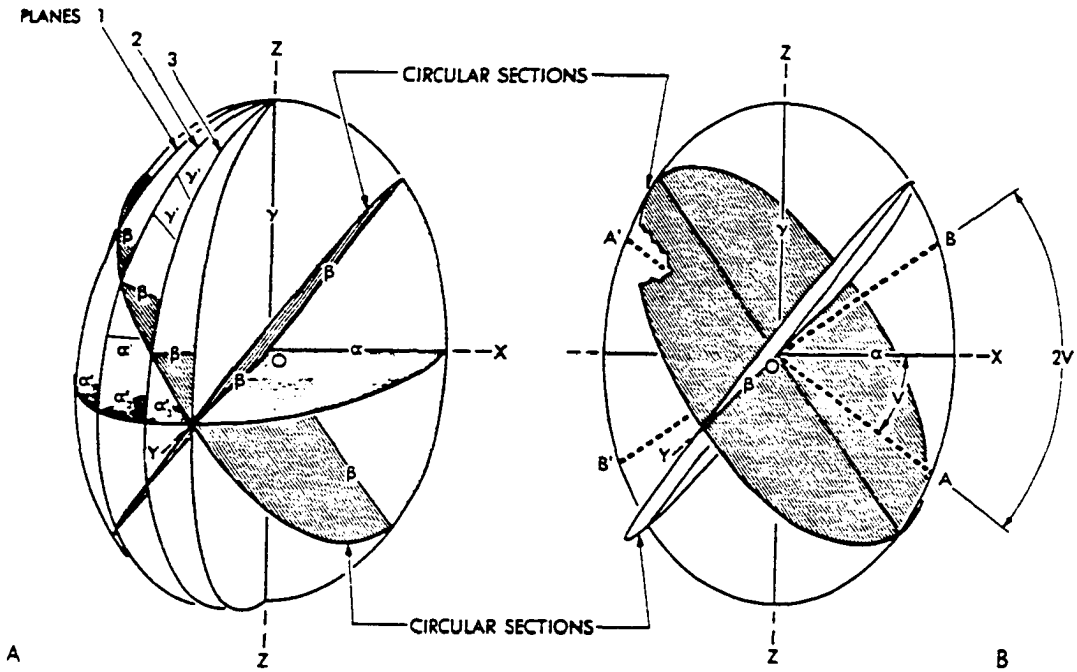

Figure 5. The biaxial indicatrix, an imaginary three -dimensional ellipsoid whose radii are proportional to the crystal's refractive index for light vibrating parallel to them. (A) Planes 1, 2, and 3 are typical of the numerous ellipses that could be drawn to hinge on ZZ. (B) The normals to the circular sections, AA' and BB', are the two optic axes

indicatrix with the face are the privileged directions of the crystal for normal incidence on the face. If the indicatrix intersects the face of a crystal in a circle, innumerable privileged directions exist. The indicatrix must have the same symmetry as the crystal. The refractive index has a real part and an imaginary part. The real part is related to the wave velocity; the imaginary part is related to the absorption. The real and imaginary parts have their own independent ellipsoids. If any crystal axis lies in the face of an orthorhomic crystal, then one of the privileged directions must always lie parallel to it. The 010 face, for example, has $\hat{a}$ and $\hat{c}$ as the privileged directions. Similarly, a face of a monoclinic crystal h0l contains the $\hat{b}$ axis, and $\hat{b}$ is one of the privileged directions. However, for all other faces of these two crystal systems and for all faces of a triclinic system, the privileged directions may vary with wavelength.

The Becke line refers to a phenomenon associated with a vertical contact of two substances of difference indices of refraction observed on the stage of a microscope. Under the microscope, the Becke line may not be seen when the microscope is exactly focused on a fragment. However, if the tube of the microscope is slightly raised, a narrow line of light (the Becke line) appears just inside or outside the contact of the fragment with the surrounding medium. If the

Becke line moves into the fragment when the microscope tube is raised, the index of the fragment is higher than that of the surrounding substance. If the Becke line moves out into the surrounding medium when the tube is raised, the fragment has a lower index than that of the surrounding medium. Lowering the tube reverses the effect in each instance. The greater the difference in the refractive indices between the fragment and immersion, the greater is the displacement of the Becke line as the microscope tube is raised or lowered. The indices of refraction of the crystal faces have been determined by means of the Becke line method (43) with a set of standard liquids prepared by the Cargille Laboratory. Steps of 0.004 in the indices of refraction were available in these standards.

The privileged directions for the face of a crystal are commonly determined with the use of a polarizing microscope. The polarizing microscope is little more than a compound microscope into which two polarizers have been integrated. One, located below the stage, is called the polarizer. The second, located above the stage, is called the analyzer. The rotatable stage is calibrated for precise measurement of angles.

With no sample on the stage and with crossed polarizers, the field of view is completely dark. The polarizer polarizes the light in one direction which then

cannot pass through the analyzer. If a crystal is placed on the stage with its privileged directions aligned with the polarizer and analyzer, then the crystal appears dark. Three successive 90 degree rotations from this orientation will also result in a dark field. In such an orientation, the incident polarized wave passes through the crystal retaining its plane polarization and is blocked out completely by the analyzer, resulting in a dark field of view. If the crystal privileged directions do not coincide with the polarizer and analyzer, then the light is split into two components along these directions. These components pass through the crystal, then re-combine as they emerge. The re-combined wave will provide transmitted light, and various interference colors will be observed for thin crystals.

In some cases, crystal dimensions were measured with the ruled eyepiece. Calibration was obtained by viewing a millimeter rule through the microscope. A cystal thickness measurement was facilitated by standing a crystal on an edge. Crystals were manipulated under microscopic observation by sewing needles or sharpened tungsten wires.

Once the extinction directions of a single crystal had been determined with the polarizing microscope, then the crystal was mounted over a hole from ca. 20 to 250 μm in diameter (dependent on crystal size), centered on a 1 cm x 2

cm x 3 mil brass or platinum plate. Silicone vacuum grease was used to hold the crystal in place on the metal plate. The metal plate with the sample was placed in a brass sample holder and the extinction directions of the crystal were re-determined in relation to the central axis of the sample holder in the spectrophotometer.

The spectrophotometer, used to record all spectra, was a Cary model 14 equipped with a model 1471200 high intensity tungsen-halogen light source and a special product number B50-025-000 Range Modifier. Various neutral density screens were used to attenuate the reference beam. Spectra could be recorded in the visible mode from 810 to 300 nm by the use of a Varian model R928HA phototube, which was sensitive at long wavelengths. However, a Cary model 1460215 phototube was used, as the spectra were recorded from 300 to 230 nm. Plane-polarization of the light beam was produced by two Glan-Taylor-type calcite polarizers. One polarizer was mounted in the sample compartment and could be rotated by means of an external crank. Under the UV-visible mode, the monochromatic light was polarized before it reached the sample. The polarizer in the reference beam was rotated by hand to match the sample polarizer, in order to balance absorption due to calcite. All spectral data were recorded on punched cards by an IBM model 29 keypunch linked to the spectrophotometer via Cary Digital System interface.

Baselines were obtained by repeating the spectral experiments with a pinhole blank in place of the sample. Baselines were subtracted and the spectra were plotted on an incremental plotter by a computer program developed previously within the research group.

To measure spectra at 5 K, the following procedure was used. First, the vacuum space of the Andonian Cryostat (see Figure 6) was pumped to a vacuum on the order of 5×10^{-5} torr by means of an oil diffusion pump. Once this vacuum was attained, the liquid helium dewar was evacuated and flushed with dry helium gas, to insure that no vapor was present that might freeze the throttle valve. After the liquid helium dewar was filled and a flow of liquid helium into the base of the sample chamber had been established, the top plug of the cryostat was removed, and the sample holding assembly lowered into the sample chamber. Once a temperature of ca. 10 K was attained, the helium flow and heater were monitored and controlled to stabilize the temperature at 5-6 K.

Polarization Ratios

A polarization ratio is the ratio of the intensity of a transition along one extinction direction to its intensity along the other extinction direction. For the vast majority of D_{4h} dimeric compounds, the molecular z-axis is

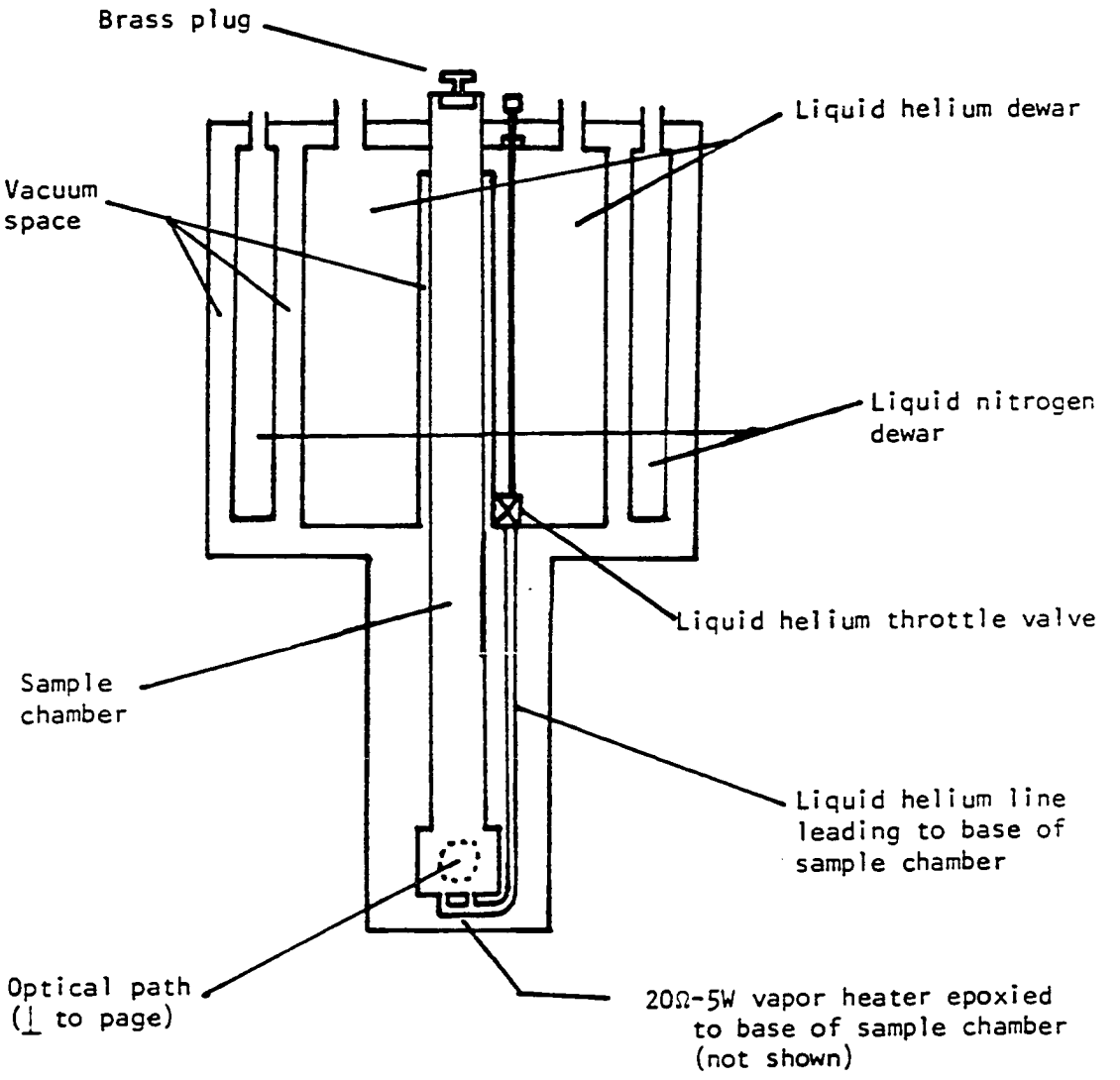

Figure 6. Simplified cross-section of the Andonian Cryogenics Cryostat

significantly closer to one of the observed extinctions than the other. To calculate a polarization ratio on the basis of the oriented molecule theory requires knowledge of Miller indices of the crystal face, the orientations of the molecules in the unit cell, and the space group of the crystals. The presence of an extinction, dependent on wavelength, will complicate the determination. For any spectral wavelength, maximum and minimum intensities will be measured when the polarized light wave travels through the crystal aligned with the extinction directions.

Polarization ratio can be calculated for an ideal case and then compared with the observed value in the spectra, e.g., for the peak of 0-0 transition. For the ideal z-polarized case, the transition moment vector can be considered to be coincident with the z symmetry axis of the molecule studied. In the ideal case of D_{4h} symmetry for the dimeric complexes in question, the unit transition moment is along the direction of metal-metal bond. $\hat{z}$, $E\hat{x}_1$, and $E\hat{x}_2$ vectors represent the z component of transition moment and the two extinction directions, respectively. The angles between $\hat{z}$ and $E\hat{x}_1$ and between $\hat{z}$ and $E\hat{x}_2$ are designated θ_1 and θ_2, respectively. For the electric vector of a wave polarized along $E\hat{x}_1$, the amplitude along $\hat{z}$ is $\varepsilon\cos\theta_1$, where ε is the electric vector amplitude of the incident wave. Since intensity is given by the amplitude squared, the intensity

absorbed from the light polarized along $\hat{Ex}_1$ is proportional to $\varepsilon^2\cos^2\theta_1$. Similarly, a quantity, $\varepsilon^2\cos^2\theta_2$, is proportional to the intensity absorbed from the wave polarized along $\hat{Ex}_2$ for the z-polarized transition. This yields a polarization ratio of $I_1/I_2 = \cos^2\theta_1/\cos^2\theta_2$. These are obtained from the dot products by $\hat{z}\cdot\hat{Ex}_1 = \cos\theta_1$ and $\hat{z}\cdot\hat{Ex}_2 = \cos\theta_2$. For a pair of degenerate and orthogonal x and y components of transition moment which are also orthogonal to $\hat{z}$ in the ideal case of D_{4h} symmetry, the polarization ratio, $I_1/I_2 = \sin^2\theta_1/\sin^2\theta_2$, is obtained (46). For space groups with different sites for the molecules in the unit cell, a variation of this calculation is used. The transition moment vectors $\hat{z}_1$ and $\hat{z}_2$ apply to the two separate sites. $\hat{z}_1$ lies at angle $\theta_{1,1}$ and $\theta_{1,2}$ from $\hat{Ex}_1$ and $\hat{Ex}_2$, respectively, and $\hat{z}_2$ lies at angle $\theta_{2,1}$ and $\theta_{2,2}$ from $\hat{Ex}_1$ and $\hat{Ex}_2$, then the polarization ratio for a z-polarized transition would be given by $I_1/I_2 = (\cos^2\theta_{1,1} + \cos^2\theta_{2,1})/(\cos^2\theta_{1,2} + \cos^2\theta_{2,2})$. To facilitate the calculations, the crystal axes and all vectors expressed in terms of an orthogonal set, viz., $\hat{i}$, $\hat{j}$, $\hat{k}$. The vector calculations were then performed on a TI-59 calculator, using a program written in the research group.

Crystallographic Indexing

A crystal to be indexed was cemented to a glass fiber with a small amount of epoxy cement and placed on a goniometer head. Careful drawings were made to show the relationship between the faces and long axis of a crystal with respect to the two horizontal adjustment axes of the goniometer head. The alignment of a crystal face parallel to an easily recognized flat surface on the goniometer head is necessary. Then, the goniometer head was placed on the Ames Laboratory four-circle diffractometer, which was controlled by a PDP-15 computer. Automatic indexing was accomplished through the interactive program ALICE developed by Dr. R. A. Jacobson (47). Omega-oscillation photographs were taken for phi values from 0^{0} to 180^{0}, usually in increments of 30^{0} in phi. The location of several diffraction spots were measured from the photographs and entered into the computerized indexing program. From a set of ten or more diffraction peaks, the crystal was indexed according to the standard guidelines published in Crystal Data (48). When the unit cell parameters were considered to be reasonably accurate, various crystallographic faces could be called (via the computer) into diffraction position, and the crystallographic axes could be placed in a vertical orientation for oscillation photographs. In this way, the observed faces and axes of a crystal could be identified.

The identity of a compound and the accuracy of the indexed unit cell parameters were determined by comparison with the values from previously reported data for that crystal in cases for which structure determinations were in the literature.

X-ray Data Collection and Structure Solution

General

Data were collected at room temperature on the Ames Laboratory automated four-circle diffractometer, which is equipped with a scintillation counter. Graphite monochromated Mo Kα X-radiation (λ = 0.71034 A) was used for data collection with a take-off angle of 4.5^{o}. A scan rate of 0.5 sec/step of 0.01^{o} steps in omega was employed, with the scan range dependent on peak width. Peaks were scanned until background was encountered, as determined by the criterion count $\leq$ background + σ(background). Stationary-crystal, stationary-counter background counts were taken at the beginning and end of each scan. All data collected were within a 2θ sphere of 50^{o}. As a check on crystal stability, the intensities of three standard reflections were remeasured every 75 reflections. The intensities of the standard reflections should not vary significantly throughout data collection.

The intensity data were corrected for absorption and Lorentz-polarization effects. Data reduction and averaging was accomplished by using the program FDATA (49). The estimated deviations in the structure factors were calculated by the finite-difference method (50). The scattering factors used for all non-hydrogen atoms were those given in the International Tables (51). Real and imaginary corrections for anomalous dispersion were obtained by linear interpolation of reported data (51). The hydrogen atom scattering factors used were those of Stewart et al. (52). The discrepancy factors used are given by $R = \Sigma||F_o| - |F_c||/\Sigma|F_o|$ and $R_w = (\Sigma w(|F_o| - |F_c|)^2/\Sigma w|F_o|^2)^{1/2}$, where F_o and F_c are observed and calculated structure factors, respectively, and $w = 1/\sigma^2(F_o)$, with $\sigma(F_o)$ representing the estimated standard deviation in F_o.

The position of atoms was subjected to least-squares refinement. Fourier synthesis for three-dimensional Patterson maps and electron density maps were performed through the computer program ALLS (53). Plots depicting molecular structure were drawn by the ORTEP program (54).

$[N(n\text{-}C_4H_9)_4]_2Re_2Br_8$

The program LATT (49) was used to calculate the following refined cell parameters based on $\pm 2\theta$ values of 14 reflections: a = 14.330(3) A, b = 15.502(2) A, c =

11.380(2) A, β = 97.08(0)^{o}, and V = 2508.7(9) A^{3}. Intensity data were collected for 10,075 reflections with $2\theta < 50^{o}$ over four octants. From these data, 2439 independent reflections with intensity greater than 3σ were utilized for the structure determination. A b-oscillation photograph exhibited the mirror symmetry of a monoclinic lattice. The monoclinic space group was identified as $P2_1/n$, based on the systematic extinction of k odd for the 0k0 reflections and of h + l odd for the h0l reflections. This space group is an alternative to $P2_1/c$ which was utilized by Cotton et al. (9) for $(TBA)_2Re_2Cl_8$. However , $P2_1/n$ is somewhat more convenient to use since β is closer to 90^{o}. The crystal plate of $(TBA)_2Re_2Br_8$, selected for X-ray diffraction, was 0.44 mm x 0.26 mm x 0.06 mm. The face for this platelet was the $10\bar{1}$ face. An empirical absorption correction was performed by means of diffractometer ϕ-scan data and the program ABSN (55). Locations of Re atoms were found from Patterson superposition techniques. A series of electron density maps provided locations of the non-hydrogen atoms. The 24 methylene hydrogen atoms were introduced at idealized positions and not refined. Positional parameters, the occupancy of the Re positions and anisotropic thermal parameters of non-hydrogen atoms were refined first by block diagonal matrices and finally by full-matrix least squares. The refinement resulted in R = 0.090 and R_w = 0.144. The

introduction of idealized positions for the hydrogen atoms did not change the R values.

$[N(n\text{-}C_4H_9)_4]_2Re_2Cl_8$

Automatic indexing was accomplished by an interactive program, ALICE (47). A transformation was applied to these axes to give a set which was tuned on 4 strong reflections with 2θ between 12 and 23° with cell parameters: a = 10.95, b = 15.32, c = 16.30 Å, α = 89.56, β = 122.76, and γ = 90.33°. This set was in quite satisfactory agreement with the monoclinic set from the structure determination by Cotton et al. (9), the cell parameters they obtained are: a = 10.933(5), b = 15.412(6), c = 16.435(5) Å, β = 122.27(3)°. The face for this platelet was the 100. For this face, the extinctions would lie along the b and c axes, and it was observed that the intense absorption or the 1.546 index of refraction applied to the b polarization. This was the same face indicated by Cowman and Gray (8) in the initial study. However, this crystal was so thick that only the very weak first absorption feature was observable. The very thin crystals for which the full absorption band was scanned did not provide sufficient diffracting intensity for X-ray confirmation of the axes.

$Re_2[O_2CC(CH_3)_3]_4Cl_2$

From a series of oscillation photographs, coordinates of 12 reflections were entered into the computer which tuned on the reflections and by means of standard programs computed cell parameters to be: a = 11.461, b = 11.461, c = 10.714 A, α = 89.96, β = 90.00, γ = 90.00°. The needle faces were 100 with $\hat{c}$ directed along the needle axis. These values are in good agreement with the values from the structure determination of Collins et al. (25). They reported from an X-ray diffraction study the crystal structure with a tetragonal cell, I4/m, a = 11.469(4), c = 10.733(1) A, Z = 2.

The monoclinic crystals of β-$Mo_2(O_2CC(CH_3)_3)_4$

Crystals with faces possessing extinctions 18° off needle axis were taken and mounted for axis determination so that the axes could be compared with Cotton's triclinic form. Instead of finding his axes, a set of monoclinic axes were obtained. b-Axis oscillation photographs possessed the mirror plane which was required by a monoclinic crystal. A total 10,759 reflections were collected of which 1948 independent reflections, having $|F_o| \geq 3\sigma(F_o)$, were used in the structure solution. The program LATT (49) was used to calculate the cell parameters of the monoclinic system of $Mo_2(piv)_4$ compound as follows: a = 12.747(3) A, b =

18.322(3) A, c = 11.369(1) A, β = 91.82(9)^{o}, and V = 2654.1(8) A^3. These refined cell parameters were based on $\pm$ 2θ values of 20 reflections. The monoclinic space group was identified as I2/c, based on the systematic extinction of h + k + l odd for the hkl reflections, of l odd for the h0l reflections, and of k odd for the 0k0 reflections.

Initial Mo atom positions were obtained from a three-dimensional Patterson map. A subsequent electron density map yielded the positions of the remaining non-hydrogen atoms. Positional parameters, and anisotropic thermal parameters of the non-hydrogen atoms were refined first by block-diagonal matrices and finally by full-matrix least squares, and resulted in R = 0.055, and R_w = 0.084. Interatomic distances, angles, and their standard deviations were calculated by the program DISTANCE (56). This monoclinic form has been designated as the β-$Mo_2(piv)_4$ to distinguish it from Cotton et al.'s triclinic α-form (4).

The orthorhombic crystals of γ-$Mo_2(O_2CC(CH_3)_3)_4$

The crystals with faces for which an extinction occurred along the needle axis were mounted for axis determination. Transformation matrices which yielded a set of possible orthorhombic axes were found. Oscillation photographs for all these axes exhibited the mirror planes required for the orthorhombic system. A total of 6118

reflections were collected, of which 1607 independent reflections having $|F_o| \geq 3\sigma(F_o)$ were used in the structure solution. The program LATT (49) was used to calculate the cell parameters of the orthorhombic system of $Mo_2(piv)_4$ based on $\pm 2\theta$ values of 15 reflections: a = 12.711(3), b = 18.351(5), c = 11.413(3) A, and V = 2662(1) A^3. The cell parameters of the orthorhombic system are strikingly close to those for the monoclinic form. The orthorhombic space group was identified as Pbcn, based on the systematic extinction of k odd for the 0kl reflections, of l odd for the h0l reflections, of h + k odd for hk0 reflections, of h odd for the h00 reflections, of k odd for the 0k0 reflections, and of l odd for the 00l reflections.

The locations of Mo atoms were found through a three-dimensional Patterson map. A subsequent electron density map yielded the positions of the remaining non-hydrogen atoms. The positional and anisotropic thermal parameters of the non-hydrogen atoms were subjected to first several cycles of block-diagonal least-squares refinement. After all the parameters had settled down, it was followed by several cycles of full-matrix refinement resulting in R = 0.057, and R_w = 0.084. The program ALLS (53) was used for least-squares refinement and Fourier synthesis was performed by the program FOUR (57). Interatomic distances, angles, and their standard deviations were calculated by the program

DISTANCE (56). This third polymorph will be designated as the γ-$Mo_2(piv)_4$.

RESULTS AND DISCUSSION

Description of Crystal Structures

Structure of $[N(n\text{-}C_4H_9)_4]_2Re_2Br_8$

It is important to know the crystal structure before the interpretation of the spectra. Table 4 summarizes crystallographic parameters for $(TBA)_2Re_2Br_8$ and $(TBA)_2Re_2Cl_8$. Tables 5 and 6 give the final positional and thermal parameters for $(TBA)_2Re_2Br_8$, and Figure 7 shows the atom labelling system. Observed and calculated structure factors are listed in Appendix A. Anisotropic thermal parameters are given for all atoms except hydrogen atoms. An isotropic thermal parameter, fixed at 4.0 A^2, was used for each hydrogen atom. The structure was refined in the space group $P2_1/n$.

The refinement for $(TBA)_2Re_2Br_8$ was rather poor since the final value of R was only 0.090. However, it does provide a satisfactory description of the $Re_2Br_8^{2-}$ ion and the orientation of the Re-Re bonds that has not been available previously for a rational interpretation of the crystal spectra. Bond lengths and bond angles for $Re_2Br_8^{2-}$ ions are in Table 7. For non-hydrogen atoms of $N(n\text{-}C_4H_9)_4N^+$ ions, they are in Table 8. The structure is very similar to that reported for $(TBA)_2Re_2Cl_8$ by Cotton et al. (9).

Table 4. Crystallographic Parameters for $(TBA)_2Re_2Br_8$

Space Group	$P2_1/n$
Crystal System	Monoclinic
a (A)	14.328(3)
b (A)	15.503(3)
c (A)	11.381(3)
β (deg)	97.10(3)
V (A^3)	2509(1)
Z	2
R	.090
R_w	.144

Table 5. Final positional parameters[a] and their estimated standard deviations[b] for $(TBA)_2Re_2Br_8$

Atom	x	y	z
Re1 (62.1(6)%)	0.0236(1)	0.4375(1)	0.5417(2)
Re2 (37.9(6)%)	0.0682(2)	0.5058(2)	0.4649(3)
Br1	0.1139(3)	0.6580(2)	0.5056(3)
Br2	0.02182(3)	0.5528(2)	0.2575(3)
Br3	0.1858(2)	0.4658(2)	0.6340(3)
Br4	0.0966(2)	0.3600(2)	0.3864(3)
N	0.348(2)	0.194(1)	0.567(2)
C1	0.365(2)	0.294(1)	0.600(3)
C2	0.403(3)	0.303(2)	0.731(3)
C3	0.439(2)	0.399(2)	0.743(4)
C4	0.475(3)	0.413(3)	0.883(4)
C5	0.442(2)	0.141(2)	0.579(3)
C6	0.516(2)	0.184(2)	0.522(3)
C7	0.605(2)	0.216(2)	0.540(3)
C8	0.693(2)	0.156(3)	0.483(5)
C9	0.287(2)	0.156(2)	0.646(3)
C10	0.190(2)	0.194(2)	0.646(3)
C11	0.131(3)	0.142(2)	0.724(4)
C12	0.033(2)	0.177(2)	0.725(4)
C13	0.300(2)	0.198(2)	0.432(3)
C14	0.268(2)	0.109(3)	0.389(3)
C15	0.226(2)	0.116(4)	0.256(3)
C16	0.199(3)	0.033(3)	0.184(5)

[a]Given in fractional coordinates.

[b]Given in parentheses for the least significant figure.

Table 6. Final thermal parameters[a] and their estimated standard deviations[b] for $(TBA)_2Re_2Br_8$

	B_{11}	B_{22}	B_{33}	B_{12}	B_{13}	B_{23}
Re1(62.1(6)%)	4.7(1)	3.84(8)	4.8(1)	0.31(7)	-0.69(7)	-0.00(7)
Re2(37.9(6)%)	4.3(1)	4.1(1)	4.5(2)	0.1(1)	-0.4(1)	-0.0(1)
Br1	7.1(1)	5.4(2)	6.9(2)	-1.5(1)	-0.1(2)	-0.6(1)
Br2	8.1(2)	5.5(2)	5.1(2)	0.1(1)	0.3(2)	0.3(1)
Br3	5.3(2)	6.6(2)	7.1(2)	1.0(1)	-1.9(2)	-1.4(1)
Br4	6.1(2)	5.6(2)	5.7(2)	1.3(1)	-0.5(1)	-0.8(1)
N	9(2)	2.9(9)	6(1)	2(1)	-1(1)	-1(1)
C1	6(2)	1.6(9)	7(2)	0(1)	-1(1)	0(1)
C2	10(3)	5(1)	6(2)	2(2)	1(2)	-0(1)
C3	5(2)	6(2)	11(3)	1(2)	-2(2)	-1(2)
C4	9(2)	9(2)	11(3)	-1(2)	-0(2)	-5(2)
C5	5(2)	7(2)	5(2)	0(1)	-3(1)	-2(1)
C6	3(1)	11(2)	5(2)	4(2)	1(1)	3(2)
C7	7(2)	7(2)	5(2)	-2(2)	-3(1)	-1(1)
C8	5(2)	9(2)	15(4)	-3(2)	2(2)	-3(2)
C9	4(1)	8(2)	6(2)	1(1)	2(1)	5(2)
C10	5(2)	6(2)	6(2)	1(1)	-1(1)	0(1)
C11	8(2)	5(2)	11(3)	1(2)	-2(2)	0(2)
C12	5(2)	9(2)	9(2)	0(2)	2(2)	-0(2)
C13	4(1)	10(2)	6(2)	-0(2)	-1(2)	3(2)
C14	4(1)	10(2)	5(2)	0(2)	-2(1)	-0(2)
C15	6(2)	18(4)	6(2)	4(3)	-1(2)	-3(3)
C16	11(3)	10(3)	15(5)	-1(3)	3(3)	-4(3)

[a]The B_{ij}'s are defined by $T = \exp[-1/4(B_{11}h^2a^{*2} + B_{22}k^2b^{*2} + B_{33}l^2c^{*2} + 2B_{12}hka^*b^* + 2B_{13}hla^*c^* + 2B_{23}klb^*c^*)]$.

[b]Given in parentheses for the least significant figure.

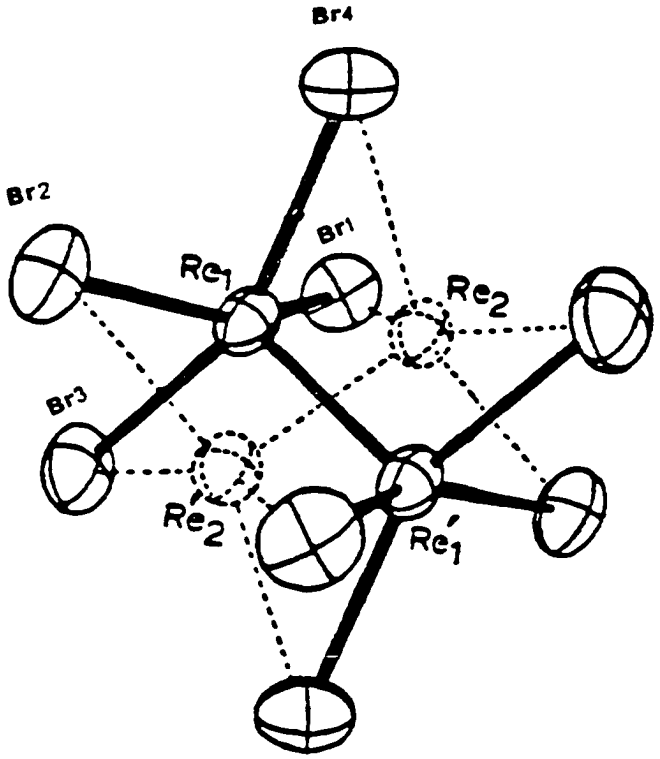

Figure 7. Atom labelling system used in the structure solution of $Re_2Br_8^{2-}$. Primes indicate atoms generated by an inversion center located at the center of the molecule

Table 7. Interatomic distances and angles and their estimated standard deviations[a] for $Re_2Br_8^{2-}$

Distances, A		Angles, degrees	
Re1-Re1	2.226(4)	Br1-Re1-Br2	86.8(1)
Re2-Re2	2.209(6)	Br1-Re1-Br4	87.1(1)
Re1-Br1	2.470(4)	Br1-Re1-Br3	152.0(1)
Re1-Br2	2.457(4)	Br2-Re1-Br3	86.4(1)
Re1-Br3	2.469(4)	Br2-Re1-Br4	151.5(1)
Re1-Br4	2.473(4)	Br3-Re1-Br4	86.1(1)
Re2-Br1	2.477(4)	Br1-Re2-Br2	86.1(2)
Re2-Br2	2.481(5)	Br1-Re2-Br3	87.4(2)
Re2-Br3	2.475(5)	Br1-Re2-Br4	152.0(2)
Re2-Br4	2.482(4)	Br2-Re2-Br4	87.8(1)
		Re1-Re1-Br1	103.7(1)
		Re1-Re1-Br2	104.0(1)
		Re1-Re1-Br3	104.3(1)
		Re1-Re1-Br4	104.6(1)
		Re2-Re2-Br1	103.6(2)
		Re2-Re2-Br2	102.9(2)
		Re2-Re2-Br3	104.3(2)
		Re2-Re2-Br4	104.4(2)

[a]Given in parentheses for the least significant figure.

Table 8. Interatomic distances and angles and their estimated standard deviations[a] for tetra-n-butylammonium ion

Distances, A		Angles, degrees	
N-C1	1.61(3)	C1-N-C5	112(2)
N-C5	1.57(4)	C1-N-C9	109(2)
N-C9	1.45(4)	C1-N-C13	103(2)
N-C13	1.60(4)	C5-N-C9	108(2)
C1-C2	1.52(5)	C5-N-C13	112(2)
C2-C3	1.58(5)	C9-N-C13	113(2)
C3-C4	1.63(6)	C1-C2-C3	104(2)
C5-C6	1.46(4)	C2-C3-C4	106(3)
C6-C7	1.55(4)	C5-C6-C7	108(3)
C7-C8	1.56(5)	C6-C7-C8	118(3)
C9-C10	1.51(4)	C9-C10-C11	112(3)
C10-C11	1.53(5)	C10-C11-C12	113(3)
C11-C12	1.51(5)	C13-C14-C15	108(3)
C13-C14	1.52(5)	C14-C15-C16	119(4)
C14-C15	1.57(5)		
C15-C16	1.55(7)		

[a]Given in parentheses for the least significant figure.

The $Re_2Br_8^{2-}$ ion occupies a crystallographic center of inversion, and there are only four crystallographically independent bromide atoms. The average of the Re-Br bonds is 0.132 A longer than the Re-Cl. Also, the unit cell volume is 7% larger for the $Re_2Br_8^{2-}$ salt than for the $Re_2Cl_8^{2-}$ salt. The average of the Re-Re bond distances, 2.218 A, is virtually the same as for the $(TBA)_2Re_2Cl_8$, 2.220 A.

Structures of $Mo_2(O_2CC(CH_3)_3]_4$

Because of their similarity, the structures of the monoclinic and orthorhombic polymorphs of $Mo_2(piv)_4$ will be discussed together. Table 9 summarizes crystallographic parameters for the three $Mo_2(piv)_4$ polymorphs. Table 10 gives the final positional and thermal vibration parameters of the monoclinic and orthorhombic systems, and Figure 8 shows the atom labelling system. Observed and calculated structure factors for monoclinic and orthorhombic systems are listed in Appendixes B, C, respectively. Both of the polymorphs of $Mo_2(piv)_4$ have four molecules in the unit cell, but the monoclinic structure has two molecules in a primitive cell, and the orthorhombic structure has four molecules in a primitive cell. There are also two molecules

Table 9. Crystallographic parameters for the triclinic, monoclinic, and orthorhombic crystals of $Mo_2(piv)_4$

	Triclinic crystal[a]	Monoclinic crystal	Orthorhombic crystal
Space Group	$P\bar{1}$	I2/c	Pbcn
a (A)	11.793(3)	12.747(3)	12.711(3)
b (A)	12.154(4)	18.322(3)	18.351(5)
c (A)	10.403(4)	11.369(1)	11.413(3)
α (deg)	90.07(3)	90.0	90.0
β (deg)	104.61(3)	91.83(1)	90.0
γ (deg)	71.33(2)	90.0	90.0
V (A^3)	1361.8(7)	2654.1(8)	2662(1)
Z	2	4	4
V/Z (A^3/molecule)	680.9	663.5	665.5

[a]Reference 4.

Table 10. Final positional parameters[a] and thermal parameters for the monoclinic and orthorhombic crystals of $Mo_2(piv)_4$

Monoclinic crystal	x	y	z
Mo	0.53843(3)	0.49597(3)	0.42058(4)
O(1)	0.5224(4)	0.3823(3)	0.4180(4)
O(2)	0.5991(4)	0.6096(3)	0.4133(4)
O(3)	0.3143(4)	0.5108(2)	0.4903(4)
O(4)	0.3943(3)	0.4979(2)	0.8199(4)
C(1)	0.3112(5)	0.50716(3)	0.3802(6)
C(2)	0.2055(5)	0.5073(3)	0.3141(6)
C(3)	0.1940(6)	0.4353(4)	0.2431(7)
C(4)	0.2014(6)	0.5736(4)	0.2297(7)
C(5)	0.1167(6)	0.5132(5)	0.4012(8)
C(6)	0.4731(6)	0.3534(4)	0.5000(6)
C(7)	0.452(1)	0.2734(5)	0.499(1)
C(8)	0.545(1)	0.230(1)	0.480(1)
C(9)	0.367(2)	0.265(1)	0.387(2)
C(10)	0.375(1)	0.2521(9)	0.592(2)

Orthorhombic crystal	x	y	z
Mo	0.53930(5)	0.49561(3)	0.57995(6)
O(1)	0.5255(4)	0.3818(3)	0.5801(6)
O(2)	0.5992(4)	0.6091(3)	0.5899(6)
O(3)	0.3138(4)	0.5098(3)	0.5055(5)
O(4)	0.3950(4)	0.5002(3)	0.6764(5)
C(1)	0.3112(6)	0.5051(4)	0.6156(8)
C(2)	0.2066(7)	0.5049(5)	0.6780(8)
C(3)	0.1961(7)	0.4341(5)	0.750(1)
C(4)	0.2019(7)	0.5727(6)	0.760(1)
C(5)	0.1172(8)	0.5103(7)	0.5882(9)
C(6)	0.4764(6)	0.3531(5)	0.4954(9)
C(7)	0.452(1)	0.2733(7)	0.499(1)
C(8)	0.541(2)	0.228(1)	0.521(2)
C(9)	0.366(2)	0.267(1)	0.606(2)
C(10)	0.380(2)	0.251(1)	0.401(2)

[a]Given in fractional coordinates.

B_{11}	B_{22}	B_{33}	B_{12}	B_{13}	B_{23}
2.68(3)	4.96(4)	2.20(3)	-0.26(2)	-0.07(2)	-0.12(2)
4.4(2)	5.2(2)	3.8(2)	-0.0(2)	0.3(2)	-0.8(2)
4.3(2)	5.0(2)	3.7(2)	-0.5(2)	0.2(2)	0.7(2)
2.9(2)	5.4(2)	2.7(2)	-0.1(1)	-0.1(2)	-0.2(1)
2.8(2)	5.4(2)	2.7(2)	0.2(1)	-0.1(2)	-0.1(1)
2.8(3)	4.9(3)	3.2(3)	-0.1(2)	-0.1(2)	0.0(2)
3.1(2)	6.5(4)	2.6(3)	0.0(2)	-0.4(2)	0.1(2)
5.2(4)	6.4(4)	4.7(4)	-1.4(3)	-1.1(3)	-0.8(3)
5.0(4)	6.4(4)	3.9(3)	1.1(3)	-0.2(3)	0.9(3)
3.2(3)	10.7(6)	4.1(4)	0.1(3)	0.1(3)	0.1(3)
4.6(3)	5.3(4)	4.5(4)	-0.0(3)	0.0(3)	-0.0(3)
10.0(7)	5.6(5)	9.4(7)	0.3(5)	2.5(5)	0.5(4)
14.2(5)	0.0	0.0	0.0	0.0	0.0
17.3(6)	0.0	0.0	0.0	0.0	0.0
15.5	0.0	0.0	0.0	0.0	0.0

B_{11}	B_{22}	B_{33}	B_{12}	B_{13}	B_{23}
2.38(3)	4.69(4)	2.80(4)	-0.30(3)	-0.13(3)	0.22(3)
3.7(3)	4.80(3)	4.6(3)	0.0(2)	-0.3(3)	0.9(3)
3.3(3)	5.1(3)	4.4(3)	-0.3(2)	0.0(2)	-0.5(3)
2.3(2)	5.8(3)	3.0(3)	-0.3(2)	-0.0(2)	0.1(2)
2.7(2)	5.3(3)	2.9(2)	0.0(2)	-0.0(2)	-0.0(2)
2.4(3)	4.0(4)	3.5(4)	-0.1(3)	-0.3(3)	-0.8(3)
2.6(3)	6.6(5)	3.4(4)	-0.4(4)	0.1(3)	0.5(4)
4.7(5)	6.3(5)	4.9(6)	-1.2(4)	1.1(4)	0.1(5)
4.2(5)	7.3(6)	4.8(6)	1.1(4)	0.5(4)	-0.9(5)
2.5(4)	13(1)	4.6(5)	-0.3(5)	-0.5(4)	0.3(6)
3.1(4)	4.7(4)	5.3(5)	-0.1(3)	0.3(5)	0.1(4)
8.8(8)	5.8(6)	10(1)	0.6(6)	-1.9(8)	-0.3(6)
14.6(7)	0.0	0.0	0.0	0.0	0.0
16.1(7)	0.0	0.0	0.0	0.0	0.0
13.9(6)	0.0	0.0	0.0	0.0	0.0

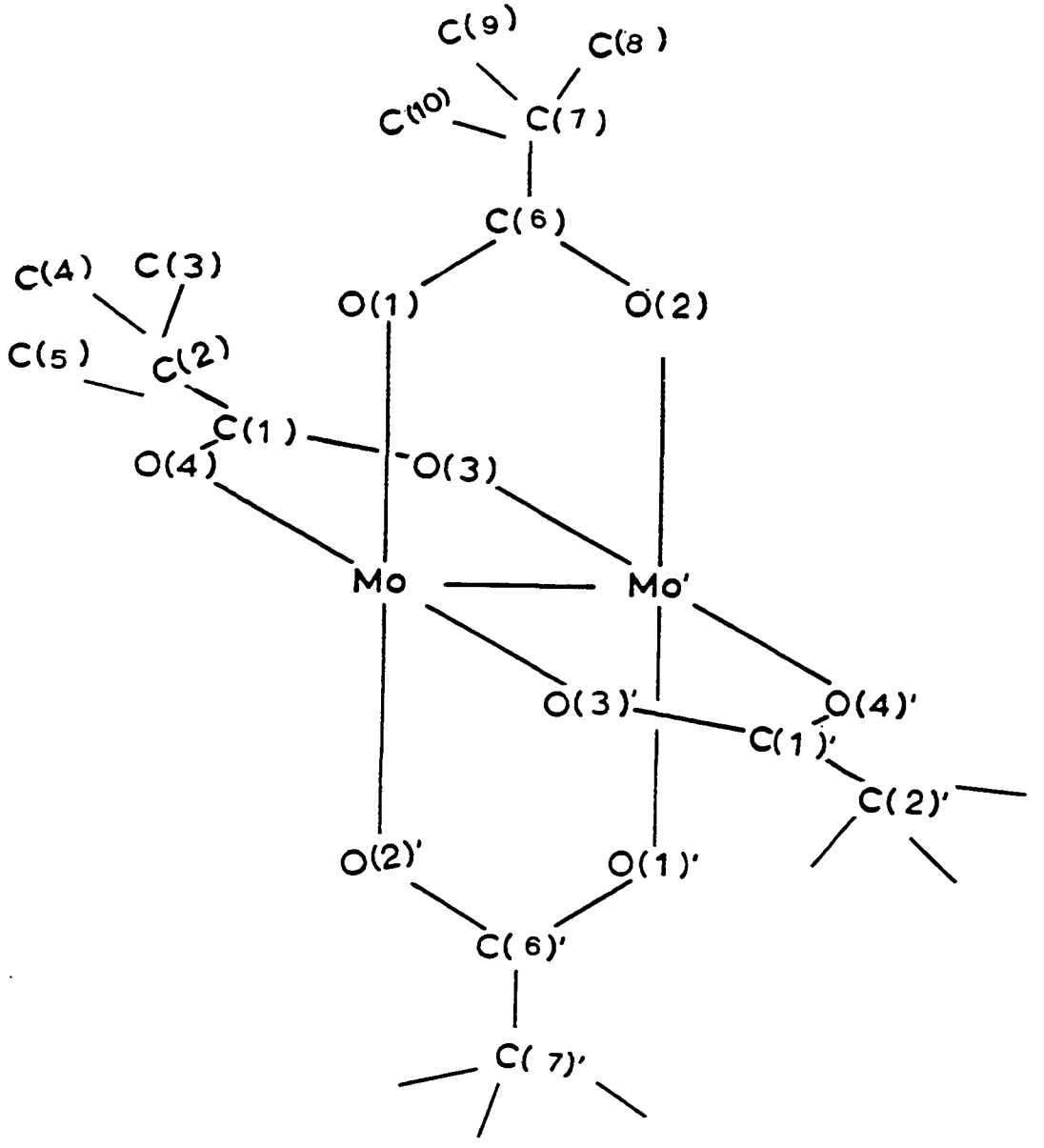

Figure 8. Atom labelling system used in the structure solution of the monoclinic and orthorhombic crystals of $Mo_2(piv)_4$

in the unit and primitive cell for Cotton et al.'s triclinic structure (4). Note in Table 9 that the two polymorphs have the c-axis dimension which is about 11.4 A in length. Each half-axis distance is a molecular stacking axis in that particular polymorph for weakly bonded one-dimensional chains. In addition to bonding with oxygens on four bridging carboxylates, each Mo atom is involved in weak axial coordination to an oxygen O(4) from an adjacent molecule. This intermolecular interaction produces chains of molecules, as depicted in Figure 9 (58). The two polymorphs have this same basic stacking arrangement. Note that all twin bonds (intermolecular bonds) in a chain lie essentially in a single plane. This type of chain structure with twin bonds between the molecules has been found in all determined structures for molybdenum(II) carboxylates with single exception of Cotton et al.'s triclinic dimolybdenum tetrapivalate. In that case, the two oxygens at opposite ends of a molecule lie in cis- rather than trans-chelate rings. An ORTEP drawing viewed along the stacking axis (showing one layer of molecules) is presented for the monoclinic and orthorhombic systems, respectively, in Figures 10 and 11. In this view, each molecule shown represents one chain. The figures are drawn to the same scale for comparison. Both structures have the same nearly close packing. If a one-dimensional chain is considered a

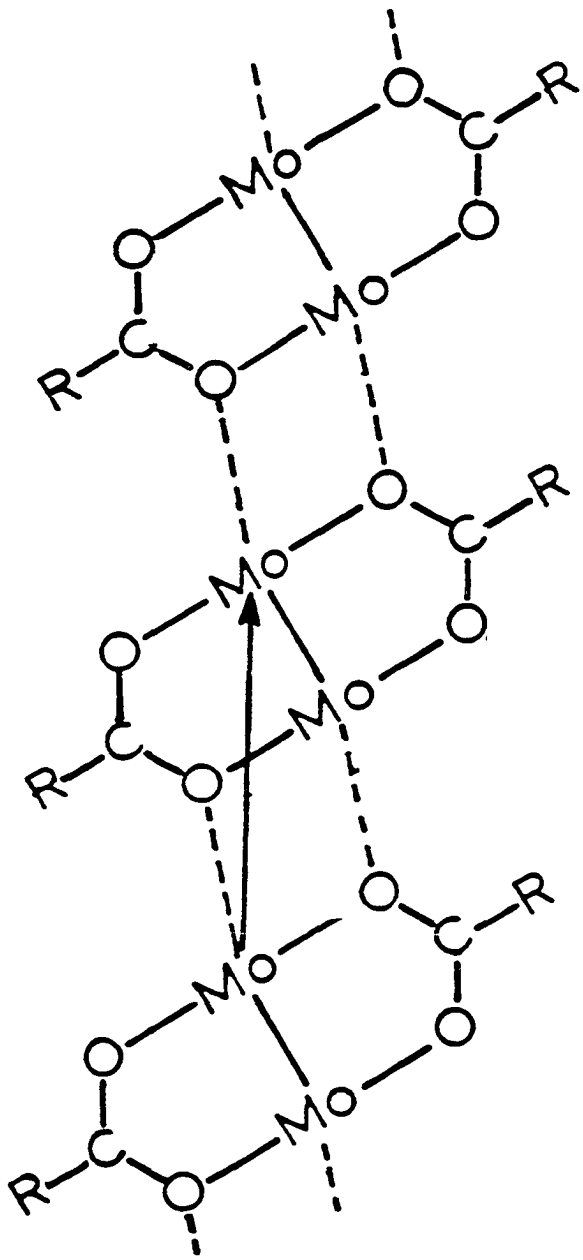

Figure 9. Intermolecular bonding in dimolybdenum tetracarboxylate complexes

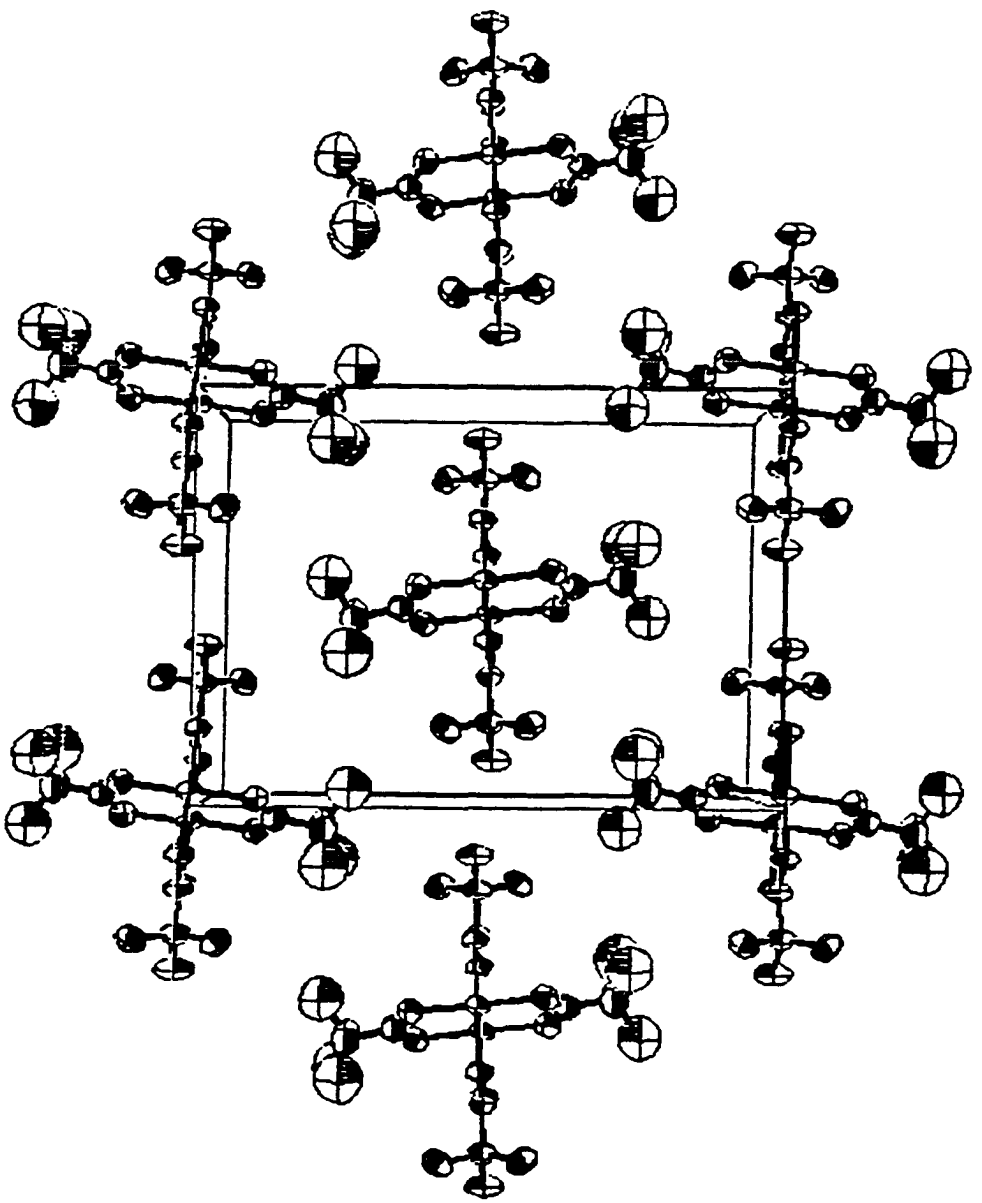

Figure 10. The molecular structure of the monoclinic crystal of $Mo_2(piv)_4$

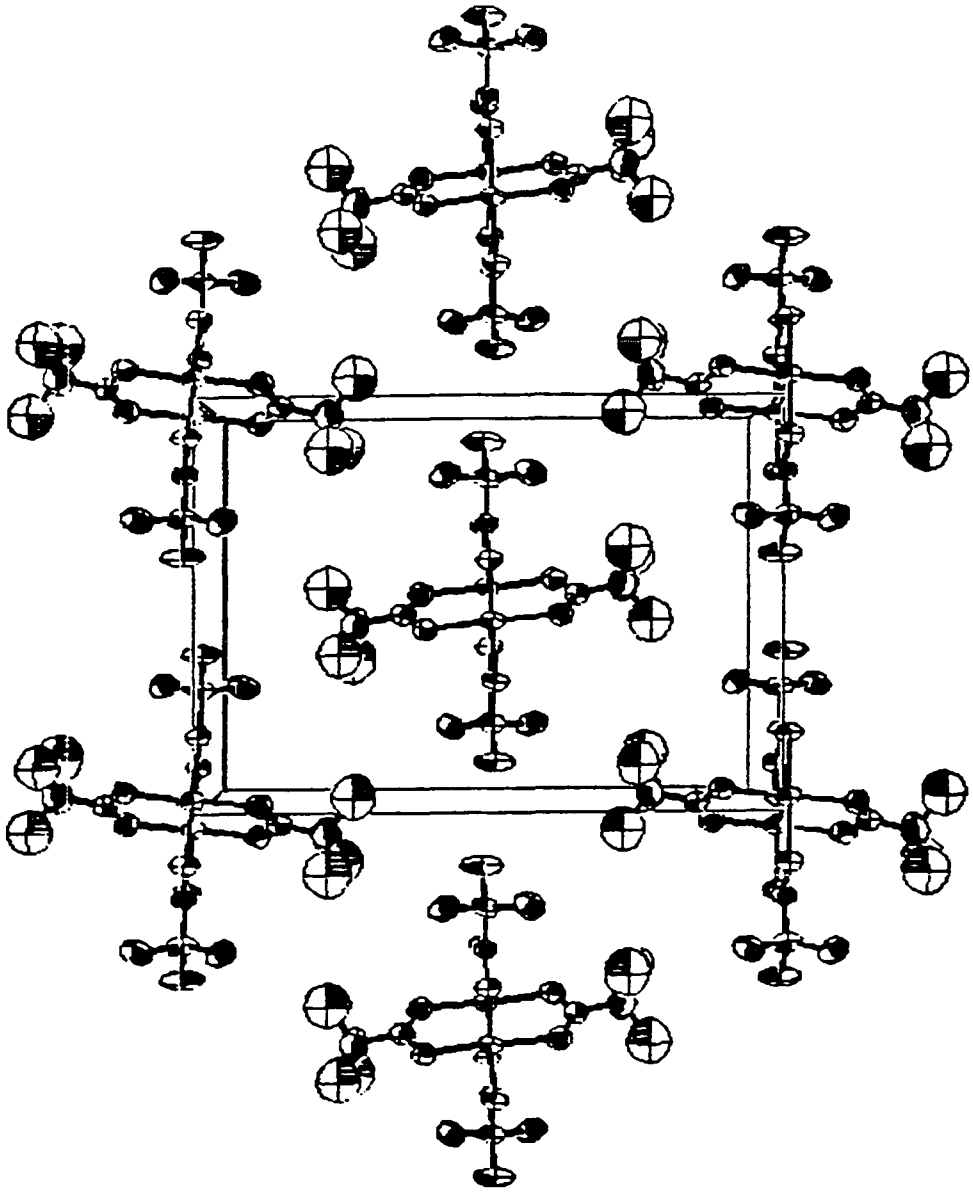

Figure 11. The molecular structure of the orthorhombic crystal of $Mo_2(piv)_4$

rod, then each rod was surrounded by six other rods. It is difficult to see any difference between Figures 10 and 11. However, the difference between structures is clearly apparent in Figures 12 and 13. In each of these figures, three molecules from two different chains are plotted as viewed from the b axis. The upper chain passes through the center of the cell, and the lower chain in each figure passes along the edge of the cell formed by the c axis. The molecules in the chains of the orthorhombic system form a herring-bone pattern. For the monoclinic system, molecules in the chains form the parallel pattern. The orthorhombic structure with the herring-bone arrangement has a slightly less efficient packing of molecules that is indicated by the larger molecular volume than the monoclinic structure with the parallel arrangement. However, triclinic structure possesses the least effective packing arrangement among these three polymorphs.

For comparison of distances and angles, two values will be considered significantly different if their difference is greater than or equal to 3σ(difference). The important interatomic distances and angles are listed in Table 11 for monoclinic crystal and in Table 12 for the orthorhombic crystal.

All types of dimeric carboxylates containing quadruple bonds evidently have some inherent capability to bind

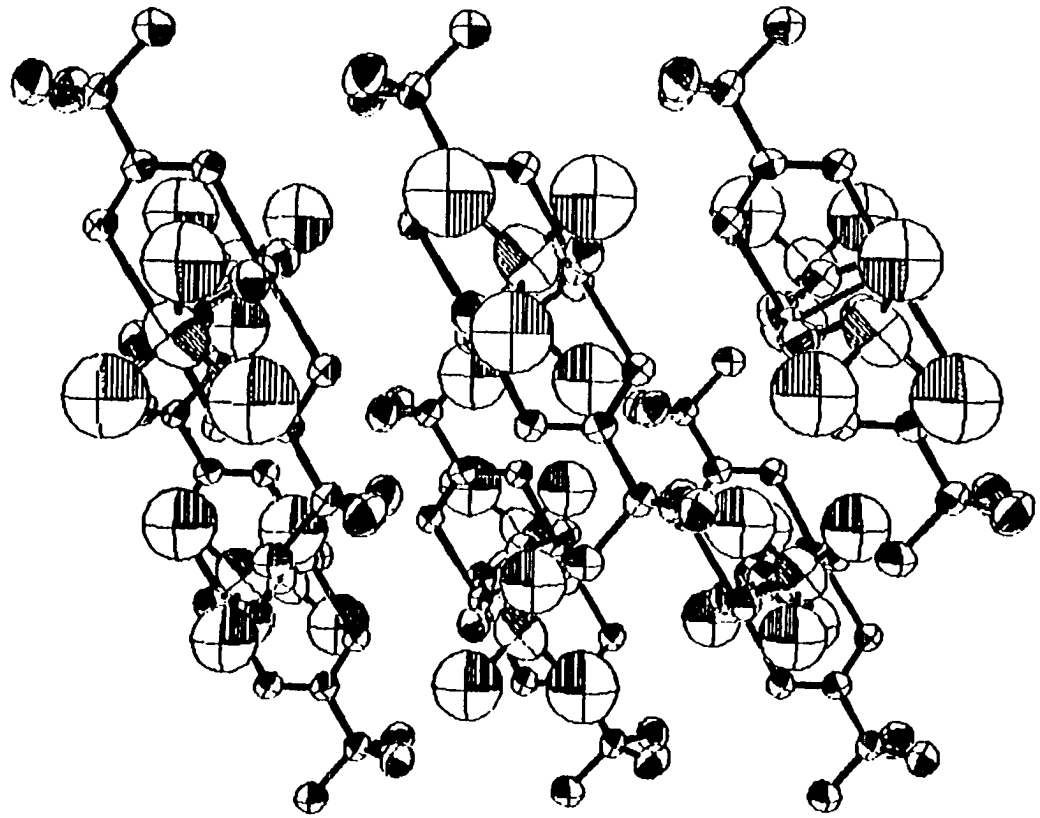

Figure 12. The molecular structure of the monoclinic crystal of $Mo_2(piv)_4$

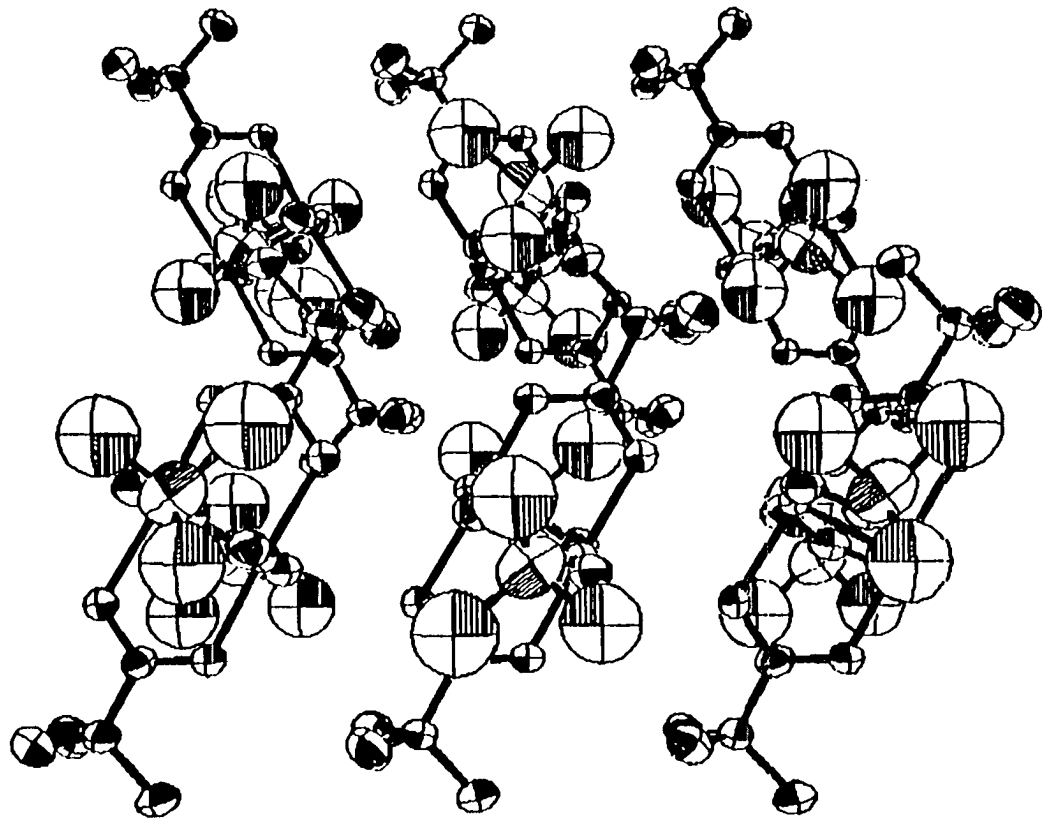

Figure 13. The molecular structure of the orthorhombic crystal of $Mo_2(piv)_4$

Table 11. Interatomic distances and angles and their estimated standard deviations[a] for the monoclinic crystal of $Mo_2(piv)_4$

	Distances, A		
Mo'-Mo	2.087(1)	C(1)-C(2)	1.52(1)
Mo-O(1)	2.092(5)	C(2)-C(3)	1.55(1)
Mo-O(2)	2.100(5)	C(2)-C(4)	1.55(1)
Mo-O(3)	2.107(5)	C(2)-C(5)	1.53(1)
Mo-O(4)	2.136(5)	C(6)-C(7)	1.49(1)
Mo-O(4) (axial)	2.894(5)	C(7)-C(8)	1.45(2)
Mo-O(4)' (axial)	3.046(5)	C(7)-C(9)	1.65(2)
O(1)-C(6)	1.257(9)	C(7)-C(10)	1.52(2)
O(2)-C(6)	1.276(9)		
O(3)-C(1)	1.254(8)		
O(4)-C(1)	1.283(8)		
	Angles, degrees		
Mo'-Mo-O(1)	92.0(1)	C(3)-C(2)-C(4)	110.1(6)
-O(2)	91.5(1)	C(3)-C(2)-C(5)	109.7(6)
-O(3)	91.4(1)	C(4)-C(2)-C(5)	109.5(6)
-O(4)	92.3(1)	C(8)-C(7)-C(9)	111(1)
Mo'-Mo-O(4) (axial)	167.5(1)	C(8)-C(7)-C(10)	121(1)
O(1)-Mo-O(3)	90.0(1)	C(9)-C(7)-C(10)	95(1)
O(2)-Mo-O(4)	92.0(1)		
O(1)-C(6)-O(2)	122.0(7)		
O(3)-C(1)-O(4)	122.5(6)		

[a]Given in parentheses for the least significant figure.

Table 12. Interatomic distances and angles and their estimated standard deviations[a] for the orthorhombic crystal of $Mo_2(piv)_4$

	Distances, Å		
Mo'-Mo	2.087(1)	C(1)-C(2)	1.51(1)
Mo-O(1)	2.095(6)	C(2)-C(3)	1.54(1)
Mo-O(2)	2.101(6)	C(2)-C(4)	1.56(1)
Mo-O(3)	2.109(5)	C(2)-C(5)	1.53(1)
Mo-O(4)	2.141(5)	C(6)-C(7)	1.50(1)
Mo-O(4) (axial)	2.905(5)	C(7)-C(8)	1.43(3)
Mo-O(4)' (axial)	3.044(5)	C(7)-C(9)	1.65(3)
O(1)-C(6)	1.27(1)	C(7)-C(10)	1.50(3)
O(2)-C(6)	1.28(1)		
O(3)-C(1)	1.26(1)		
O(4)-C(1)	1.28(1)		

	Angles, degrees		
Mo'-Mo-O(1)	92.2(2)	C(3)-C(2)-C(4)	110.4(8)
-O(2)	91.6(2)	C(3)-C(2)-C(5)	110.3(8)
-O(3)	91.3(2)	C(4)-C(2)-C(5)	108.7(8)
-O(4)	92.1(2)	C(8)-C(7)-C(9)	110(1)
Mo'-Mo-O(4) (axial)	166.6(1)	C(8)-C(7)-C(10)	117(1)
O(1)-Mo-O(3)	90.4(2)	C(9)-C(7)-C(10)	97(1)
O(2)-Mo-O(4)	89.6(2)		
O(1)-C(6)-O(2)	122.0(9)		
O(3)-C(1)-O(4)	121.7(7)		

[a]Given in parentheses for the least significant figure.

ligands trans to the metal-metal bond, i.e., in their axial positions. The strength of such bonding varies greatly. A long Mo-O(4) bond length (ca. 2.14 A) is found relative to the corresponding values observed for another oxygen atom (ca. 2.10 A) as shown in Tables 11 and 12. In each system, the Mo-O(b) distances are about 0.04 A longer than the Mo-O(nb) one. These differences are statistically significant. The Mo-Mo-O angles for O(4) are not significantly different from other oxygen atoms. In the monoclinic crystal, two axial contact distances are 2.894(5) and 3.046(5) A, and in the orthorhombic crystal 2.905(5) and 3.044(5) A. By comparison, in Cotton et al.'s $P\bar{1}$ crystals (4), the axial contacts are at distances of 2.870(5) and 2.926(5) A. The axial interaction involves the d_{z^2}-p_z hybrid orbital of the metal which has maximum value 180^0 from the metal-metal bond and the sp^2 hybrid orbital on the oxygen. These two orbitals will have maximum overlap, when Mo-Mo-O bond angles is somewhat less than 180^0. Figure 14 illustrates the axial interaction involving these Mo and O orbitals.

The interatomic distances and angles are essentially the same for the two polymorphs. The $Mo_2(piv)_4$ molecules for the two polymorphs have $\bar{1}$ site symmetry and deviate slightly from the local D_{4h} symmetry due to adjacent molecular interaction. The data of the Mo···O bond length

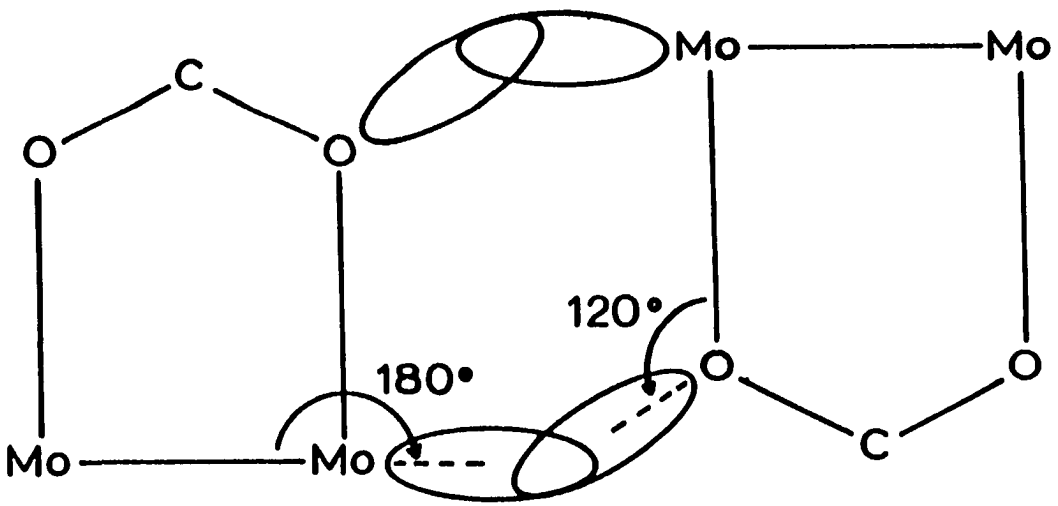

Figure 14. Diagram of the Mo-O axial interaction showing orbital geometries

suggest the Mo···O bond is the stronger in the Cotton et al.'s $P\bar{1}$ system than in the other two polymorphs, but the Mo-Mo bond length is essentially the same for the three polymorphs.

Crystal Spectra

$[N(n\text{-}C_4H_9)_4]_2Re_2Cl_8$

The $[Re_2Cl_8]^{2-}$ ion was the first example to have a demonstrated quadruple bond of any kind. It is important to understand the relatively recent and rare electronic structure. The orientation of the electric vector of the two plane-polarized light waves transmitted for the 100 face will be along the b-axis (b-polarization) and along the c-axis (c-polarization). Scans of the complete 14500cm^{-1}-band for a crystal 2.2 μm thick at 300 and 6 K for the b- and c-polarizations are shown in Figure 15. A plot of the 6 K spectra with an extended wavenumber scale revealed striking detail and is shown in Figure 16.

The relative intensities of absorptions have been calculated from the oriented molecule model. Under D_{4h} symmetry, an absorption feature will have either molecular z-polarization or molecular x, y-polarizations for two degenerate transitions. The z-axis lies along the metal-metal bond.

For convenience, all vector calculations were performed

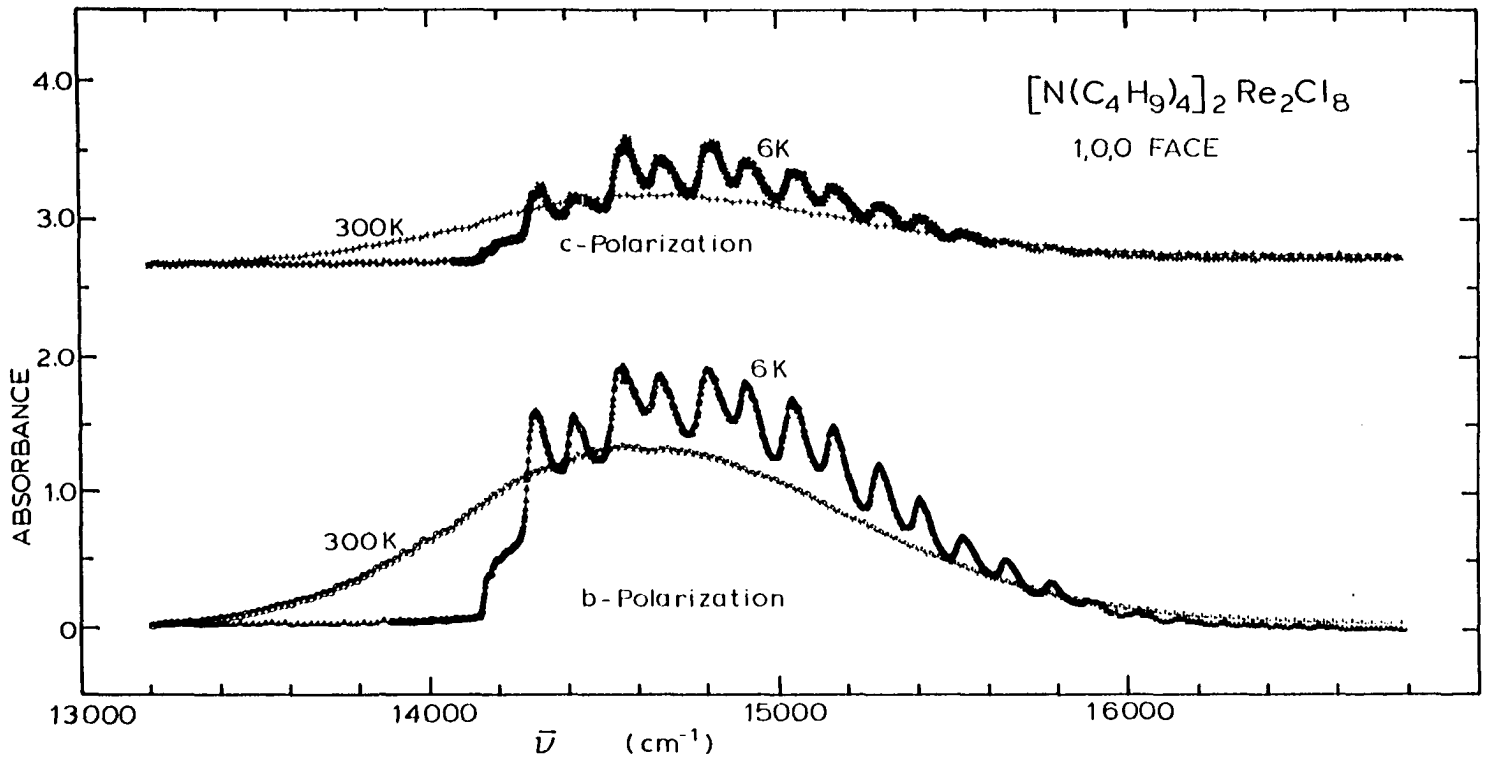

Figure 15. Polarized spectra of the entire band for a crystal of $(TBA)_2Re_2Cl_8$ that was 2.2 μm thick at 300 and 6 K

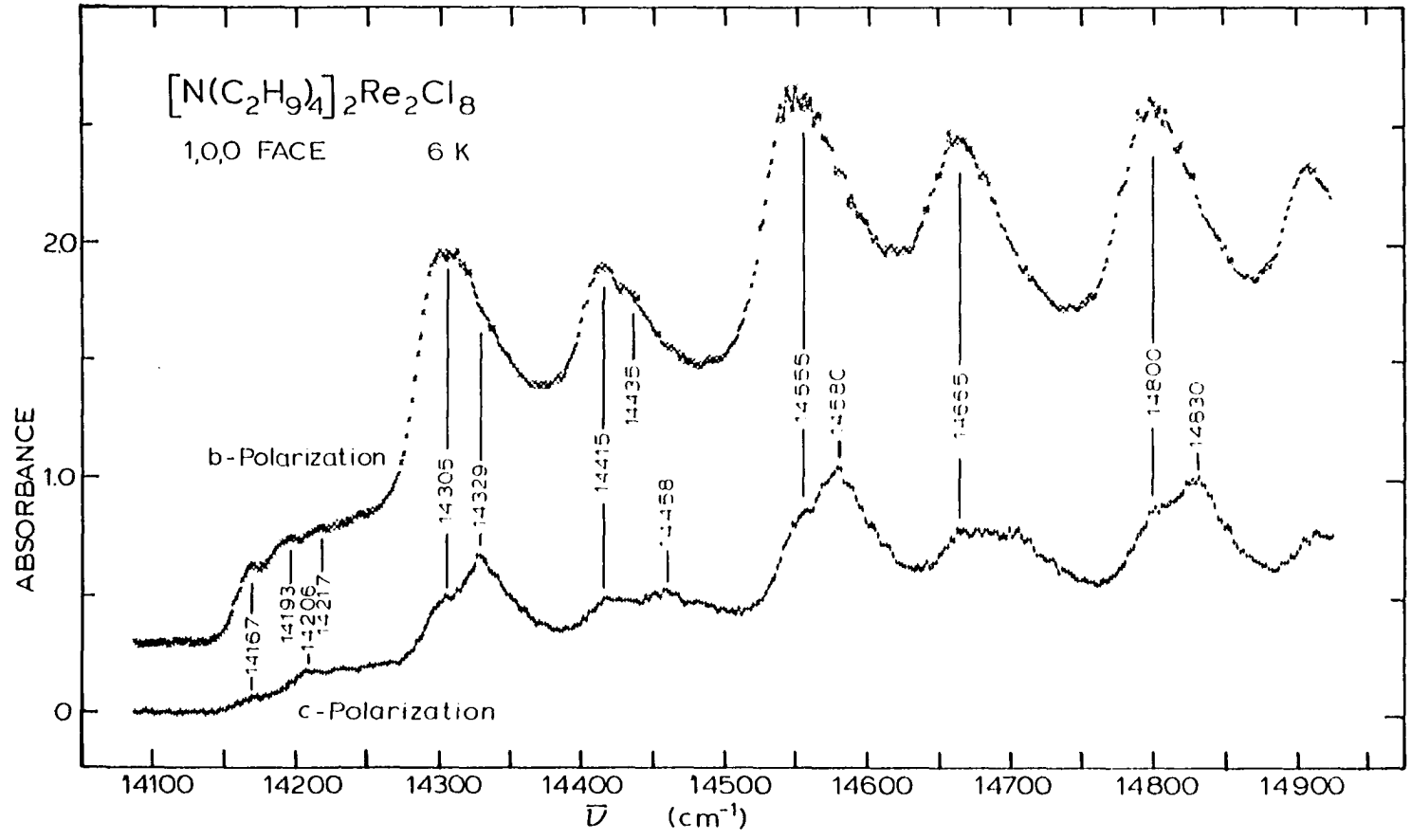

Figure 16. Polarized spectra in the low-energy region with an extended wavenumber scale for a crystal of $(TBA)_2Re_2Cl_8$ that was 2.2 μm thick at 6 K

in an orthogonal coordinate system with unit vectors, i.e., $\hat{i}$, $\hat{j}$, and $\hat{k}$. The following expressions relate the crystallographic coordinates to an orthogonal system:

$$\hat{a} = 0.84554\hat{i} - 0.53391\hat{k}$$

$$\hat{b} = \hat{j}$$

$$\hat{c} = \hat{k}$$

The observed extinctions were represented by the following vectors:

$$\hat{Ex}_1 = \hat{b} = \hat{j}$$

$$\hat{Ex}_2 = \hat{c} = \hat{k}$$

The $\hat{z}$ for the major site (1) and minor site (2) cases are listed below:

$$\hat{z}_1 = -0.18321\hat{i} + 0.87654\hat{j} + 0.44509\hat{k}$$

$$\hat{z}_2 = -0.85890\hat{i} + 0.06303\hat{j} - 0.50825\hat{k}$$

The following results were obtained from the unit dot products of the $\hat{z}_1$ and $\hat{z}_2$ molecular axes with the extinction vectors:

$$\hat{z}_1 \cdot \hat{Ex}_1 = 0.87656 = \cos\theta_{1,b} = \cos 28.77^\circ$$

$$\hat{z}_1 \cdot \hat{Ex}_2 = 0.44510 = \cos\theta_{1,c} = \cos 63.57^\circ$$

$$\hat{z}_2 \cdot \hat{Ex}_1 = 0.06296 = \cos\theta_{2,b} = \cos 86.39^\circ$$

$$\hat{z}_2 \cdot \hat{Ex}_2 = 0.50829 = \cos\theta_{2,c} = \cos 59.45^\circ$$

The intensity of absorption for a unit molecular z-polarization transition with the major $Re_2Cl_8^{2-}$ orientation appearing in b polarization is $0.739\cos^2\theta_{1,b} = 0.567$ and appearing in c polarization is $0.739\cos^2\theta_{1,c} = 0.143$. The expected polarization ratio, $(I_b/I_c)_{1,z}$ is 3.88.

The intensity from the two x- and y-polarized unit transitions appearing in b polarization is $0.739\sin^2\theta_{1,b}$ = 0.171 and appearing in c polarization is $0.739\sin^2\theta_{1,c}$ = 0.590 with the polarization ratio, $(I_b/I_c)_{1,xy}$ = 0.289.

Thus, the b-axis intensity for a z-polarized transition of the minor $Re_2Cl_8^{2-}$ is $0.261\cos^2\theta_{2,b}$ = 0.0010, and the c-axis intensity is $0.261\cos^2\theta_{2,c}$ = 0.0674 with the polarization ratio of $(I_b/I_c)_{2,z}$ =0.015. For x, y-polarized transitions, the b-axis intensity is calculated from $0.261\sin^2\theta_{2,b}$ =0.260 and the c-axis intensity from $0.261\sin^2\theta_{2,c}$ = 0.194 with the polarization ratio $(I_b/I_c)_{2,xy}$ = 1.34. The above calculated values can only serve as guides rather than precise predictions because of crystal field perturbations which may lower the site symmetry from D_{4h}. A relative minor crystal field might alter the polarization by moving the transition moment of a molecular z-polarized transition away from the metal-metal bond. A major perturbation might break the degeneracy of the two x, y transitions to give two bands with very different intensities and polarization ratios.

The first absorption band is predicted from Xα-SW calculations (37) to be the $\delta \rightarrow \delta^*$ transition, $^1A_{1g} \rightarrow {}^1A_{2u}$, which will have z polarization. Cotton et al. were the first to use structural data and the equations which were modified from Piper's equations (46). They concluded from

the overall band intensity polarization that the ca. 700nm transition of $Re_2Cl_8^{2-}$ is z-polarized.

In Figure 15, it can be seen that although the band has sharpened and vibrational structure appeared in low-temperature spectra, the integrated intensity of the band is virtually identical at the two temperatures. This feature indicates an electric dipole-allowed transition. The relative intensities of the general features are in very good agreement with those of Cowman and Gray (8). The spectrum shown in Figure 16 indicates the component at 14,167 cm^{-1} is the lowest energy feature. This is followed by a rather broad region of absorption in which at least two weak maxima can be discerned in each polarization. This absorption lies on a rising absorption associated with much more intense features at 14,305 cm^{-1} and followed by another intense feature at 14,329 cm^{-1}. It is noted that at 14,415 cm^{-1} in each polarization, just 248 cm^{-1} above the first feature, there is a sharp peak followed by a broad area of absorption in each polarization. The average 249 (2) cm^{-1} occurs between all successive major elements in Franck-Condon progression in the band. Only one of the three totally symmetric vibrations of the anion gives the excited Franck-Condon lines. This vibration is generally considered to be the metal-metal stretching vibration for these dimeric complexes. The Raman spectra for $(TBA)_2Re_2Cl_8$ places this

vibration at 271.9 cm^{-1} in the ground electronic state (59). The lower value in the excited electronic state is consistent with a weaker metal-metal bond that would occur with $\delta \rightarrow \delta^*$ excitation. Such detailed features, less well-resolved but still recognizable, are in the peak 14,650-14,770 cm^{-1}. Therefore, it is concluded that the feature at 14,150-14,270 cm^{-1} is really the origin of the long progression that continues 14,440-14,520, 14,650-14,770 cm^{-1}, etc. The difference in the shape of the first feature arises from the fact that it lies on the rising absorption of the major component at 14,305 cm^{-1} whereas the later members of the progression each lie between much more intense components. The polarization ratio of the members of this progression, I_b/I_c, can be estimated to be about 3 with considerably uncertainty. This might be considered consistent with a z-polarized absorption of the major component. However, at 14,206 cm^{-1}, there is clearly a weak maximum in c polarization just where there is a minimum in b-polarization. Hence, there is probably a contribution from the minor component with z-polarization.

In b-polarization, there is the intense peak at 14,305 cm^{-1} with subsequent members of a Franck-Condon progression spacing 249 $\pm$ 2 cm^{-1}. However, in c-polarization, a rather sharp maximum is at 14,329 cm^{-1}, 24 cm^{-1} higher than the b-polarization peak; and there is clearly a shoulder at 14,305

cm^{-1}. There is no discernible component at 14,329 cm^{-1} in b-polarization. The observed polarization ratio at 14,305 cm^{-1} is estimated to be 3.3. Therefore, it is proposed that 14,305 cm^{-1} is the origin of a z-polarized progression for the major component, whereas 14,329 cm^{-1} is the origin for the minor component. The predicted c-polarized relative intensity for the unit transition moment is 0.146 on the major site, whereas it is 0.067 on the minor site. However the 14,329 cm^{-1} feature appears somewhat sharper than the 14,305 cm^{-1} band, and the higher peak at 14,329 cm^{-1} may be a consequence of a smaller width even though its integrated intensity is lower. The feature of a shoulder on a narrow peak is evident in the higher members of the Franck-Condon progression as well. The progressions with origins at 14,305 and 14,329 cm^{-1} therefore are consistent with the spin-allowed $\delta \rightarrow \delta^*$ transition, i.e., electric dipole allowed, z-polarized for the major and minor sites, respectively, indicated in the crystal structure and with a site splitting of 24 cm^{-1}.

The source of the additional progression based on the broad, multiple-component origin, 14,150-14,270 cm^{-1}, is not evident from the crystal structure. It is proposed that it arises from additional disorder in the crystal. The intensity of peaks at 14,150-14,270 cm^{-1} appears to be 20-30% of the more intense peak at 14,270-14,350 cm^{-1}. It is

disturbing that no such alternative disorder was evident from the crystal structure where the refinement produced an R of 0.042 (9). Since the site difference with the alternative metal-metal bond orientation shifted the origin by only 24 cm^{-1}, the shift of up to 138 cm^{-1} indicates a much larger crystal field shift. It is possible that a different orientation of parts of the cations at low temperature cause the large shift by significant electrostatic effects on the Re orbitals. The breadth and complexity of the origin indicate that there are a number of different disordered perturbations. But, none were identified in the averaging by the X-ray diffraction at room temperature.

Cowman and Gray (8) suggested vibrational assignments for this first band for $(TBA)_2Re_2Cl_8$. The lowest energy component of the band was quite weak, and they assigned it as the 0-0 line, which with their low resolution they placed at 14183 cm^{-1}. There was then one strong progression based on higher origin. The two progressions had the same spacing. They assigned the spacing of the two progressions, $\bar{\nu}_2$, to the totally symmetric metal-metal stretching frequency. Since this was a dipole-allowed transition, the distances of the origin of the progression above the 0-0 energy was assigned to $\bar{\nu}_3$, the other totally symmetric vibration of the $Re_2Cl_8^{2-}$ ions, viz., the Re-Re-Cl bends.

Such an assignment requires that the $\nu = 1$ vibrational line of the $\bar{\nu}_3$ (14298 cm^{-1}) Franck-Condon progression is much more intense than all the other members of the progressions. This pattern of Franck-Condon progression is not logical.

Trogler et al. (42) and Bursten et al. (37) described a very weak absorption, designated by them as band I, in $(TBA)_2Re_2Cl_8$ in the vicinity of 16,000-18,500 cm^{-1}. This absorption, above the $\delta \rightarrow \delta^*$ transition, had well-resolved vibrational structure for which Bursten et al. tabulated wavenumbers for four Franck-Condon progressions. The four progressions were based on progression separations of 225 $\pm$ 10 cm^{-1}, somewhat lower than the separation for the $\delta \rightarrow \delta^*$ band. These low values indicate an especially weak metal-metal bond in the excited state. They concluded that progressions a, c, and d are z-polarized while progression b is x, y-polarized. In addition, there are several peaks that remained unassigned. Since the origin of their fourth progression, designated d, was 1687 cm^{-1} above the first origin, they proposed that both the $\pi \rightarrow \delta^*$ ($^1A_{1g} \rightarrow {}^1E_g$) and $\delta \rightarrow \pi^*$ ($^1A_{1g} \rightarrow {}^1E_g$) transitions are contained in this band. The band obtained in this research were similar to theirs. The spectroscopic face is 100 which is different from their 110 face. This probably accounts for the fact that the b:c peak height ratio was about 4.0 whereas their $\perp$c:c ratio was

reported as 2.6. The origins of the b, c, and d progression lie 280, 380, and 1680 cm^{-1} above the a-origin, respectively. It does not seem possible to assign the c, d and perhaps the b to different vibronic origins for the same transition. These wavenumbers would presumably have to represent the difference in frequencies for two vibrations of $Re_2Cl_8^{2-}$ and the highest frequencies observed in Raman and IR spectra for the ground state are 356.5 and 346 cm^{-1}. Hence, the b, c, and d progressions alternatively might originate from either different sites or different transitions.

$[N(n\text{-}C_4H_9)_4]_2Re_2Br_8$

A search of the crystals of $(TBA)_2Re_2Br_8$ failed to locate any as thin as those which were available for $(TBA)_2Re_2Cl_8$. Polarized spectra for the thinnest spectroscopic crystal (3.4 μm thick) are shown in Figure 17. Even so, the intensity of the band was so great that it was not possible to scan over the highest peaks for b-polarization. The spectroscopic face was identified from the diffractometer angles as the $10\bar{1}$ face for the $P2_1/n$ cell. This is the same face indicated in the $P2_1/c$ space group that was found for $(TBA)_2Re_2Cl_8$ crystals. One optical extinction is required to be parallel to the b axis and the other perpendicular to the b axis. Since this latter

direction is not that of the crystallographic c axis, these two crystal polarizations for the spectra are designated as the b and $\perp$b.

The following expressions relate the crystallographic coordinates to an orthogonal system:

$$\hat{a} = 0.99236\hat{i} - 0.12339\hat{k}$$

$$\hat{b} = \hat{j}$$

$$\hat{c} = \hat{k}$$

The observed extinctions were given by:

$$\hat{Ex}_1 = \hat{b} = \hat{j}$$

$$\hat{Ex}_2 = \perp b = 0.82849\hat{i} + 0.55999\hat{k}$$

The $\hat{z}$ unit vector represented a z-polarized transition moment vector for the major site (1) and minor site (2). These are listed below:

$$\hat{z}_1 = 0.30137\hat{i} - 0.87070\hat{j} + 0.38860\hat{k}$$

$$\hat{z}_2 = 0.87840\hat{i} + 0.08125\hat{j} - 0.47094\hat{k}$$

The following results were obtained from dot products of $\hat{z}$ unit vectors with the extinction vectors:

$$\hat{z}_1 \cdot \hat{Ex}_1 = -0.87066 = \cos\theta_{1,b} = \cos 29.47^\circ$$

$$\hat{z}_1 \cdot \hat{Ex}_2 = 0.46744 = \cos\theta_{1,\perp b} = \cos 62.13^\circ$$

$$\hat{z}_2 \cdot \hat{Ex}_1 = 0.08124 = \cos\theta_{2,b} = \cos 85.34^\circ$$

$$\hat{z}_2 \cdot \hat{Ex}_2 = 0.46377 = \cos\theta_{2,\perp b} = \cos 62.37^\circ$$

The predicted intensity of a unit molecular z-polarized transition for the major $Re_2Br_8^{2-}$ orientation appearing in b-polarization is $0.621\cos^2\theta_{1,b} = 0.471$ and appearing in $\perp$b

polarization is $0.621\cos^2\theta_{1,\perp b}$ =0.136. The predicted polarization ratio is $(I_b/I_{\perp b})_{1,z}$ = 3.46. The intensity from the two x, y-polarized unit transitions appearing in b polarization is $0.621\sin^2\theta_{1,b}$ = 0.150 and appearing in $\perp$b polarization is $0.621\sin^2\theta_{1,\perp b}$ = 0.485 with the polarization ratio $(I_b/I_\perp)_{1,xy}$ =0.309. For z polarization, the b-axis intensity for the minor $Re_2Br_8^{2-}$ orientation is $0.379\cos^2\theta_{2,b}$ =0.0025, and the $\perp$b intensity is $0.379\cos^2\theta_{2,\perp b}$ = 0.0185 with the polarization ratio $(I_b/I_{\perp b})_{2,z}$ = 0.031. For the x, y-polarization, the b intensity is calculated from $0.379\sin^2\theta_{2,b}$ =0.376 and the $\perp$b intensity from $0.379\sin^2\theta_{2,\perp b}$ =0.297 with the predicted polarization ratio, $(I_b/I_{\perp b})_{2,xy}$ = 1.28.

Polarized spectra in the low-energy region were shown in Figure 17. In the $\perp$b-polarization, four members of two strong progressions are clearly resolved with origins at 13,720 and 13,790 cm^{-1}, respectively, a splitting of 70 cm^{-1}. Only the first member of each progression was observable in b-polarization. The b-polarized component at 13,720 was considerably less intense than the $\perp$b polarized component, whereas the b-polarized peak at 13,790 cm^{-1} is at least 3 times as intense as the $\perp$b component. Therefore, the 13,790 cm^{-1} line was assigned as the 0-0 line ($\delta \rightarrow \delta^*$ transition) of a z-polarized transition for a major component, and the 13,720 cm^{-1} line as the 0-0 line for a z-

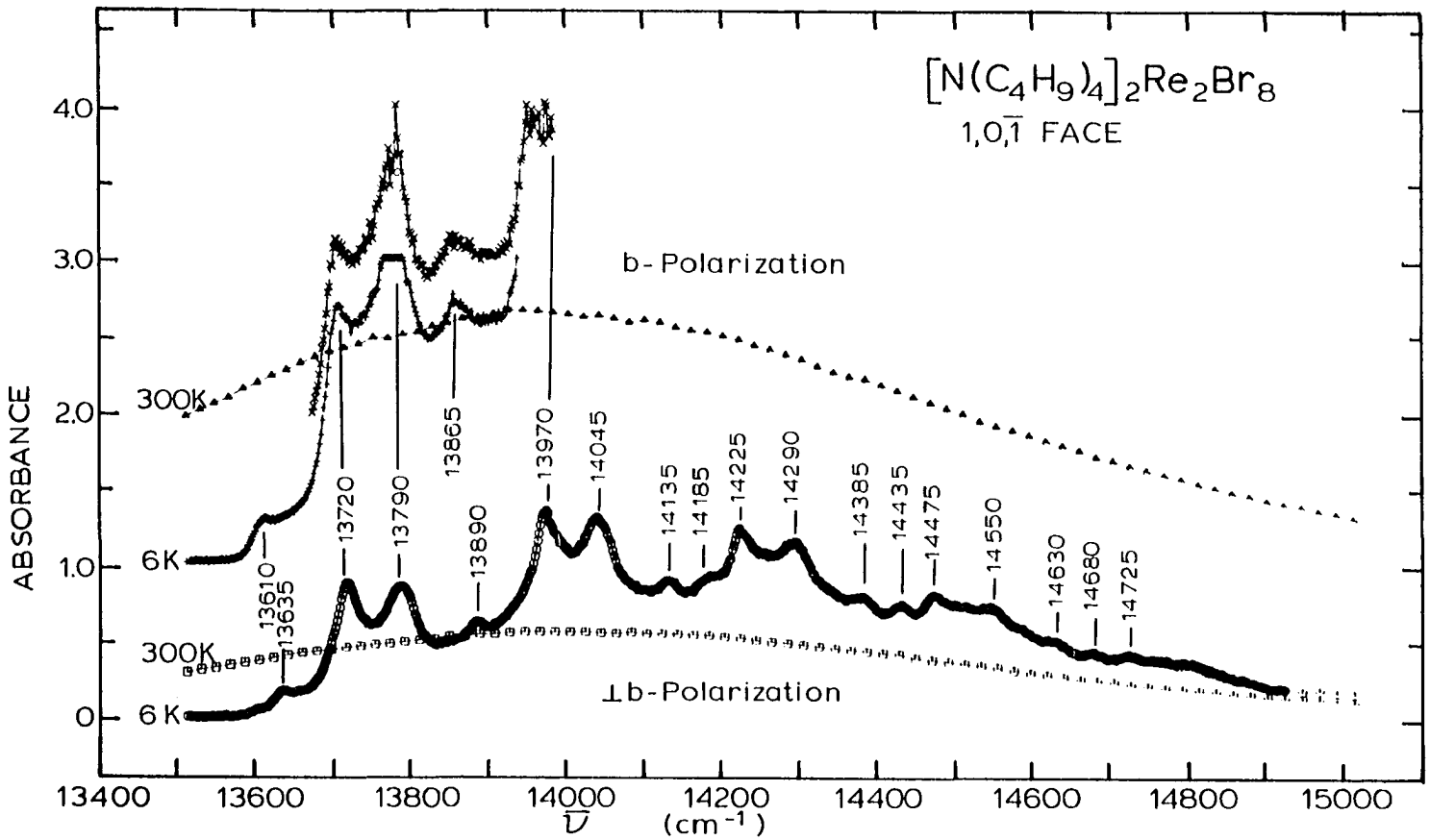

Figure 17. Polarized spectra in the low-energy region with an extended wavenumber scale for a crystal of $(TBA)_2Re_2Br_8$ 3.4 μm thick at 6 K. The short segment above the b polarization was obtained with a higher range extender setting that increased the noise

polarized transition in the minor component. The intensity of the 13,720 cm^{-1} line is obviously higher than that predicted from the expected polarization ratio for the ideal D_{4h} symmetry. This feature can well be due to a moderate deviation of the transition moment vector from the molecular z-axis caused by the crystal fields. Also, the intensity of the 13,790 line should be about 1.66 times of the 13,720 line for the ideal case. The 13,720 cm^{-1} component is slightly higher although this may be in part due to the fact that it is somewhat narrower. Again, it is probably another consequence of the crystal-field effect on the transition moment alignment. If the assignment is correct, it indicates that the origin of z-polarized band, presumably the $\delta \rightarrow \delta^*$ transition, has been red-shifted by 70 cm^{-1} in the minority component.

Below the two intense origins, there is evidence of some absorption in the region of 13,570-13,680 cm^{-1}. Higher progression terms based on the origins in this region are clearly seen in both polarizations. These origins are suspected to result from the same sort of unspecified disorder that also occurred in the $(TBA)_2Re_2Cl_8$. In the case of the bromide salt, the disorder must be nearly an order of magnitude less abundant, because these progressions are such minor features in the spectra. A very minor origin was also noted to occur at 14,185 in the $\perp$b-spectrum. This

is 395 cm^{-1} above the 13,790 cm^{-1} origin and appears to be too high to be a vibronic origin. The highest energy of the vibrational mode for $[Re_2Cl_8]^{2-}$ anion is 365.5 cm^{-1} belonging to $\bar{\nu}$(Re-Cl) (57). The line at 14,185 cm^{-1} may indicate a further minor disorder.

There is some vibrational structure in the region 13,570-13,680 cm^{-1} that is more clearly seen in the spectra for a thicker crystal in Figure 18. Thus, the two peaks, 13,610 and 13,643, which are more intense in b-polarization, can be attributed to the major site in z-polarization, and the peaks at 13,635 and 13,660, which are much more intense in $\perp$b, can be attributed to the minor site in z-polarization. For these components, the orientation of metal-metal bonds is assumed to be the same in each major and minor site as for the other components. It is only a difference in the configuration in cations.

A very weak absorption in the region of 16,000-18,500 cm^{-1} is shown in Figure 19. A crystal 37 μm thick was used for these spectra. Mishowski (60) found a very similar band for crystals of $Cs_2Re_2Br_8$. He noted that the majority of lines could result from two vibronic origins with two Franck-Condon progressions. According to his suggestion, the observed vibrational structure of $(TBA)_2Re_2Br_8$ in this region is assigned in Table 13. The two vibronic origins at 16,330 and 16,450 cm^{-1}, designated 0-0 + ν_i and 0-0 + ν_j,

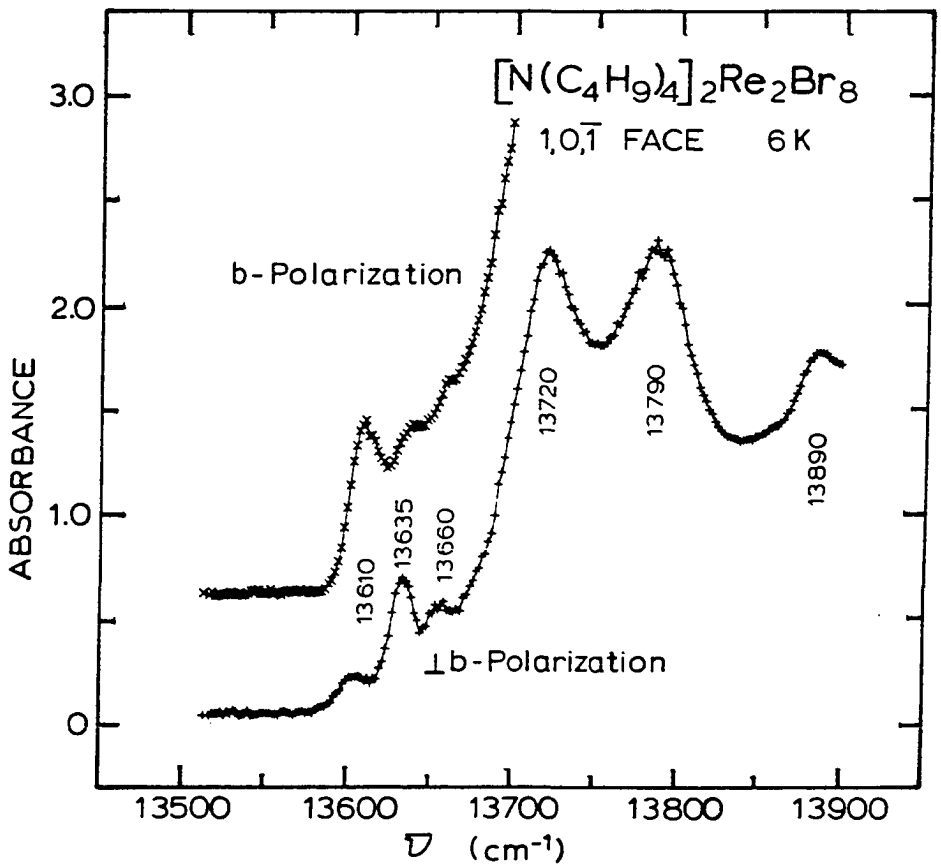

Figure 18. Polarized spectra for a $(TBA)_2Re_2Br_8$ crystal that is 8.5 μm thick

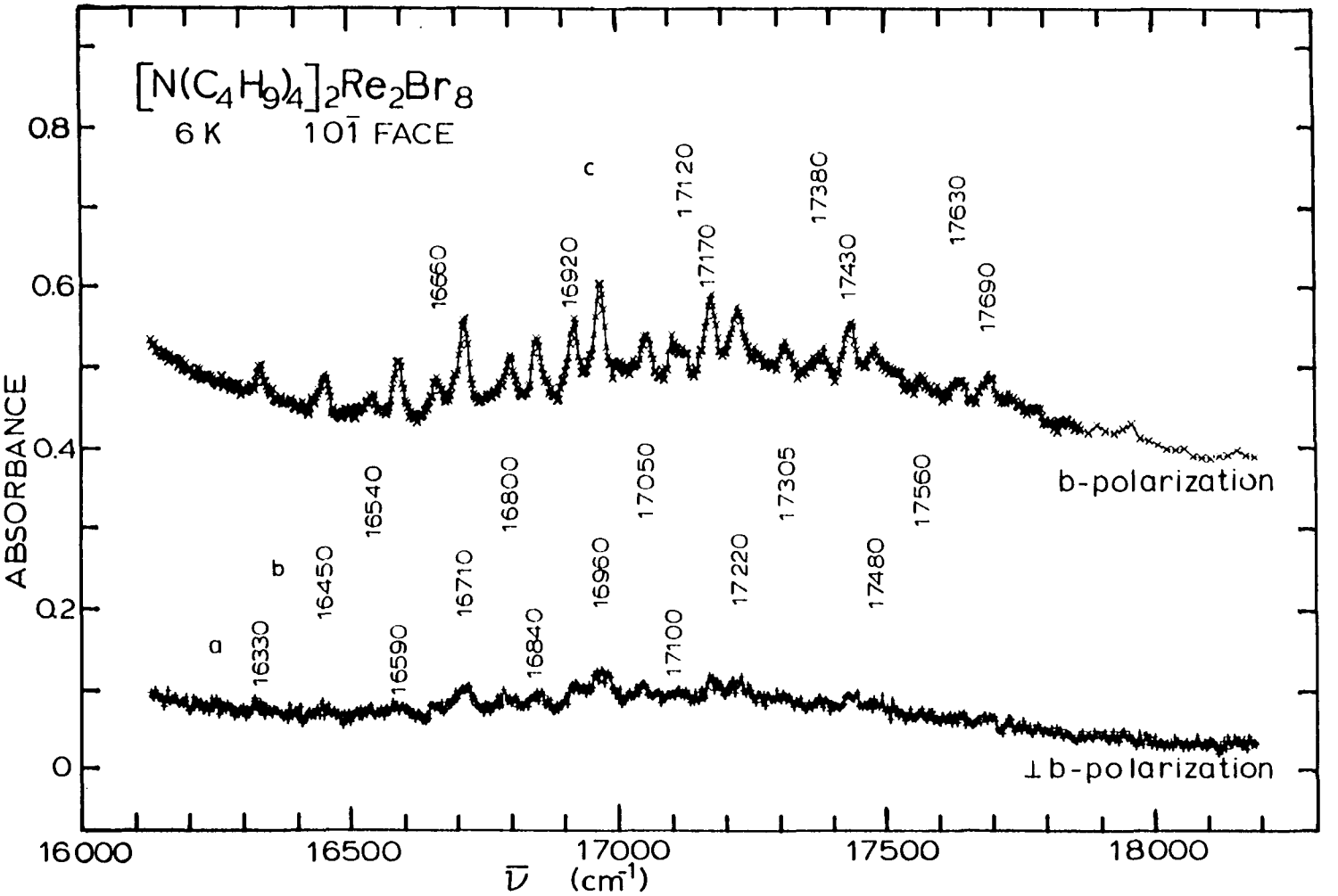

Figure 19. Polarized spectra for a 37 μm thick $(TBA)_2Re_2Br_8$ crystal in the region of the weak band, 16000-18000 cm^{-1}

Table 13. Vibrational Structure in the region of 16000-18500 cm^{-1} for $(TBA)_2Re_2Br_8$ at 6 k

$\bar{\nu}^a$, cm^{-1}	$\bar{\nu}^b$, cm^{-1}	assignment
16540	16538	$0\text{-}0 + \nu_i + \nu_2$
16590	16586	$0\text{-}0 + \nu_i + \nu_1$
16660	16658	$0\text{-}0 + \nu_j + \nu_2$
16710	16706	$0\text{-}0 + \nu_j + \nu_1$
16800	16794	$0\text{-}0 + \nu_i + \nu_2 + \nu_1$
16840	16842	$0\text{-}0 + \nu_i + 2\nu_1$
16920	16914	$0\text{-}0 + \nu_j + \nu_2 + \nu_1$
16960	16962	$0\text{-}0 + \nu_j + 2\nu_1$
17050	17050	$0\text{-}0 + \nu_i + 2\nu_1 + \nu_2$
17100	17098	$0\text{-}0 + \nu_i + 3\nu_1$
17170	17170	$0\text{-}0 + \nu_j + 2\nu_1 + \nu_2$
17220	17218	$0\text{-}0 + \nu_j + 3\nu_1$
17305	17306	$0\text{-}0 + \nu_i + 3\nu_1 + \nu_2$
17380	17376	$0'\text{-}0' + \nu_k + \nu_1$
17430	17426	$0\text{-}0 + \nu_j + 3\nu_1 + \nu_2$
17480	17484	$0'\text{-}0' + \nu_k + \nu_1 + \nu_2$
17560	17562	$0\text{-}0 + \nu_i + 4\nu_1 + \nu_2$
17630	17632	$0'\text{-}0' + \nu_k + 2\nu_1$
17690	17680	$0\text{-}0 + \nu_j + 4\nu_1 + \nu_2$

[a] Observed frequencies.

[b] Calculated frequencies.

respectively, are based on the 0-0 line ($\pi \rightarrow \delta^*$ or $\delta \rightarrow \pi^*$ transition). Another vibronic origin at 17120 cm^{-1}, designated $0'-0' + \nu_k$, lie 790 cm^{-1} above an origin. Hence, the c progression must originate from either different transitions or different sites. There are two totally symmetric vibrations, designated ν_1 and ν_2, with wavenumbers 256.0 and 208.0 cm^{-1} which yield Franck-Condon progressions. The ν_1 vibration produces long Franck-Condon progression with four members above the origin discernible, whereas ν_2 produces short progression with only one member above the origin. Therefore, ν_1 was assigned to the a_{1g} Re-Re stretching vibration, and ν_2 was assigned to the a_{1g} Re-Br stretching vibration. Progressions a, b,and c, which are z-polarized, couple a vibrational wave function of overall E_u symmetry to the electronic wave function to give a vibronic state of A_{2u} symmetry. Since the origin of the third progression, designated c, was 790 cm^{-1} above the a-origin, it was concluded that this absorption represents a different transition or a different site.

Trogler et al. (42) commented that in their sample of $(TBA)_2Re_2Br_8$ they observed some thin tan crystals that they attributed to a different face from the normal specimens. They indicated it was partially due to this observation that they concluded the 14,000 cm^{-1} band must be z-polarized; for

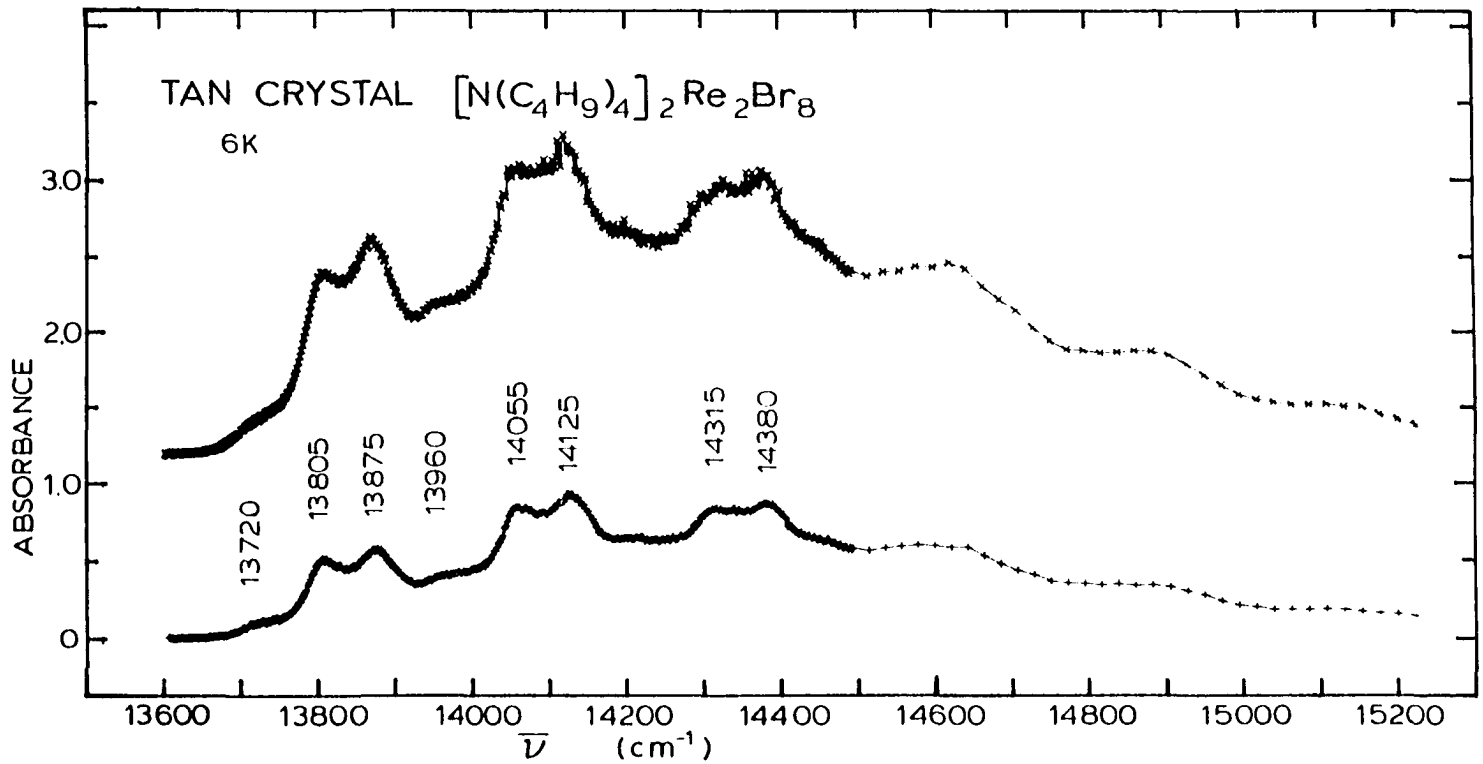

Figure 20. Polarized spectra of a tan crystal found in the preparation of $(TBA)_2Re_2Br_8$

if the green color was due to an x, y-polarization, there would be no face where this component would not be seen in at least one polarization. Some thin tan crystals were found among green crystals of $(TBA)_2Re_2Br_8$ in this research. Polarized spectra for the 14,000 cm^{-1} band of such a cystal are shown in Figure 20. There are two intense progressions seen in each polarization and a third weaker progression based on an origin below the other two. The pattern is clearly similar to the bands in Figure 17 for $(TBA)_2Re_2Br_8$. However, lines in the tan crystals are about 80 cm^{-1} higher in energy than in the green crystals. This result has been confirmed with a second crystal as well. Therefore, it is concluded that the tan crystals represent a different crystal structure from the green which does contain the $Re_2Br_8^{2-}$ anion, and that the 80 cm^{-1} shift of the vibrational lines results from the different crystal environment.

The intensity ratio of the tan crystal at room temperature appeared to be approximately 1.7 in the two polarizations, whereas in the green crystal it was estimated to be 2.9. In examination of the extended spectra for the tan crystals, which are presented in Figure 21, it was noted that a band peaking at 21,100 cm^{-1} with equal intensity in each polarization is about the same intensity as the 14,000 cm^{-1} band in the polarization with low intensity. The room

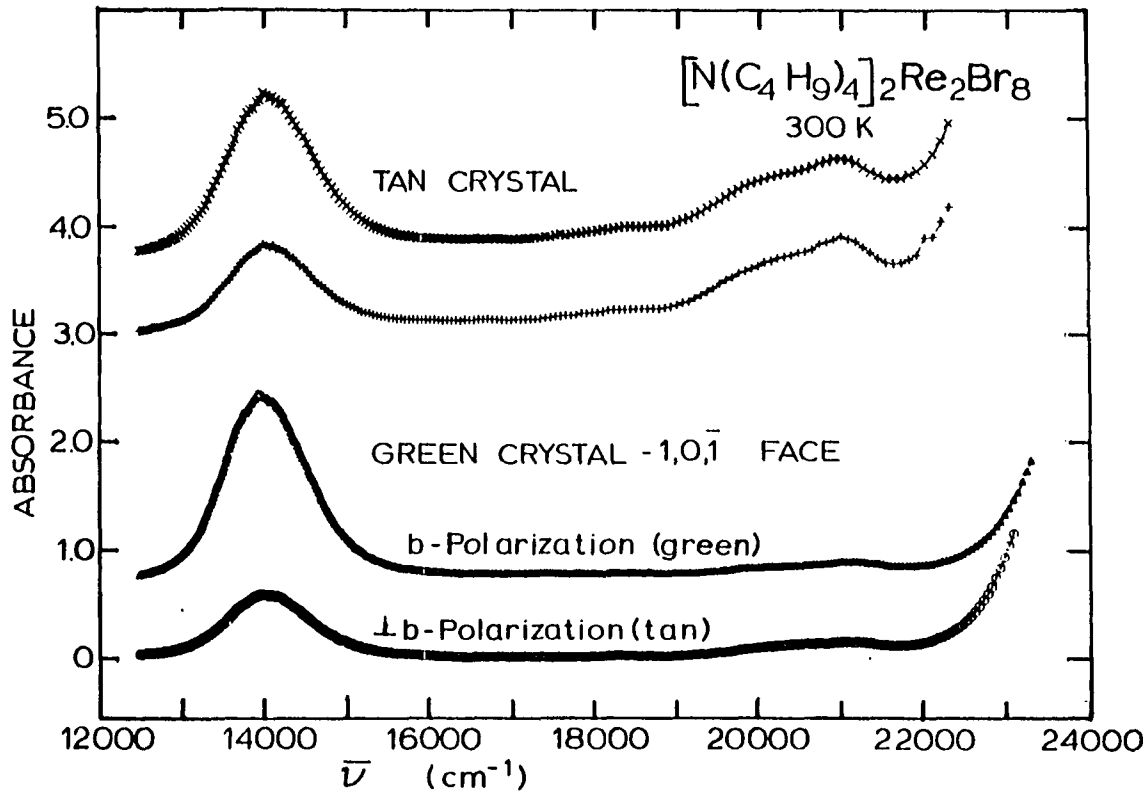

Figure 21. Room-temperature polarized crystal spectra for tan and green crystals of $(TBA)_2Re_2Br_8$

temperature scans for the green crystal are also shown in Figure 21, and they show a 21,000 cm^{-1} peak the intensity of which is only 10-20% of the $\perp$b-polarization of the 14,000 cm^{-1} band. It seems likely that the 21,000 cm^{-1} band may be due to an impurity component. In any event, the 21,000 cm^{-1} band appears to play an important role in establishing the color of the tan crystals. For the green crystals, the relative intensity of the 14,000 cm^{-1} band, primarily with little absorption at 21,000 cm^{-1}, serves to provide the responses which the eye interprets as green and tan colors for the different polarizations.

Comparison of $(TBA)_2Re_2Cl_8$ and $(TBA)_2Re_2Br_8$

There are similarities in the first band of these two compounds, but also some distinct differences as well. First of all, the bands have nearly the same energy with maxima in the region of 14,000-14,500 cm^{-1}. Room temperature oscillator strengths, calculated for a particular polarization from the equation:

$$f = 4.32 \times 10^{-9} \int \varepsilon d\bar{\nu},$$

were similar as well. For $(TBA)_2Re_2Cl_8$, $f_b = 2.6 \times 10^{-2}$ and $f_c = 9.5 \times 10^{-3}$. For $(TBA)_2Re_2Br_8$, $f_b = 2.0 \times 10^{-2}$ and $f_{\perp b} = 6.8 \times 10^{-3}$. Since the thinnest crystal of $(TBA)_2Re_2Br_8$ was about 50% thicker than $(TBA)_2Re_2Cl_8$, it was not possible to scan over the b-polarized spectrum of this compound.

The average separation in Franck-Condon progressions were nearly equal for each compound, 249(2) cm^{-1} for $(TBA)_2Re_2Cl_8$ and 252(4) cm^{-1} for $(TBA)_2Re_2Br_8$ in the first band. These progressional frequencies are due to an excited state Re-Re stretch. These values are very reasonable in view of the corresponding stretching frequencies for the ground state of 271.9 and 275.4 reported by Clark and Franks (59) from their resonance Raman study of these compounds. The most intense progression of each compound is based on an origin that can be considered the 0-0 line of a dipole-allowed, z-polarized transition of the majority component in the disordered crystals. This line for $(TBA)_2Re_2Br_8$ was 515 cm^{-1} below the corresponding line for the $(TBA)_2Re_2Cl_8$. The corresponding 0-0 line of the minority component in the crystal of $(TBA)_2Re_2Cl_8$ was blue-shifted only 24 cm^{-1} above that for the major component, and the two lines were barely resolvable. On the other hand, this line for the minor component of $(TBA)_2Re_2Br_8$ was red-shifted by 70 cm^{-1} so the two progressions were clearly resolved. A complex pattern of absorption below these 0-0 lines occurred for both compounds which are attributed to a disorder not revealed by X-ray diffraction at room temperature. The considerable difference in the relative intensities for these additional absorptions and the progression based on them are consistent with their assignment to such a disorder component. They

indicate a much lower occurrence of such an anomalous component in the bromide compound. This feature may well account for the better resolution of the major vibrational components in the $(TBA)_2Re_2Br_8$.

The features of absorption are quite different in the region of 16,000-18,500 cm^{-1} for these two compounds. For the $(TBA)_2Re_2Br_8$, all line intensities are high in b-polarization. There are no lines resolvable that can be assigned as x, y-polarized for the major orientation or z-polarized for the minor orientation. A majority of the lines can be described by two vibronic origins with two a_{1g} vibrations which produce Franck-Condon progressions. It was necessary to include a second site or transition to account for a few lines. For $(TBA)_2Re_2Cl_8$, Franck-Condon progressions based on a single a_{1g} vibration were observed. At least three different sites or separate transitions were required to account for lines and one progression was more intense in c-polarization.

$Re_2[O_2CC(CH_3)_3]_4Cl_2$

As Collins et al. (25) indicated, the structure of $Re_2[O_2CC(CH_3)_3]_4Cl_2$ is ideal for crystal spectroscopy. There is only one molecule in a primitive cell, and the site symmetry is 4/m. The needle faces were 100 with c directed along the needle axis. The molecular z-axis which is along

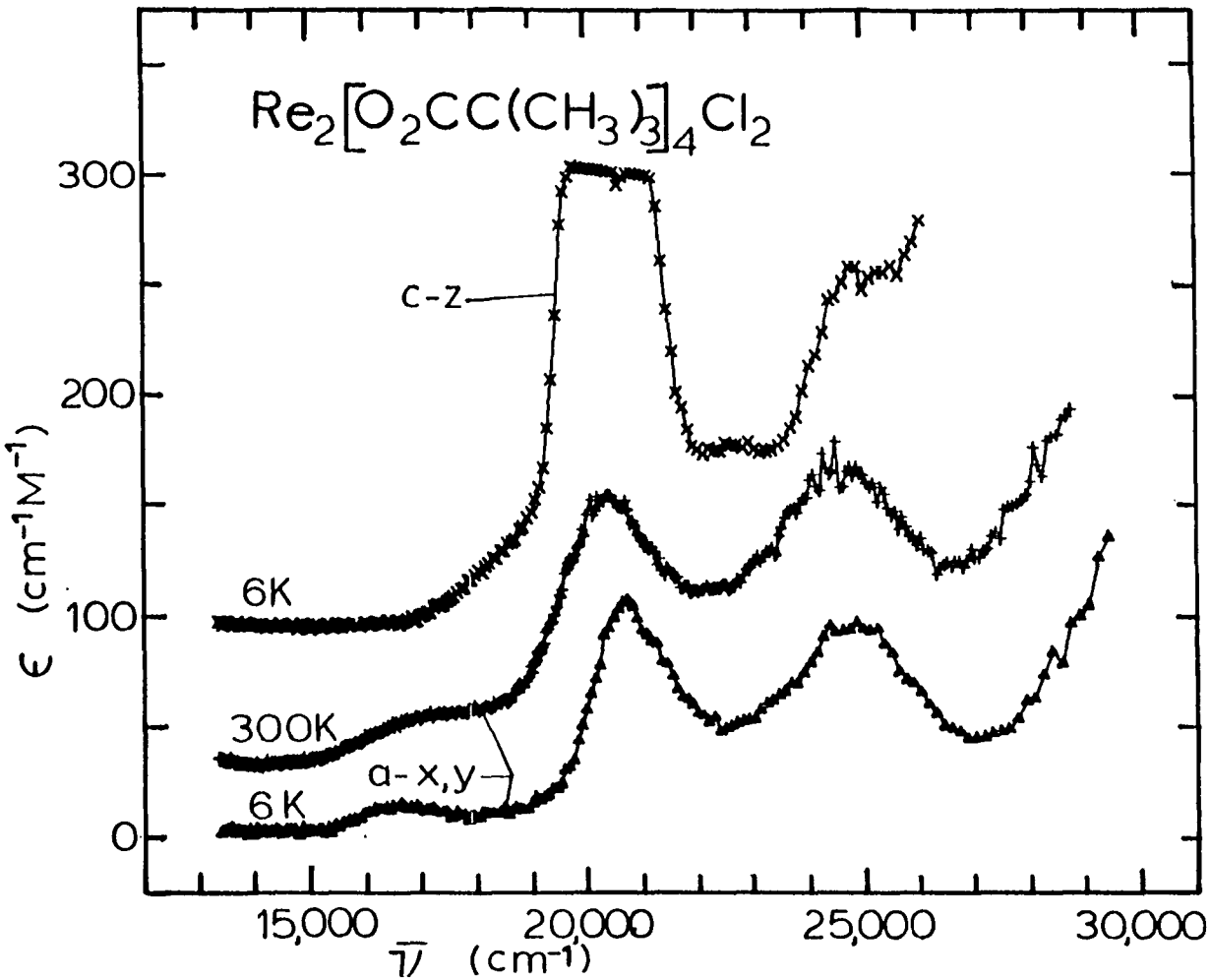

Figure 22. Polarized spectra for a $Re_2[O_2CC(CH_3)_3]_4Cl_2$ crystal that was 41 μm thick

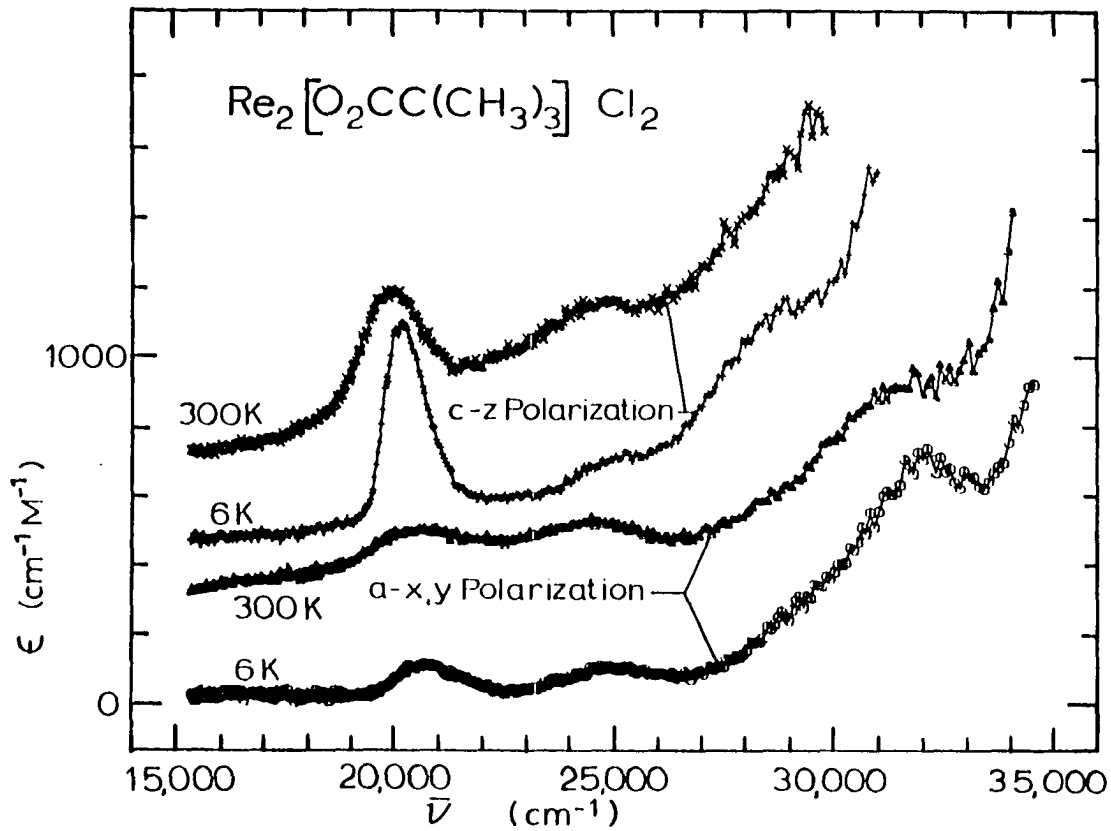

Figure 23. Polarized spectra for a $Re_2[O_2CC(CH_3)_3]_4Cl_2$ crystal that was 2.3 μm thick

Table 14. Electronic transitions, polarized intensities, and proposed assignments for $Re_2[O_2CC(CH_3)_3]_4Cl_2$

z-Polarization		x, y-Polarization		Proposed
$\bar{\nu}$, cm^{-1}	Osc. str., f^a	$\bar{\nu}$, cm^{-1}	Osc. str., f^a	assignment
		16500	5×10^{-5}	$^1A_{1g} \rightarrow {}^3A_{2u}$, $\delta \rightarrow \delta^*$
20200	3×10^{-3}	20600	7×10^{-4}	$^1A_{1g} \rightarrow {}^3A_{2u}$, $\delta \rightarrow \delta^*$
b	b	21600	1×10^{-5}	$^1A_{1g} \rightarrow {}^3E_g$, $\pi \rightarrow \delta^*$
24700	1.5×10^{-4}	24700	7×10^{-4}	$^1A_{1g} \rightarrow {}^1E_g$, $\pi \rightarrow \delta^*$
29000	8×10^{-4}	29000	$< 2 \times 10^{-4}$	$^1A_{1g} \rightarrow {}^1E_g$, $\delta \rightarrow \pi^*$
c	c	32000	1.6×10^{-3}	spin-forbidden
	$\pi \rightarrow \pi^*$ or CT			

[a]Oscillator strengths at 6 K calculated by the expression $f = 4.32 \times 10^{-9} \int \varepsilon d\bar{\nu}$.

[b]Not resolved.

[c]Beyond range.

the Re-Re bond is directed along the crystallographic c-axis, the c- and a-polarization absorptions give directly the molecular z and x, y absorptions, respectively. The locations of the maxima for the bands of the experimental spectra in Figures 22 and 23 together with the indicated intensities, polarizations, and proposed assignment are listed in Table 14.

In the thick-crystal spectra, Figure 22, the most intense feature is a band in z-polarization whose intensity was well beyond the capabilities of the instrumentation. However, with the thin crystal, Figure 23, it was possible to scan over this peak with a maximum of ca. 600 cm^{-1} M^{-1} at 20,200 cm^{-1} and 6 K. The peak height at 6 K in z-polarization for this 20,200 cm^{-1} band is distinctly higher than at 300 K. This band is clearly electric dipole-allowed in this polarization since the higher peak height implies that the intensity does not fall off significantly at low temperatures as should that for a vibronically-allowed but dipole-forbidden band. It seems appropriate to assign this band to the $^1A_{1g} \rightarrow {}^1A_{2u}$ ($\delta \rightarrow \delta^*$) which is electric dipole-allowed in the z-direction. The absorption in x, y-polarization peaking at 20,600 cm^{-1} would then be attributed to vibronic excitation of this electronic transition that would require an E_g degenerate pair of vibrations under D_{4h} symmetry. In this case, the vibronic intensity is about 15%

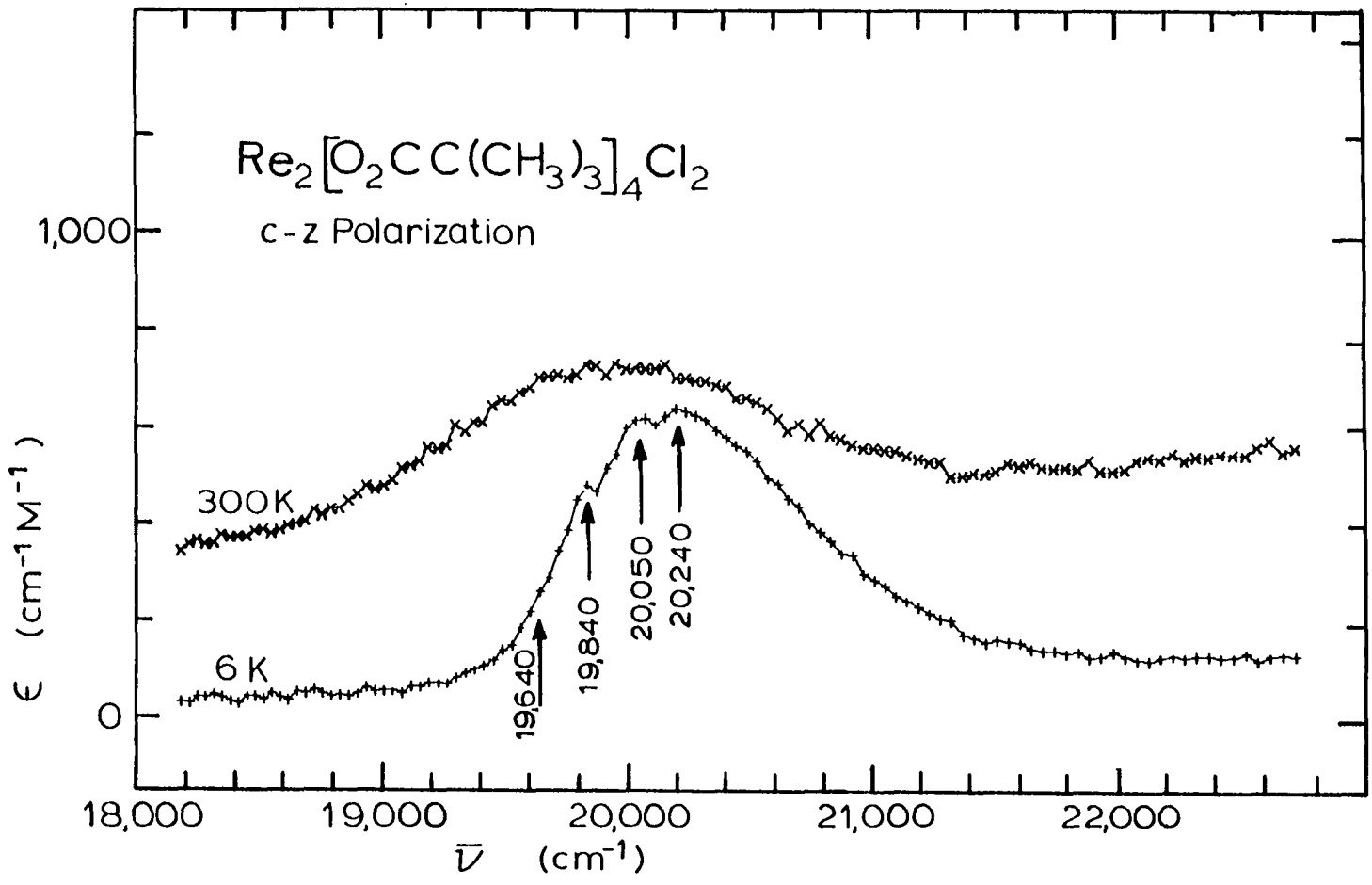

Figure 24. Expanded scale plot of the 20200 cm^{-1} peak in c polarization for the $Re_2[O_2CC(CH_3)_3]_4Cl_2$ crystal that was 2.3 μm thick

that of the electric dipole-allowed portion seen in z-polarization.

Poorly resolved vibrational structure was clearly evident on the z-polarized peak of $Re[O_2CC(CH_3)_3]_4Cl_2$ at 20,200 cm^{-1}. The plots in Figure 24 show this band with an extended scale where three maxima are seen. A fourth component as a shoulder at 19,640 cm^{-1} is barely discernible. The separation of the components is 200 cm^{-1}. This behavior is certainly different from the dimolybdenum tetracarboxylate crystal spectra at liquid helium temperature where very sharply resolved vibration lines form progressions on not only the 0-0 but on several vibronic origins. The dimolybdenum tetracarboxylate crystal spectra will be discussed in the next section. The slit for the spectrum in Figure 24 was sufficiently narrow to provide a dispersion of 25 cm^{-1} so the lack of resolution was not instrumental. The average separations in Franck-Condon progressions were 200 cm^{-1} which is 31% below the 289 cm^{-1} assigned to the ground state Re-Re stretch by Bratton et al. (27) and indeed is very close to their value of 199 cm^{-1} assigned to the Re-Cl stretch. When the vibrational structure exhibits a regular energy spacing, it is interpreted in terms of a single mode (61). There are no totally symmetric Infrared or Raman bands which can explain this excited state vibration. It may well be that this

progression is an example of the missing mode effect (MIME). Tutt et al. (62) demonstrated this effect in a spectrum of $W(CO)_5(C_5H_5N)$ where they found that an electronic band, observed in emission, with poor resolution of vibrational structure could exhibit, as a consequence of two totally symmetric modes, a single apparent Franck-Condon progression with the separation of maxima corresponding to a wavenumber which was intermediate to the wavenumbers of the two normal modes. The separation indicated in the progression in Figure 24 lies between the expected wavenumbers of the totally symmetric modes of Re-Re and Re-Cl stretching vibrations for the exited state.

The 20,600 cm^{-1} band in x, y-polarization had a very weak shoulder on the high energy side, indicated at 21,600 cm^{-1} in Table 14. This shoulder was evident in scans of several crystals. It has been assigned as a spin-forbidden transition $\pi \rightarrow \delta^*$ ($^1A_{1g} \rightarrow {}^3E_g$) corresponding to one of the spin-allowed bands at higher energy.

The x, y-polarized spectrum, Figure 22, shows a weak band at 16,300 cm^{-1}, below the spin-allowed $\delta \rightarrow \delta^*$ transition. This band is missing in z-polarization. A $^1A_{1g} \rightarrow {}^3A_{2u}$ transition by spin-orbit coupling would be electric dipole-forbidden in z-polarization but allowed in x, y-polarization under double group D_4' symmetry. Therefore, it is assigned as the spin-forbidden transition. In this case,

the separation of $^3A_{2u}$ and $^1A_{2u}$ states would be 3900 cm^{-1}. This is a rather normal separation for a transition-metal complex. No corresponding spin-forbidden band has been found below the band which is dipole-allowed with z-polarization for any of the dimeric molybdenum complexes. However, rhenium with the higher atomic number than molybdenum is expected to have a considerably higher spin-orbit coupling and consequently higher intensity for the spin-forbidden bands. Bursten et al. (37) did assign a band (designated II) which centered at about 478 nm to the orbitally allowed, spin-forbidden $\pi \rightarrow \pi^*(^1A_{1g} \rightarrow {}^3A_{2u})$ transition of their crystal, $(TBA)_2Re_2Cl_8$. However, no spin-forbidden $\delta \rightarrow \delta^*$ transition has been reported for any molybdenum or rhenium dimer previously. Hay (63) predicted the $\delta \rightarrow \delta^*(^1A_{1g} \rightarrow {}^3A_{2u})$ transition in $Re_2Cl_8^{2-}$ would occur at about 3200 cm^{-1} in his theoretical treatment. The spin-forbidden transition below the spin-allowed transition in the x, y-polarization would at one time have been accepted as an unambiguous justification for the assignment if this was the first dimer to yield polarized spectra. There is always the possibility that a weak feature such as the band at 16,500 cm^{-1} is due to a minor impurity component in a crystal. However, the band was observed reproducibly in several crystals whose spectra were measured.

The assignment of the higher energy bands in the

spectra is based on the earlier studies (31, 8, 64) of $Re_2Cl_8^{2-}$ and a paper by Bursten et al. (37). This latter paper describes a SCF-Xα-Scattered wave calculation for $Re_2Cl_8^{2-}$ which includes inner-shell and valence relativistic effects. This calculation indicated that the first orbital excitation above the $\delta \rightarrow \delta^*$ should be the $\pi \rightarrow \delta^*$. Accordingly, the band at 24,700 cm^{-1} with about the same intensity in z- as in x, y-polarization has been assigned as the spin-allowed $^1A_{1g} \rightarrow {}^1E_g$ ($\pi \rightarrow \delta^*$) with the spin-forbidden $^1A_{1g} \rightarrow {}^3E_g$ ($\pi \rightarrow \delta^*$) as the shoulder seen at 21,600 cm^{-1} in x, y-polarization. This places the $^1A_{1g} \rightarrow {}^1E_g$ at 4100 cm^{-1} above the $\delta \rightarrow \delta^*$, comparable to the 3,800 cm^{-1} difference between the corresponding bands assigned by Bursten et al. (37). The peak at 29,000 cm^{-1}, some 8500 cm^{-1} above the $\delta \rightarrow \delta^*$ band, was assigned as $^1A_{1g} \rightarrow {}^1E_g$ ($\delta \rightarrow \pi^*$). The band at 32,000 cm^{-1} is likely a spin-forbidden $\pi \rightarrow \pi^*$ or charge-transfer transition. Since the computations of Norman and Ryan (65) indicated that in $Mo_2Cl_8^{4-}$ and $Mo_2(O_2CH)_4$ the carboxylate stabilizes both the π and π^* orbitals with respect to the δ and δ^*, there is the possibility that the $\delta \rightarrow \pi^*$ and $\pi \rightarrow \delta^*$ assignments are reversed.

The monoclinic $Mo_2(O_2CC(CH_3)_3)_4$

The microscopic observations of these crystals indicated a distinct wavelength dependence of the extinction

direction. Experience has shown for similar cases that the polarizer angle in the spectrophotometer cannot be safely set at the extinctions observed in the polarizing microscope.

For the monoclinic crystals, the first absorption band at 300 K has a maximum at ca. 23,000 cm^{-1}. At 6 K, this band develops a rich vibrational structure. An extended plot of the low-energy region of this band observed for the $1\bar{1}0$ face at 6 K is presented in Figure 25. Wavenumbers of resolvable vibrational peaks and shoulders have been recorded and the assignment of progression lines has been made in Table 15. When the plane of polarized light entering a crystal face is rotated, the observed absorbance will be a maximum or a minimum at the extinction angles. Crystal spectra were recorded for steps of 10^{o} in the polarizer angle. The two curves shown in Figure 25 have the maximum and minimum values for the A lines. These indicated extinctions coincided within experimental error with the optical extinctions assigned by the polarizing microscope.

Every absorption feature occurred as three lines, e.g., the three A_o lines (A_o^1, A_o^2, and A_o^3). Extended Franck-Condon progressions based on each of the three origins could be identified. The first member A_o^1 is quite weak. At 25 cm^{-1} higher energy, there is a considerable stronger line, A_o^2,

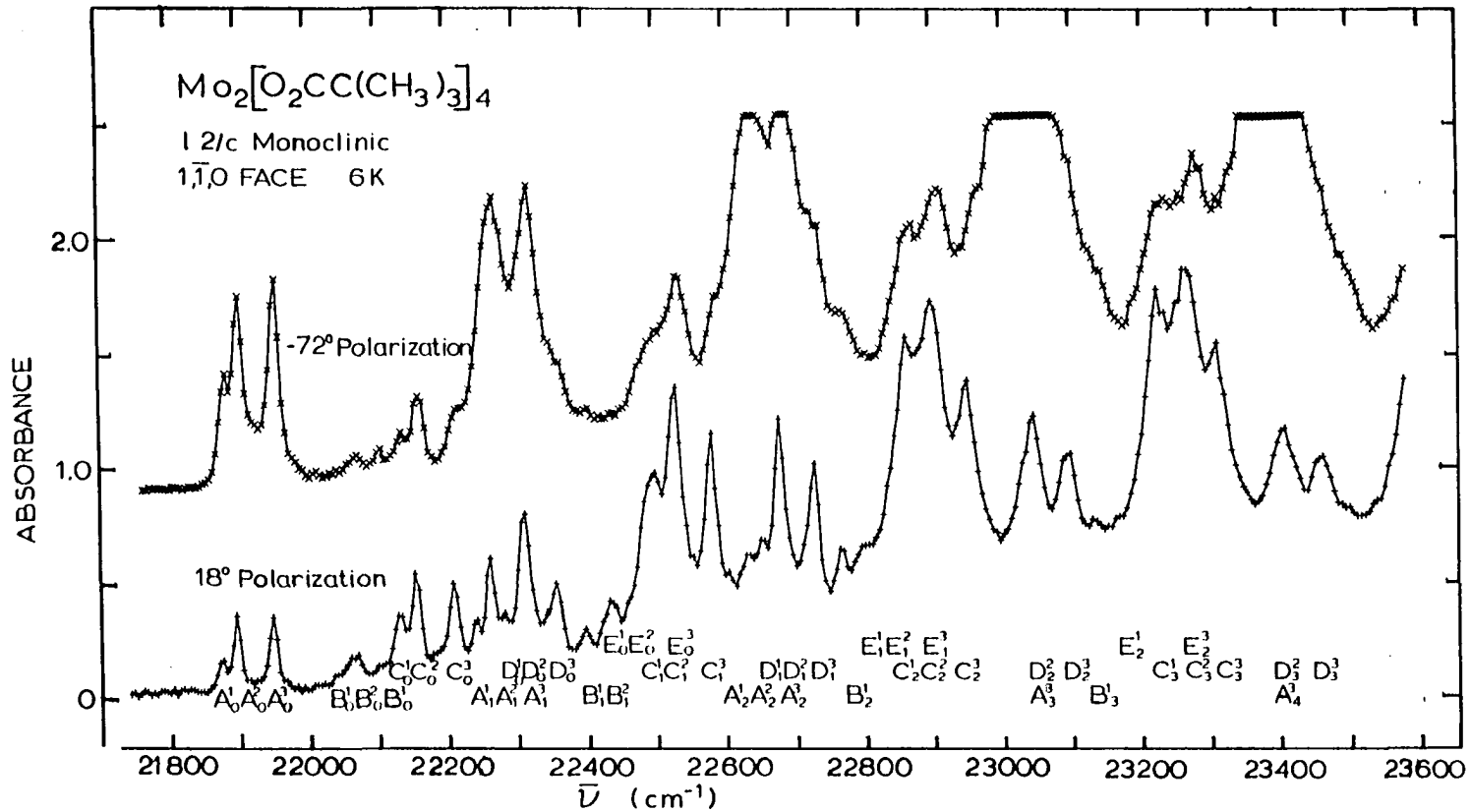

Figure 25. Resolution of vibrational structure in the first band for a crystal of the monoclinic crystal of $Mo_2(piv)_4$, 52 ± 10 μm thick

Table 15. Vibrational details in the low energy absorption band of the monoclinic crystal of $Mo_2(piv)_4$ at 6 K

Assignment	$\bar{\nu}$, cm^{-1}	$\Delta\bar{\nu}$,[a] cm^{-1}
A_o^1	21875	
A_o^2	21900	(25)
A_o^3	21950	(75)
B_o^1	22040	(165)
B_o^2	22070	(195)
B_o^3	22115	(240)
C_o^1	22130	(255)
C_o^2	22150	(275)
C_o^3	22210	(335)

[a]Values in parentheses give the difference, $\Delta\bar{\nu}$, from the A_o^1 line. Values without parentheses give the $\Delta\bar{\nu}$ values from the preceding line in a progression.

Table 15. Continued

Assignment	$\bar{\nu}$, cm^{-1}	$\Delta\bar{\nu}^a$, cm^{-1}
A_1^1	22240	365
A_1^2	22260	360
D_0^1	22280	(405)
A_1^3, D_o^2	22310	360, (435)
D_o^3	22360	(485)
B_1^1	22400	360
E_o^1	22430	(555)
E_o^2	22460	(585)
C_1^1	22500	370
C_1^2, E_o^3	22525	375, (650)
C_1^3	22580	370
A_2^1	22600	360
A_2^2	22630	370
D_1^1	22650	370
A_2^3, D_1^2	22675	365
D_1^3	22725	365
B_2^1	22760	365

Table 15. Continued

Assignment	$\bar{\nu}$, cm^{-1}	$\Delta\bar{\nu}^a$, cm^{-1}
E_1^1	22800	370
E_1^2	22830	370
C_2^1	22860	360
C_2^2, E_1^3	22890	365
C_2^3	22945	365
A_3^3, D_2^2	23040	365
D_2^3	23090	365
B_3^1	23130	370
E_2^1	23160	360
C_3^1	23220	360
C_3^2, E_2^3	23260	370
C_3^3	23305	360
A_4^3, D_3^2	23400	360
D_3^3	23455	365

and 75 cm^{-1} higher still is a A_o^3 line with intensity comparable to A_o^2. The observed polarization ratios I_{-72^o}/I_{18^o} is about 2.8. A peaks dominate the -72^o spectrum. In the 18^o spectrum, the B, C, D, and E progressions are evident, and the C^1, C^2, and C^3 peaks have comparable intensities to the corresponding A^1 A^2, and A^3 peaks. The high intensity of the component at 22,310 cm^{-1} is due to the near coincidence of A_1^3 and D_0^2 components. The B, C, and D components have comparable intensity in the two polarizations, and indeed showed little change in the intensity as polarizer angle was rotated.

The possibility of Davydov splitting to account for the observed multiple lines was considered (the treatment of Davydov splitting for this monoclinic structure is shown in Appendix D). Although there are two Davydov states, the excitation for a z-polarized transition to one of these states should have only a very low intensity in each of the polarizations for the $1\bar{1}0$ face. Hence, Davydov splitting cannot explain triple lines which are observed. Three components for each feature indicate three different sites, and the lowest energy site appeared to be of minor abundance. Such minor sites have been observed for other spectra of molybdenum carboxylates, i.e., $Mo_2(O_2CCF_3)_4$ and γ-$Mo_2(O_2CH)_4$. However, the second and the third sites produce very similar intensities so that they must have

nearly equal abundance.

The crystal structure with I2/c space group contains only a single molecular site, therefore the spectral evidences are inconsistent with the structure. The rotational orientations of the tert-butyl groups, $(CH_3)_3C$, may produce different sites. The fact that anisotropic thermal parameters could not be refined and fairly large isotropic thermal parameters were required for the methyl carbons are consistent with this explanation. Since the crystal structure was performed at room temperature, there is an interesting possibility that a phase transition occurred between room temperature and 6 K. Since the crystals maintain an integrity as they cycle between room temperature and 6 K, such transition would probably have to be the second-order type. The spectra were recorded at various temperatures from 6 to 85 K. The splittings disappeared between 65 to 75 K. If there were a second-order phase transition, it might occur at about 65-75 K. As a consequence of the second-order phase transitions, some symmetry operations of the space group will be lost, so inequivalent molecular sites might occur. There is another possibility that the herring-bone and parallel arrangements of the orthorhombic and monoclinic forms occur in the same spectroscopic specimen. Hence, such disordered or twinned crystal could have two types of orientation. Some sort of

crystallographic defect cannot be ruled out. Defects in the chain orientation and stacking can certainly occur. Any such defect would have to result in additional spectral components. However, spectra were recorded for several crystals and all of them had essentially the same features.

For the monoclinic crystal of $Mo_2(piv)_4$, the c-axis is contained in the spectroscopic face $11\bar{0}$. The following relationships were used to transform vectors defined in the cystallographic system to orthogonal coordinates:

$$\hat{a} = 0.99949\hat{i} - 0.03192\hat{k}$$
$$\hat{b} = \hat{j}$$
$$\hat{c} = \hat{k}$$

The extinction, designated $\hat{Ex}_1$, was found to lie 18° from $\hat{c}$. The extinctions in the $1\bar{1}0$ face are given by:

$$\hat{Ex}_1 = \cos 18^\circ \hat{c} + \sin 18^\circ \perp \hat{c}$$
$$= 0.17642\hat{i} + 0.25371\hat{j} + 0.95106\hat{k}$$
$$\hat{Ex}_2 = -\sin 18^\circ \hat{c} + \cos 18^\circ \perp \hat{c}$$
$$= 0.54297\hat{i} + 0.78083\hat{j} - 0.30902\hat{k}$$

Molecular z-axis vectors for sites 1 and 2 were defined along the Mo-Mo bonds and represented z-polarized transitions in the ideal case. These are listed below:

$$\hat{z}_1 = -0.46924\hat{i} + 0.07079\hat{j} + 0.88022\hat{k}$$
$$\hat{z}_2 = -0.46924\hat{i} - 0.07079\hat{j} + 0.88022\hat{k}$$

For a transition moment along the z-axis, the polarization ratio was calculated as follows:

$$\hat{z}_1 \cdot \hat{Ex}_1 = 0.77232$$

$\hat{z}_1 \cdot \hat{Ex}_2 = -0.47151$

$\hat{z}_2 \cdot \hat{Ex}_1 = 0.73640$

$\hat{z}_2 \cdot \hat{Ex}_2 = -0.58206$

$I_2/I_1 = [(-0.58)^2+(-0.47)^2]/[(0.74)^2+(0.77)^2] = 0.493$

This prediction is in serious disagreement with the observed polarization ratio of 2.8 for the combined A_0 peaks. As stated in the introduction, Martin et al. (22) found the transition moment vector was shifted 34^o away from the metal-metal bond or the molecular z axis for $Mo_2(O_2CCH_3)_4$. Therefore, similar shifts of the transition moment as were used for acetate were tested for a series of angles in 5^o steps. The best agreement with the observed polarization ratio was found for a shift of the transition moment by 30^o away from the metal-metal bond for pivalate. These are shown as follows:

$\hat{z} = \hat{Mo\text{-}Mo}$

$\hat{y} = (\hat{Mo\text{-}i}) \times (\hat{i\text{-}O_4})$

$\hat{x} = \hat{y} \times \hat{z}$

The unit $\hat{x}$, $\hat{y}$, and $\hat{z}$ axes are orthogonal for a molecule, and the molecular inversion center was designated as i.

$\mu(\theta) = \sin\theta\hat{x} + \cos\theta\hat{z}$

$\mu_1(30^o) = -0.84601\hat{i} + 0.088799\hat{j} + 0.52572\hat{k}$

$\mu_2(30^o) = -0.84601\hat{i} - 0.088799\hat{j} + 0.52572\hat{k}$

$\mu_1(30^o) \cdot \hat{Ex}_1 = 0.37327$

$\mu_1(30^o) \cdot \hat{Ex}_2 = -0.55247$

$\mu_2(30^o) \cdot \hat{Ex}_1 = 0.32821$

$$\mu_2(30^0)\ \hat{Ex}_2 = -0.69115$$

$$I_2/I_1 = [(-0.69)^2+(-0.55)^2]/[(0.33)^2+(0.37)^2] = 3.17$$

It has been concluded that the A progression represents a series of single transition vibrational lines with z-polarization, for which the molecular polarization has been shifted from the molecular axis by the crystal field perturbation. The major crystal field perturbation to the molecular D_{4h} symmetry can resonably be attributed to the intermolecular interactions that exist in the one-dimensional chains of loosely bonded dimeric molecules along the c axis.

Other strong progressions (labeled C, D, and E) have origins 255, 405, and 555 cm^{-1} respectively, above A_0. In addition, a weaker progression, labeled B, has an origin 165 cm^{-1} above A_0. The assignment of A, B, C, D, and E progressions follows that used in the description of $Mo_2(O_2CCH_3)_4$ (22). The polarization ratios of the B, C, D, and E lines are near unity. Also, it noted that the polarization ratio is comparable for the 1, 2, and 3 sites. Therefore, it seems likely that the orientations of the transition moment vectors are the same for three different sites.

A number of vibrations in the excited state may be assigned from the spectra in addition to the A_{1g} metal-metal stretch of 365 ± 5 cm^{-1}. The 255 cm^{-1}, 408 cm^{-1} and the 563

cm^{-1} (the average frequencies from three sites) vibrations which excite the C, D, and E progressions are presumably E_g vibrations which will have vibronically allowed character under D_{4h} symmetry. Apparently, only three of the five E_g degenerate pairs of vibrations of the Mo-O-C framework interact effectively with the electronic states to give intense vibronic lines with x, y-polarizations seen in the spectra.

There are no Raman spectra for $Mo_2(piv)_4$ available. Here, the Raman spectrum of dimolybdenum(II) tetraacetate was used for reference (27). There is a weak 299 cm^{-1} line in the Raman spectrum of acetate which would correspond to the vibration exciting the C progression. This would presumably be primarily an Mo-O stretch. There also is a very weak Raman line reported at 567 cm^{-1} for acetate which would correspond to the vibration exciting the C progression. This vibration is presumably a ring deformation which will involve motion of the molybdenum atoms. There are no peaks in Raman spectra of acetate that can account for the D lines. However, there are four electron-donating tert-butyl groups in $Mo_2[O_2CC(CH_3)_3]_4$. They might produce peaks in the vicinity of 425 cm^{-1} for $Mo_2(piv)_4$.

It was apparent from the spectrum in Figure 25 that there was an absorption feature, labeled B, at 22040 cm^{-1},

165 cm^{-1} above A_0. The 165 cm^{-1} vibration which would be required to excite the B_0 line is in the expected region of Mo-Mo-O bending vibrations. Apparently, such vibrations are not as effective as a Mo-O stretch in the vibronic excitation process. The average spacing between successive lines in the Franck-Condon progressions is 365 ± 5 cm^{-1}. This spacing corresponds to the frequency for a totally symmetric vibration, presumably the metal-metal stretch, which has been observed to be 406 cm^{-1} in the Raman spectra for $Mo_2(O_2CCH_3)_4$ (27). When the relative heights of successive peaks are examined in Figure 25, it can be seen that they follow the same pattern for the A, C, D, and E progressions. The third peak for each progression is the highest which is designated A_2, C_2, D_2, and E_2 in Table 15.

For the carboxylate dimers of molybdenum(II), the rather uncommon resolution of vibrational structure in the lowest electronic absorption band at low temperatures has provided the information that the lowest energy peak is a weak electric dipole-allowed transition derived from the z polarization. The intensity is sufficiently weak that vibronically excited lines have intensities comparable to the progressions based on the 0-0 origin. The z-polarization of this peak is expected for a $\delta \rightarrow \delta^*$ transition. The exceptionally low intensity may result from some electron density transfer from metal to carboxylate

orbitals. It is recognized that for the carboxylates the lowest unoccupied orbital is the π^* orbital involving carbon and oxygen p orbitals. The symmetry-adapted linear combination of the carboxylate π^* orbitals are the bases for the a_{2g}, e_u, and b_{2g} irreducible representations. It is possible that this orbital somewhat mixes with the Mo-Mo δ orbital, b_{2g}. In fact, the relatively high transition energy of the first band for the carboxylate complexes might result from this stabilization of the δ orbital, for there is no b_{1u} linear combination for the carboxylate π^* orbitals. Involvement of the carboxylate orbitals results in withdrawal of electron population from the vicinity of the metal-metal bond. Since the transition is essentially an intermetallic electron transfer between the Mo d_{xy} orbitals, this removes electron density from between the metals where the overlap in the transition moment integral occurs.

The orthorhombic $Mo_2(O_2CC(CH_3)_3)_4$

The polarized spectra of a crystal of $Mo_2(piv)_4$, ca. 20 μm thick, were recorded at 300 and 6 K for the spectroscopic face 110. The lowest energy band observed at room temperature has a maximum at ca. 23,000 cm^{-1}. The band is somewhat more intense in the $\perp$c-polarization than in the c-

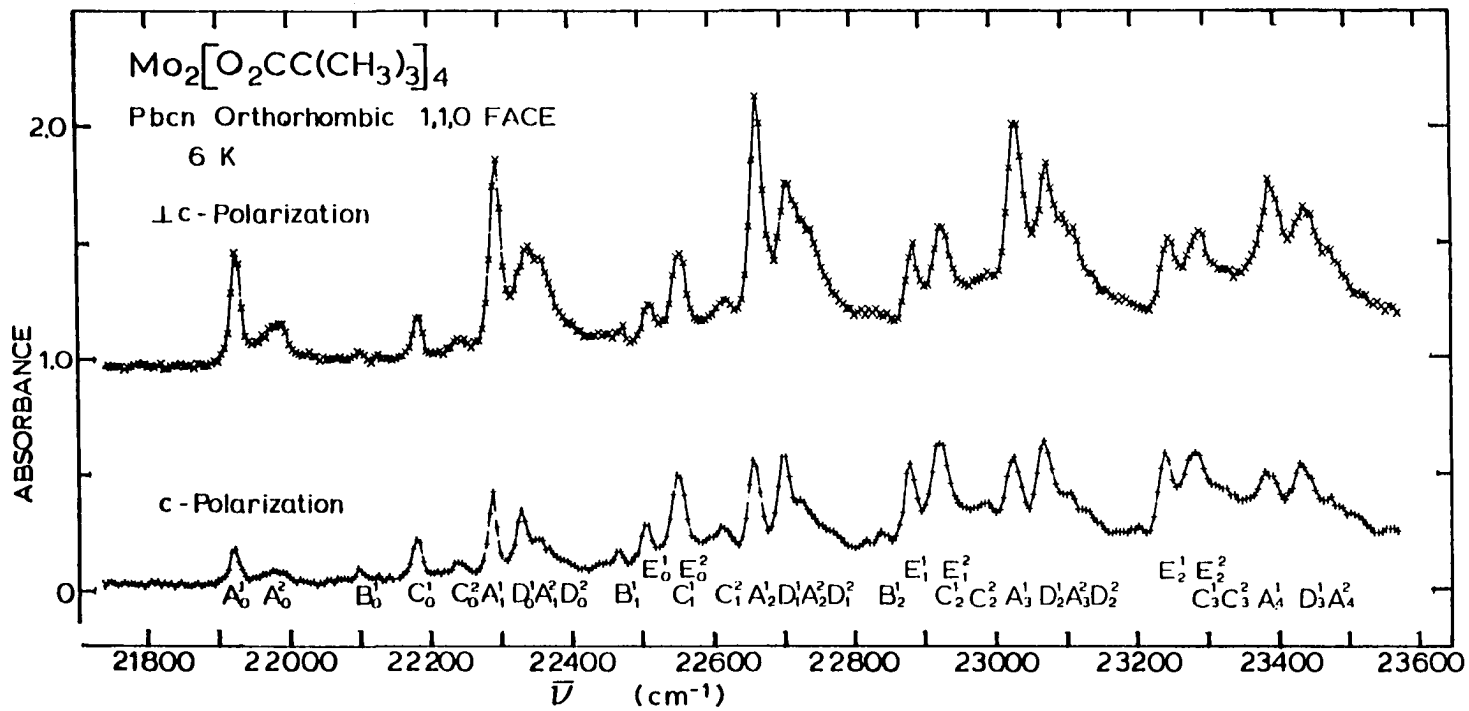

Figure 26. Resolution of vibrational structure in the first band for a crystal of the orthorhombic crystal of $Mo_2(piv)_4$, 20 ± 10 μm thick

polarization. Scans of the low-energy region of this band are shown in Figure 26. Some interesting differences between these spectra and the spectra of the monoclinic system can be noted. There are two components for each feature in this spectra. The first component is a very narrow high peak and the second is a rather broad low peak occurring with maximum about 60 cm^{-1} higher than the sharp peak. However, it appears that the integrated intensity of the two components is comparable (the ratio of intensities for two components was estimated to be 1.3/1). The broad peak might be a multiple-component origin with lower occupancies. According to the treatment of Davydov splitting (Appendix D), there are four Davydov states. A transition to only one Davydov state is allowed in c-polarization. Transitions to two Davydov states, differing from the one allowed in c-polarization, are allowed in $\perp$c-polarization. For a transition moment aligned with the Mo-Mo bond, the two transitions in $\perp$c polarization would collectively have only 15% of the intensity of the c-polarized transition. The splitting of the vibrational lines in the band are therefore inconsistent with Davydov splitting and must be assigned to different sites. Table 16 gives the details of the observed vibrational progressions in the orthorhombic $Mo_2(piv)_4$. In this table, the superscript 1 indicates the sharp peak, and the superscript

Table 16. Vibrational details in the low energy absorption bands of the orthorhombic crystals of $Mo_2(piv)_4$ at 6 K

Assignment	$\bar{\nu}$, cm^{-1}	$\Delta\bar{\nu}$[a], cm^{-1}
A_o^1	21925	
A_o^2	21985	(60)
B_o^1	22100	(175)
C_o^1	22185	(260)
C_o^2	22245	(320)
A_1^1	22290	365
D_0^1	22330	(405)
A_1^2	22350	(425)
D_o^2	22390	(465)
B_1^1	22470	370
E_o^1	22510	(585)

[a]Values in parentheses give the difference, $\Delta\bar{\nu}$ from the A_o^1 line. Values without parentheses give the difference $\Delta\bar{\nu}$ from the preceding line in the progression.

Table 16. Continued

Assignment	$\bar{\nu}$, cm^{-1}	$\Delta\bar{\nu}$,[a] cm^{-1}
C_1^1	22555	370
C_1^2	22615	370
A_2^1	22660	370
D_1^1	22705	375
A_2^2	22720	370
D_1^2	22765	375
B_2^1	22845	375
E_1^1	22885	375
C_2^1	22930	375
C_2^2	22990	375
A_3^1	23030	370
D_2^1	23075	370
A_3^2	23100	380
D_2^2	23130	365
B_3^1	23210	365
E_2^1	23250	365
C_3^1	23290	360
A_4^1	23390	360
D_3^1	23440	365

Table 17. Energies of the origins of corresponding intense vibrational progressions in the monoclinic and orthorhombic crystals of $Mo_2(piv)_4$

System	A_o, cm^{-1}	$B_o^i - A_o^i$, cm^{-1}	$C_o^i - A_o^i$, cm^{-1}	$D_o^i - A_o^i$, cm^{-1}	$E_o^i - A_o^i$ cm^{-1}
Monoclinic	21900	167	255	408	563
Orthorhombic	21925	175	260	405	585

2 represents the broad peak. There are B, C, D, and E progressions identifiable for which the origin separations and relative intensities are very similar to those of the monoclinic form. The separations of origins of the B, C, D, and E progressions from the A origin are also given in parentheses in the column, $\Delta\bar{\upsilon}$, of Table 16 which also listed the separation of the higher members of each progression from the preceding member. The separation of progression members is 370 ± 5 cm^{-1}, presumably representing the Mo-Mo stretch in the excited state. The lowest energy origin in the spectra is a line at 21,925 cm^{-1}, labeled A_o^1. The energies of the first intense A origins and the distances of the B_o^i, C_o^i, D_o^i, and E_o^i lines above A_o^i lines are given for two systems of $Mo_2(piv)_4$ in Table 17. The lowest energy component for the orthorhombic system was blue-shifted 25 cm^{-1} above the first intense peak for the monoclinic system. The differences for the B_o^i, C_o^i, and D_o^i lines above the A_o^i line are quite comparable for two polymorphs. The molecular environment must be very similar for the two systems.

Again, the crystal structure solved from X-ray diffraction studies at room temperature did not reveal any site difference. The rotational orientations of the tert-butyl groups in the molecule, or a second-order phase transition occurring above 65-75 K, or an impure spectroscopic specimen might explain the site difference.

For the orthorhombic system of $Mo_2(piv)_4$, the unit $\hat{a}$, $\hat{b}$, and $\hat{c}$ axes are orthogonal and were taken as $\hat{i}$, $\hat{j}$, and $\hat{k}$, respectively. The spectroscopic face was found to be 110. The crystal face contained the c-axis, therefore $\hat{Ex}1$ was taken as the extinction direction parallel to the c-axis (needle axis). $\hat{Ex}_2$ was the extinction direction perpendicular to $\hat{Ex}_1$. The observed extinctions were given by:

$$\hat{Ex}_1 = \hat{c} = \hat{k}$$

$$\hat{Ex}_2 = 0.56941\hat{i} - 0.82206\hat{j}$$

The molecular z-axis vector was defined along the Mo-Mo bond and is given by

$$\hat{z} = 0.47872\hat{i} - 0.07715\hat{j} + 0.87456\hat{k}$$

The following expected polarization ratio was calculated for the oriented-molecule model:

$$\hat{z}\cdot\hat{Ex}_1 = 0.87457$$

$$\hat{z}\cdot\hat{Ex}_2 = 0.33608$$

$$I_1/I_2 = (0.87)^2/(0.34)^2 = 6.77$$

This prediction is in serious disagreement with the observed polarization ratio of 0.377 for the sharp and broad component origins. The same calculation was performed as for monoclinic system and it was found that if the transition moment vector was shifted 40^0 away from the metal-metal bond, a satisfactory agreement with the

experimental polarization ratio was obtained as shown below:

$$\hat{\mu}(\theta) = \sin\theta\hat{x} + \cos\theta\hat{z}$$

$$\hat{\mu}(40^0) = 0.929\hat{i} - 0.086\hat{j} + 0.360\hat{k}$$

$$\hat{\mu}(40^0)\cdot\hat{Ex}_1 = 0.35977$$

$$\hat{\mu}(40^0)\cdot\hat{Ex}_2 = 0.59976$$

$$I_1/I_2 = (0.36)^2/(0.60)^2 = 0.36$$

It has been concluded that the combined A_o peaks represent an electric-dipole allowed transition $\delta \rightarrow \delta^*$ ($^1A_{1g} \rightarrow {}^1A_{2u}$) under D_{4h} symmetry from different sites. The B_o, C_o, D_o, and E_o lines correspond to different normal modes of enabling vibrations. The 260, 405, and 585 cm^{-1} vibrations which excite the C, D, and E progressions are presumably E_g vibrations. The E_g vibrations will provide the electric dipole-forbidden but vibronic-allowed transitions in x,y-polarization under D_{4h} symmetry. The A^2_{i+1} peaks overlap somewhat with the D^1_i peaks. The C^1_{i+1} peaks overlap strongly with the E^2_i peaks. The long progressions are the result of a highly relaxed metal-metal bond in the excited state.

CONCLUSIONS

This research has provided further information about the lowest energy band in the optical spectra for the dimeric complexes of rhenium(III) and molybdenum(II) which possess d^8 electronic configuration in each dimer. Recent theoretical treatments of these systems (29, 31, 63, 34) have generally indicated that the lowest energy electronic excitation in such dimers should be $\delta \rightarrow \delta^*$ transitions for the quadruple bonds.

In the present study, the spectra of $(TBA)_2Re_2Cl_8$ and $(TBA)_2Re_2Br_8$ are reported for the bands which peak about 14,000 cm^{-1}, with better resolution than those of earlier work. These spectra have provided additional insight into the vibrational assignments of the first absorption band. The present results are consistent with the assignment as the spin-allowed $\delta \rightarrow \delta^*$ ($b_{2g} \rightarrow b_{1u}$) transition which would be $^1A_{1g} \rightarrow {}^1A_{2u}$ under D_{4h} symmetry. An X-ray diffraction structure determination for $(TBA)_2Re_2Br_8$ has indicated a disordered structure similar to that of $(TBA)_2Re_2Cl_8$. This disorder provides major and minor orientations in the crystal whose different contribution could be identified in the spectra. However, other components were found in the spectra that indicated further disorder. However, the

crystal structure did not reveal such further disorder. It would be worthwhile to expend some effort on seeking salts of these anions with other cations which would provide purer spectra without these disorder effects.

Single-crystal spectra for tetrakis(carboxylato)-bridged rhenium(III) dimeric complexes have not been reported previously. The present study provides the spectra for such a complex, viz., $Re_2[O_2CC(CH_3)_3]_4Cl_2$. A possible assignment of resolvable bands has been made in the region from 15,000 to 35,000 cm^{-1}. The first strong peak at 20,600 cm^{-1} is assigned to the electric-dipole-allowed transition $\delta \rightarrow \delta^*$ ($^1A_{1g} \rightarrow {}^1A_{2u}$) in z-polarization. A weak band at 16,500 cm^{-1} was observed in the spectra. Such a band which might correspond to a spin-forbidden $\delta \rightarrow \delta^*$ transition has not been observed for any molybdenum or rhenium dimer previously. The appearance of this weak feature was therefore unexpected. It would be helpful to confirm and assign this band if spectra for other rhenium carboxylate dimers could be measured.

The assignment of the lowest energy band in the electronic absorption spectra of the tetrakis(μ-carboxylato)dimolybdenum(II) complexes has involved greater controversy. Crystals of these compounds have highly resolved, unusually rich vibrational structures for the band at liquid-helium temperatures. The spectra have frequently

been compromised by the low crystal site symmetries and by the presence of defect components. Cotton et al.'s crystals of $Mo_2(piv)_4$ (α-$Mo_2(piv)_4$) have different intermolecular bonding arrangement from any other known molybdenum carboxylates which have a planar array of twin bonds (two intermolecular bonds). Two other polymorphs, the monoclinic β-$Mo_2(piv)_4$ and the orthorhombic γ-$Mo_2(piv)_4$, were found instead of Cotton et al.'s triclinic α-$Mo_2(piv)_4$ in the synthesis of $Mo_2(piv)_4$. The cystals of β-$Mo_2(piv)_4$ and γ-$Mo_2(piv)_4$ form the same type of planar array of twin bonds which occur in the crystals of $Mo_2(O_2CCH_3)_4$ and $Mo_2(O_2CCF_3)_4$. Site splittings in these spectra were unexpected since the X-ray diffraction structure at room temperature each possessed only single sites. The observed polarization ratios for the 0-0 line of the electric-dipole allowed transition disagree with the prediction of oriented-molecular theory for two systems of $Mo_2(piv)_4$. Polarization ratios observed could be accounted for by crystal field perturbation which shifted the transition moment vectors away from the Mo-Mo bond by 30-40 degrees. The investigation of some closely related systems and low-temperature X-ray diffraction studies of the crystals of $Mo_2(piv)_4$ are still needed to characterize fully the complexes of molybdenum(II) with carboxylic bridges. However, the results in this study are consistent with the

assignment of the energy excitation of the d^8-dimers as the $\delta \rightarrow \delta^*$ transition.

BIBLIOGRAPHY

1. Bertrand, J. A.; Cotton, F. A.; Dollase W. A. J. Am. Chem. Soc. 1963, 85, 1349; Inorg. Chem. 1963, 2, 1166.

2. Bennett, M. J.; Cotton, F. A.; Walton, R. A. J. Am. Chem Soc. 1966, 88, 3866; Proc. R. Soc., London, Ser. A. 1968, 303, 1975.

3. Cotton, F. A., et al., Science, 1964, 145, 1305; Inorg. Chem. 1965, 4, 334.

4. Cotton, F. A.; Extine, M; Gage, L. D. Inorg. Chem. 1978, 17, 172.

5. Cotton, F. A.; Pipal, J. R. J. Am. Chem. Soc. 1971, 93, 5441.

6. Cotton, F. A.; Gage, L. D.; Mertis, K.; Shive, L. W.; Wilkinson, G. J. Am. Chem. Soc. 1976, 98, 6922.

7. Cotton, F. A. Chem. Soc. Rev. 1975, 4, 27.

8. Cowman, C. D.; Gray, H. B. J. Am. Chem. Soc. 1973, 95, 8177.

9. Cotton, F. A.; Frenz, B. A.; Stults, B. R.; Webb, T. R. J. Am. Chem. Soc. 1976, 98, 2768.

10. Brencic, T. J. V.; Cotton, F.A, Inorg. Chem. 1969, 8, 7.

11. Lawton, D.; Mason, R. J. Am. Chem. Soc. 1965, 87, 921.

12. Cotton, F. A.; Mester, Z. C.; Webb, T. R. Acta Cryst. 1974, B30, 2768.

13. Abel, E. W.; Singh, A.; Wilkinson, G. J. Chem. Soc. 1959, 3097.

14. Bannister, E.; Wilkinson, G. Chem. and Ind. 1960, 319.

15. Stephenson, T. A.; Bannister, E.; Wilkinson, G. J. Chem. Soc. 1964, 2538.

16. Brignole, A. B.; Cotton, F. A. Inorg. Synth. 1972, 13, 81.

17. Bino, A; Cotton, F. A.; Dori, Z. J. Am. Chem. Soc. 1981,

103, 243.

18. Cotton, F. A.; Martin, D. S.; Webb, T. R.; Peters, T. J. Inorg. Chem., 1976, 15, 1199.

19. Cotton, F. A.; Martin, D.S.; Fanwick, P. E.; Peters, T. J.; Webb, T. R. J. Am. Chem. Soc. 1976, 98, 4681.

20. Fanwick, P. E.; Martin, D. S.; Webb, T. R.; Robbins, G. A.; Newman, R. A. Inorg. Chem. 1978, 17, 2723.

21. Trogler, W. C.; Solomon, E. I.; Trjberg, I; Ballhausen, C. J.; Gray, H. B. Inorg. Chem. 1977, 16, 828.

22. Martin, D. S.; Newman, R. A.; Fanwick, P. E. Inorg. Chem. 1979, 18, 2511.

23. Cotton, F. A.; Curtis, N. F.; Johnson, B. F. G.; Robinson; W. R. Inorg. Chem. 1965, 4, 326.

24. Webb, T. R.; Espenson, J. H. J. Am. Chem. Soc. 1974, 96, 6289.

25. Collins, D. M.; Cotton, F. A.; Gage, L. D. Inorg. Chem. 1979, 18, 1712.

26. Cotton, F. A.; De Boer, B. G.; Jeremic, M. Inorg. Chem. 1970, 9, 2143.

27. Bratton, W. K.; Cotton, F. A.; De Beau, M.; Walton, R. A. J. Coord. Chem. 1971, 1, 121.

28. Slater, J. C.; Johnson, K. H. Phys. Rev. 1972, B5, 844.

29. Norman, J. G., Jr.; Kolari, H. J. J. Am. Chem. Soc. 1975, 97, 33.

30. Norman, J. G., Jr; Kolari, H. J. J. Chem. Soc. Chem. Commun. 1974, 303.

31. Mortola, A. P.; Moskomitz, J. W.; Rosch, N.; Cowman, C. D.; Gray, H. B. Chem. Phys. Lett. 1975, 32, 283.

32. Mortola, A. P.; Moskowitz, J. W.; Rosch, N. Int. J. Quantum. Chem. 1974, Symp. No.8, 161.

33. Cotton, F. A. Inorg. Chem. 1964, 3, 334.

34. Norman, J. G.; Kolari, H. J. J. Chem. Soc., Chem.

Commun. 1975, 649.

35. Norman, J. G., Jr.; Kolari, H. J.; Gray, H. B.; Trogler, W. C. Inorg. Chem. 1977, 16, 987.

36. Cotton, F. A.; Kalbacher, B.J. Inorg. Chem. 1977, 16, 2386.

37. Bursten, B. E.; Cotton, F. A.; Fanwick P. E.; Stanley, G. G. J. Am. Chem. Soc. 1983, 105, 3082.

38. Noodleman, L.; Norman, J. G., Jr. J. Chem. Phys. 1979, 70, 4903.

39. Cotton, F. A.; Walton, R. A. "Multiple Bonds Between Metal Atoms", John Wiley and Sons: New York, 1982; p426.

40. Goddard III, W. A.; Dunning, T. H., Jr.; Hunt, W. J.; Hay, P. J. Acc. Chem. Res. 1973, 6, 368.

41. Cotton, F. A.; Curtis, N. F.; Robinson, W. R. Inorg. Chem. 1965, 4, 1696.

42. Trogler, W. C.; Cowman, C. D.; Gray, H. B.; Cotton, F. A. J. Am. Chem. Soc. 1977, 99, 2993.

43. Wahlstrom, E. E. "Optical Crystallography", 4th ed.; Wiley: New York, 1972; p106.

44. McCarley, R. E.; Templeton, J. L.; Colburn, T. J.; Katovic, V.; Hoxmeier, R. J. Adv. Chem. Ser. 1976, 150, 318.

45. Bloss, F. D. "An Introduction to the Methods of Optical Crystallography"; Holt, Rinehart and Winston: New York, 1961; Chapter 5, pp. 50-53.

46. Piper, T. S. J. Chem. Phys. 1961, 35, 1240.

47. Jacobson, R. A. "An Algorithm for Automatic Indexing and Bravais Lattice Selection: The programs BlIND and ALICE". Ames Laboratory-USAEC Report 1s-3469, Iowa State University, Ames, Iowa, 1974.

48. "Crystal Data Determinative Tables", 2nd Ed.; American Cryst. Assoc., Williams and Heinz Map Corp.: Washington, D.C., 1963; pp. 2, 3.

49. Takausagawa, F. Ames Laboratory USDOE, Iowa State University, Ames, Iowa, unpublished.

50. Lawton, S. L.; Jacobson, R. A. Inorg. Chem. 1968, 7, 2124.

51. Templeton, D. H. "International Tables for X-ray Crystallography"; The Kynoch Press: Birmingham, England, 1962; Vol. III.

52. Stewart, R. F.; Davidson, E. R.; Simpson, W. T. J. Chem. Phys. 1965, 42, 3175.

53. Lapp, R. L.; Jacobson, R. A."ALLS: A Generalized Crystallographic Least-Squares Program", USDOE Report Is-4798, Iowa State University, Ames, Iowa, 1980.

54. Johnson, C. K. AEC Report ORNL-3794, Oak Ridge Tenn., March 1971 (second revision).

55. Karcher, B. A. Ph.D. Thesis, Iowa State University, 1961.

56. Jenson, W. Private communication, South Dakota State University, Brookings, South Dakota.

57. Powell, D. R.; Jacobson, R. A. "FOUR: A Generalized Crystallographic Fourier Program: Ames Laboratory-DOE Report Is-4737, Iowa State University, Ames, Iowa, 1980.

58. Martin, D. S.; Newman, R. A.; Fanwick, P. E. Inorg. Chem. 1982, 21, 3400.

59. Clark, R. J. H.; Franks, M. L. J. Am. Chem. Soc. 1976, 98, 2673.

60. Mishowski, V. M. private communication, California Institute of Technology, Pasadena, California, 1985.

61. Herzberg, G. "Electronic Spectra of Polyatomic Molecules"; Van Nostrand: New York, 1966.

62. Tutt, L; Tannor, D; Heller, E. J.; Zink, J. I. Inorg. Chem. 1982, 21, 3858.

63. Hay, P. J. J. Am. Chem. Soc. 1978, 100, 2897.

64. Cowman, C. D.; Trogler, W. C.; Gray, H. B. Isr. J. Chem. 1976/77, 15, 308.

65. Norman, J. G., Jr.; Ryan, J. B. J. Comput. Chem. 1980, 1, 59.

ACKNOWLEDGMENTS

I wish to thank Dr. D. S. Martin for his help, guidance, and support throughout my time as a graduate student. From him I have learned much indeed.

I wish to thank my parents for their encouragement and wholehearted support throughout my academic career.

I gratefully acknowledge the advice and assistance of Dr. R. A. Jacobson and members of the X-ray crystallography group with many aspects of the crystal structures.

APPENDIX A: OBSERVED AND CALCULATED STRUCTURE FACTORS FOR $[N(n\text{-}C_4H_9)_4]_2Re_2Br_8$

H =-16

K	L	FO	FC
-6	2	314	129
-2	5	194	-183

H =-15

K	L	FO	FC
-8	1	244	-247
-5	3	162	241
-4	2	205	228
-1	6	210	-224
0	1	198	271
0	5	200	-151
3	-3	195	-199
5	-1	120	129
6	-1	208	-234

H =-14

K	L	FO	FC
-10	2	156	223
-9	1	424	377
-8	2	223	73
-7	2	298	-309
-6	1	172	-159
-6	3	258	-254
-5	2	382	-466
-4	1	257	-331
-4	2	335	277
-4	3	303	-345
-3	1	171	220
-3	2	385	-363
-3	3	363	423
-2	1	364	-355
-2	2	166	218
-2	4	387	396
-2	6	188	209
-2	8	176	80
-1	1	240	-277
-1	3	290	284
0	4	281	333
0	6	405	311
6	-1	143	-193

H =-13

K	L	FO	FC
-10	1	389	-339
-8	4	168	-210
-7	1	276	277
-6	2	346	406
-5	1	435	417
-5	3	350	347
-5	4	143	-133
-4	1	408	-410
-4	2	603	599
-4	3	518	-539
-3	1	389	398
-3	2	700	-658
-3	4	566	-556
-2	2	420	426
-2	3	258	-282
-2	5	259	202
-2	9	164	106
-1	1	262	266
-1	2	205	-237
-1	4	372	-386
-1	6	232	-211
0	1	321	338
0	3	413	-422
0	5	258	-272
0	7	307	-313
4	-6	141	-132
8	-1	107	-128
9	-2	207	-181
10	-3	210	161

H =-12

K	L	FO	FC
-13	2	272	279
-12	0	252	61
-12	1	261	212
-11	2	154	177
-10	2	248	179
-9	4	231	268
-7	0	143	-191
-7	3	324	-296
-6	1	325	-338
-6	3	152	-185
-5	1	229	223
-5	2	426	-411
-5	3	211	226
-5	4	104	-111
-5	6	406	-404
-4	1	721	-734
-4	2	623	596
-4	3	244	-247
-4	4	403	414
-4	5	173	-179
-3	1	453	430
-3	2	568	-557
-3	3	932	877
-3	5	230	284
-3	7	202	244
-2	1	383	-371
-2	2	602	559
-2	4	463	433
-2	6	267	289
-2	8	274	279
-1	1	124	159
-1	2	226	-306
-1	3	467	487
-1	4	265	267
-1	7	574	521
0	2	453	453
0	4	279	311
0	6	464	420
0	8	475	451
7	-4	153	-206

H =-11

K	L	FO	FC
-13	1	233	-261
-13	3	191	-192
-12	2	328	-309
-12	3	141	-213
-11	2	166	-187
-11	4	178	-265
-8	3	300	308
-7	4	280	285
-6	0	253	238
-6	1	307	-264
-6	2	107	175
-6	3	241	269
-6	4	167	167
-6	6	460	439
-5	1	336	400
-5	2	326	-299
-5	3	322	419
-5	5	314	444
-4	2	498	503
-4	3	409	-389
-4	6	417	435
-3	1	487	461
-3	2	268	-269
-3	3	405	395
-3	4	178	-219
-3	6	297	-279
-2	2	368	386
-2	3	600	-615
-2	4	142	-139
-2	5	332	-360
-2	7	615	-566
-2	8	286	-262
-1	2	356	-305
-1	4	388	-438
-1	6	643	-549
-1	8	723	-599
0	1	414	-441
0	3	250	-250
0	7	1057	-852
0	9	371	-330
5	-2	137	139
7	0	161	-218
7	-1	166	-306
8	-3	210	-237
9	-3	159	263
10	-3	316	-343

H =-10

K	L	FO	FC
-14	2	205	190
-14	4	224	119
-13	1	173	212
-13	3	223	268
-12	1	171	239
-12	2	451	310
-12	3	207	226
-12	4	256	214
-12	6	313	110
-11	2	205	212
-10	0	311	-442
-10	1	175	195
-10	2	150	-207
-10	4	169	-151
-9	3	536	-553
-9	7	159	-172
-8	1	291	328
-8	2	178	-138
-8	4	520	-537
-8	6	287	-219
-7	1	323	301
-7	2	168	-166
-7	3	405	-402
-7	4	197	-228
-7	5	233	-282
-7	8	231	234
-6	3	308	-339
-6	5	285	-273
-5	2	553	-595
-5	4	209	-192
-5	6	491	-461
-4	1	547	-511
-4	2	564	-555
-4	3	645	-627
-4	4	156	156
-4	5	309	-324
-4	6	212	238
-4	9	195	210
-3	1	618	-584
-3	2	669	-680
-3	5	440	465
-3	7	494	459
-3	8	413	369
-2	1	196	-245
-2	2	165	-246
-2	3	474	-464
-2	4	465	397
-2	5	233	248
-2	6	485	457
-2	7	309	270
-2	8	391	383
-2	9	164	211
-1	2	339	-328
-1	3	435	404
-1	4	199	-314
-1	5	438	416
-1	7	1009	834
-1	8	383	328
-1	9	284	309
0	2	582	477
0	4	686	663
0	6	1042	923
0	8	888	759
0	-2	129	-135
3	0	105	164

H = -9

K	L	FO	FC
-14	1	353	-287
-14	2	294	-270
-13	1	214	-202
-13	2	321	-324
-12	1	244	-173
-12	2	242	-233
-12	8	161	217
-11	1	139	-197
-11	2	158	242
-11	4	168	179
-10	1	373	393
-10	3	691	663
-10	4	190	209
-9	0	498	509
-9	1	211	-240
-9	2	487	543
-9	3	365	429
-9	4	745	788
-9	6	137	239
-8	2	334	337
-8	3	823	811
-8	4	297	319
-8	5	387	388
-8	7	223	213
-8	9	168	-172
-7	3	504	526
-7	4	443	460
-7	10	222	-224
-6	2	702	772
-6	3	161	236
-5	1	553	541
-5	2	427	464
-5	3	489	472
-5	11	174	-97
-4	1	1197	1247
-4	2	898	955
-4	3	277	338
-4	5	246	-253
-4	8	311	-270
-3	1	456	508
-3	2	1072	1156
-3	3	897	927
-3	4	253	-262
-3	6	364	-349
-3	7	214	-216
-3	9	296	-294
-2	1	1000	973
-2	2	1057	1037
-2	3	240	-292
-2	4	259	258
-2	5	429	-416
-2	7	651	-579
-2	8	548	-486
-1	1	142	143
-1	2	275	-293
-1	3	324	381
-1	4	1043	-997
-1	6	637	-574
-1	8	690	-612
-1	12	180	-168
0	1	160	-89
0	3	1444	-1354
0	5	822	-697
0	7	885	-683
0	9	296	-265
0	11	418	-339
6	-3	126	-171
10	-2	191	352

H = -8

K	L	FO	FC
-14	2	431	193
-14	6	314	79
-13	1	181	190
-12	3	155	194
-12	4	359	-93
-12	6	283	242
-12	8	194	49
-11	1	278	-346
-11	2	141	183
-11	3	767	-746
-10	1	214	231
-10	2	868	-834
-10	4	902	-878
-9	0	461	315
-9	1	481	-343
-9	2	327	-336
-9	3	1167	-1164
-9	4	274	-276
-9	5	434	-444
-9	7	238	-262
-8	1	271	-261
-8	2	429	-467
-8	3	653	-695
-8	4	793	-774
-8	6	402	-358
-7	2	811	-826
-7	5	293	-301
-7	7	285	-357
-6	1	828	-767
-6	2	395	-227
-6	3	348	-327
-6	4	175	-249
-6	5	579	602
-6	10	284	242
-5	1	686	-748
-5	2	1001	-1093
-5	3	481	-503
-5	4	789	779
-5	12	280	227
-4	1	890	-961
-4	2	1106	-1162
-4	3	357	-375
-4	5	821	805
-4	9	312	310
-4	10	191	-23
-3	1	1634	-1600
-3	2	1278	-1253
-3	3	119	-221
-3	8	487	424
-2	1	521	-493
-2	2	611	-237
-2	3	1082	-1076
-2	4	796	758
-2	5	271	-327
-2	8	365	273
-2	9	260	293
-1	1	196	-331
-1	2	644	-641
-1	3	1838	1694
-1	4	425	-420
-1	5	387	372
-1	7	473	380
-1	9	226	169
-1	11	379	299
0	2	1176	1109
0	4	1722	1468
0	8	645	497
0	10	396	362
6	-3	101	-218
7	-1	535	-629
10	-3	253	-340
11	0	336	-405

H = -7

K	L	FO	FC
-14	4	155	180
-14	5	143	-196
-13	1	116	112
-12	1	188	231
-12	2	247	-254
-12	3	466	500
-12	8	258	307
-11	1	160	-206
-11	2	787	768
-11	3	168	-215
-11	4	581	573
-10	1	709	737
-10	2	261	-342
-10	3	1157	1176
-10	5	264	303
-9	1	147	-177
-9	2	841	853
-9	4	943	946
-9	5	311	319
-9	6	188	217
-9	7	383	388
-9	8	193	246
-8	0	117	336
-8	1	440	463
-8	2	523	537
-8	3	800	826
-8	4	136	190
-8	5	412	454
-8	6	554	553

H = -6

K	L	FO	FC
-16	2	200	138
-16	3	137	140
-16	4	174	241
-15	3	329	336
-15	5	167	249
-14	4	469	317
-14	5	169	-218
-13	1	273	-281
-13	8	238	-321
-12	2	618	-496
-12	3	178	223
-12	4	380	357
-12	6	228	-65
-12	9	272	-320
-11	1	621	-646
-11	2	623	640
-11	3	876	-853
-11	4	123	135
-11	5	295	-309
-10	1	543	593
-10	2	275	291
-10	3	444	444
-10	4	869	-880
-10	5	276	-325
-10	6	388	-190
-10	7	270	-295
-10	8	156	-200
-9	1	468	-471
-9	2	373	411
-9	3	896	-722
-9	4	130	-214
-9	5	358	-400
-9	6	748	-764
-9	7	418	-472
-9	8	188	-275
-8	2	864	-886
-8	4	920	-916
-8	5	457	-443
-8	6	536	-479
-8	7	666	-644
-8	8	313	-496
-7	1	944	-1002
-7	2	208	-177
-7	3	965	-1006
-7	4	112	243
-7	5	622	-680
-7	6	367	-339
-7	7	808	-814
-6	2	1039	-1078
-6	4	1103	-1127
-6	5	615	638
-6	6	587	-617
-6	8	624	-524
-6	9	274	330
-6	10	280	30
-5	1	972	-964
-5	2	227	-229
-5	3	1292	-1316
-5	4	1124	1119
-5	5	1003	-1043
-5	6	349	318
-5	7	200	-253
-5	8	679	637
-4	1	188	198
-4	2	255	-328
-4	4	1045	-998
-4	5	839	836
-4	6	405	-302
-4	8	668	419
-4	9	722	686
-4	12	170	-14
-3	1	684	734
-3	2	241	-249
-3	3	181	-258
-3	5	475	-501
-3	6	278	-315
-3	7	521	480
-3	8	494	455
-3	10	304	330
-2	1	403	-395
-2	2	236	-136
-2	4	410	-79
-2	5	303	-266
-2	6	377	-334
-2	7	396	-408
-2	8	777	558
-2	9	457	420
-2	10	243	-96
-1	1	319	262
-1	3	765	710
-1	4	421	-440
-1	5	351	-435
-1	6	714	-652
0	2	562	607
0	4	720	665
0	6	510	-501
0	10	404	-328
10	-2	224	204
10	-1	283	-310
16	0	137	106

H = -5

K	L	FO	FC
-17	2	166	-192
-16	1	199	-230
-16	2	217	-226
-16	3	400	-379
-15	2	360	-272
-15	4	448	-428
-14	2	152	-207
-14	3	328	-286
-14	8	161	232
-13	2	130	168
-13	5	218	316
-13	9	253	295
-12	1	257	278
-12	3	420	456
-12	4	177	233
-12	5	400	408
-12	7	350	367
-11	1	730	-724
-11	3	201	-257
-11	4	718	760
-11	5	498	519
-11	6	336	345
-11	7	200	222
-10	2	720	-713
-10	3	853	832
-10	4	251	283
-10	5	523	542
-10	6	370	398
-10	7	258	299
-9	1	467	-492
-9	2	165	209
-9	3	302	-332
-9	4	929	989
-9	5	445	414
-9	6	293	316
-9	7	440	440
-9	8	177	297
-9	10	245	-296
-8	0	222	-209
-8	1	976	1030
-8	2	461	-456
-8	3	777	828
-8	5	300	328
-8	6	353	345
-8	7	628	606
-7	1	694	-773
-7	2	1558	1559
-7	3	279	320
-7	4	1493	1530
-7	6	491	539
-7	8	736	691
-7	9	255	-264
-6	1	1895	1985
-6	2	549	578
-6	3	1869	1966
-6	4	184	-201
-6	5	1097	1110
-6	6	291	-361
-6	7	743	723
-6	8	621	-627
-6	9	354	328
-5	1	725	-760
-5	2	896	989
-5	3	836	836
-5	4	1210	1233
-5	5	576	-637
-5	6	330	613
-5	7	477	-481
-5	9	748	-722
-4	0	224	-261
-4	1	559	-556
-4	3	1101	1035
-4	4	320	-371
-4	5	768	798
-4	6	227	-325
-4	7	165	-246
-4	8	840	-747
-4	9	245	-223
-3	1	194	-201
-3	4	365	374
-3	5	345	-351
-3	8	936	-907
-3	9	750	-694
-2	1	853	-793
-2	2	312	-338
-2	3	579	-539
-2	6	391	411
-2	7	443	-408
-2	8	220	-290
-2	10	329	-357
-1	1	669	-635
-1	2	1034	1131
-1	3	402	-418
-1	4	460	-433
-1	7	271	312
-1	10	699	637
0	1	1445	1489
0	3	518	466
0	5	230	178
0	9	802	713
0	11	399	390
4	-12	301	336
6	-3	98	205
11	-4	90	124
14	0	115	92
14	-6	239	252

H = -4

K	L	FO	FC
-17	1	345	355
-17	3	244	274
-16	2	434	399
-16	3	294	309
-16	4	372	337
-15	1	389	367
-15	2	331	303
-15	3	430	395
-14	2	153	164
-14	5	148	-224
-14	8	200	-105
-13	2	153	225
-13	3	163	-276
-13	4	287	-331
-13	5	121	-210
-13	7	155	-219
-12	1	324	292
-12	2	167	117
-12	4	783	-777
-12	5	620	-634
-12	6	400	-393
-12	8	179	-196
-11	2	135	-119
-11	3	444	-436
-11	4	612	-671
-11	5	825	-834
-11	6	376	-413
-11	7	312	-349
-10	1	447	471
-10	2	358	367
-10	4	856	-901
-10	5	438	-447
-10	6	221	-290
-10	7	261	-264
-9	1	84	-83
-9	2	621	637
-9	3	645	-670
-9	5	489	-490
-9	6	325	-287
-9	8	223	-302
-8	1	715	795
-8	2	977	-977
-8	4	1399	-1408
-8	5	329	365
-8	6	212	-292
-8	8	452	-488
-7	1	1956	-1997
-7	3	1904	-2068
-7	5	657	-689
-7	6	436	516
-7	7	584	-589
-7	8	480	487
-7	9	314	-394
-6	1	633	685
-6	2	1956	-1959
-6	3	1190	-1222
-6	4	1625	-1604
-6	5	461	496
-6	6	628	-393
-6	7	474	446
-6	8	724	-570
-6	9	502	480
-6	11	218	-232
-6	12	198	-43
-5	1	835	-859
-5	2	1254	-1327
-5	3	1209	-1309
-5	4	546	-551
-5	5	990	-1036
-5	6	696	649
-5	7	391	-482
-5	8	821	803
-4	1	782	824
-4	3	1345	-1409
-4	4	477	-86
-4	5	648	719
-4	6	521	-441
-4	7	481	479
-4	8	327	-144
-4	9	787	742
-4	10	587	-72
-3	1	1305	1336
-3	2	234	-228
-3	3	268	280
-3	4	766	747
-3	6	413	427
-3	8	511	492
-3	10	240	217
-2	1	965	1035
-2	2	666	-613
-2	3	564	519
-2	4	931	967
-2	5	1382	1377
-2	6	397	-350
-2	8	419	-41
-2	9	457	461
-2	10	425	-481
-1	1	2038	-2009
-1	3	393	354
-1	4	764	798
-1	5	487	514
-1	6	281	334
-1	8	276	312
-1	9	950	-938
-1	10	185	213
-1	11	324	-399
0	2	2752	-2752
0	4	1149	1043
0	8	554	-270
0	10	1142	-1019
6	-2	356	-137
15	-5	221	306
15	-3	212	289
17	-1	186	261

H = -3

K	L	FO	FC
-18	1	179	-218
-17	2	330	-307
-17	4	172	-209
-16	1	492	-486
-16	2	226	-210
-16	3	254	-300
-15	2	163	-214
-15	3	316	-366
-14	1	277	-311
-14	2	291	-299
-13	1	257	-259
-13	4	330	346
-13	5	483	498
-12	1	192	-231
-12	2	102	85
-12	3	379	398
-12	4	682	726
-12	5	375	422
-12	6	348	389
-11	1	177	189
-11	2	396	-439

-11	3	359	354	-3	2	1133	-1065	-12	7	258	-249	-3	4	1717	1656	-11	1	595	667	-3	4	717	-656	2	2	1514	106
-11	4	796	842	-3	3	230	210	-12	8	280	-274	-3	5	164	-276	-11	2	358	-322	-3	5	2079	-2076	2	3	830	853
-11	5	645	662	-3	4	1441	-1373	-12	9	266	-307	-3	6	1332	1283	-11	5	653	674	-3	6	1363	1417	2	4	726	663
-11	6	165	190	-3	5	1740	-1798	-11	2	401	-413	-3	7	1258	-1315	-11	6	147	-180	-3	8	346	439	2	5	1348	-1281
-11	7	327	338	-3	6	868	909	-11	4	424	-434	-3	8	302	311	-11	7	386	421	-3	9	505	-538	2	6	276	-207
-11	8	200	275	-3	7	402	-418	-11	6	651	-648	-3	9	397	-410	-11	8	479	557	-3	10	576	622	2	7	414	-384
-11	9	417	430	-3	8	518	585	-11	7	283	-321	-2	1	149	206	-11	9	219	315	-2	1	2287	-2406	2	9	449	-449
-10	1	475	-505	-3	9	609	-602	-11	8	465	-459	-2	2	1831	1626	-10	1	897	870	-2	3	1432	-1430	2	10	803	-795
-10	2	283	277	-3	10	265	319	-10	1	756	-786	-2	3	1183	1065	-10	2	363	365	-2	4	1823	-1846	2	11	199	259
-10	3	409	433	-2	1	161	-185	-10	2	282	-72	-2	4	1774	1481	-10	3	216	220	-2	5	369	454	2	12	349	-340
-10	4	161	208	-2	2	1013	-969	-10	4	667	-707	-2	5	2779	2723	-10	6	248	268	-2	6	1330	-1339	3	1	1397	1497
-10	5	395	397	-2	3	1374	-1407	-10	7	374	-400	-2	6	1093	-1199	-10	7	284	352	-2	7	556	603	3	2	627	-730
-10	6	173	189	-2	4	2206	-2243	-10	8	478	-498	-2	7	621	596	-10	8	292	348	-2	8	506	-552	3	3	93	-78
-10	7	428	485	-2	5	282	-302	-10	9	466	-465	-2	8	488	-418	-10	9	287	344	-2	9	309	356	3	4	575	-602
-10	8	454	464	-2	6	1332	-1306	-9	1	692	-765	-2	9	457	461	-9	2	297	316	-2	11	522	542	3	5	184	197
-10	10	264	310	-2	7	371	399	-9	2	159	-178	-2	10	686	-605	-9	3	130	-171	-1	1	762	984	3	6	1232	-1191
-9	2	235	232	-2	8	209	-239	-9	3	982	-1046	-1	1	1349	1384	-9	4	926	950	-1	2	2715	-2782	3	7	413	-423
-9	4	1039	1154	-2	9	468	485	-9	4	756	808	-1	2	583	636	-9	5	435	-461	-1	3	491	-520	3	8	675	-672
-9	5	483	-496	-2	10	274	-276	-9	5	383	-430	-1	3	1846	1870	-9	8	460	521	-1	4	1423	-1394	3	9	718	-722
-9	8	345	422	-2	12	214	-276	-9	6	326	398	-1	4	1647	1819	-8	1	642	708	-1	5	1607	-1579	3	10	204	-271
-8	1	1193	1217	-1	1	631	-581	-8	2	720	-666	-1	6	1126	1157	-8	2	205	-173	-1	6	555	604	3	11	575	-593
-8	3	1457	1513	-1	2	1358	1222	-8	3	708	724	-1	7	194	-289	-8	3	880	936	-1	7	592	-620	4	0	1505	-894
-8	4	873	-887	-1	3	857	-811	-8	4	1364	-1386	-1	9	285	-316	-8	4	903	-893	-1	8	506	-531	4	1	2959	-2937
-8	5	464	472	-1	4	1879	-1804	-8	5	1341	1411	-1	11	330	-340	-8	5	417	464	-1	10	563	594	4	2	370	-270
-8	6	617	-669	-1	5	1625	-1569	-8	6	368	283	-1	13	268	-282	-8	6	307	-340	-1	12	238	359	4	3	927	-898
-7	1	649	-713	-1	6	342	362	-8	8	391	-408	0	2	1945	862	-7	1	867	-899	0	1	3952	-4511	4	4	290	248
-7	2	1684	1701	-1	7	424	-412	-7	1	635	-736	0	4	1920	2026	-7	3	632	-686	0	3	1307	-1334	4	5	1303	-1272
-7	3	369	393	-1	10	849	808	-7	2	233	145	0	6	641	-595	-7	4	1062	1048	0	7	530	-514	4	6	208	56
-7	4	1426	1503	0	1	486	-268	-7	3	1212	-1279	0	8	332	394	-7	5	990	-1060	0	9	207	-284	4	7	191	-215
-7	5	1149	-1219	0	3	239	-321	-7	4	1134	1157	0	10	632	-633	-7	6	379	-385	0	11	667	646	4	8	406	-390
-7	7	422	-414	0	5	901	-897	-7	5	378	-410	0	12	285	-297	-7	8	279	-330	0	13	313	369	4	9	935	-978
-7	8	333	430	0	7	570	648	-7	6	700	696	3	-12	147	-216	-7	9	382	-344	9	-10	206	-268	4	10	309	-493
-7	9	167	-209	0	9	855	877	-6	1	478	446	9	-9	288	368	-7	10	320	-350	11	-7	155	29	5	1	628	621
-6	1	1577	1607	0	11	558	563	-6	2	469	-458	10	-4	110	-118	-6	1	665	-690	12	-2	108	117	5	2	2187	-2229
-6	2	771	798	4	-1	430	-414	-6	3	480	-478	15	-6	134	-234	-6	2	1275	-1273	15	-6	232	219	5	3	121	194
-6	3	1542	1635	7	-1	242	210	-6	4	817	-840	17	-3	194	168	-6	4	790	-760					5	4	961	-964
-6	4	116	164	14	-3	171	-235	-6	5	843	923					-6	7	259	-304		H =	0		5	5	248	172
-6	5	475	521	15	-4	221	-210	-6	9	662	622		H =	-1		-6	9	268	-325	K	L	FO	FC	5	6	268	-285
-6	6	588	-616	16	-5	147	-179	-6	10	452	156	K	L	FO	FC	-6	10	466	-477	-14	3	128	166	5	7	275	296
-6	7	408	459					-5	2	655	-697	-18	1	199	-242	-5	1	1118	-1130	-8	1	111	197	5	8	362	-435
-6	8	619	-607		H =	-2		-5	3	311	273	-17	2	146	-161	-5	2	904	-784	-2	-8	136	127	5	10	652	-613
-6	9	277	377	K	L	FO	FC	-5	4	251	341	-17	4	355	-317	-5	3	391	-478	-1	12	231	-184	6	0	1693	1446
-5	1	170	-143	-18	2	178	203	-5	5	483	-549	-16	1	183	-234	-5	5	809	-810	0	2	2341	2254	6	1	2424	-2368
-5	2	269	299	-17	1	377	392	-5	7	508	-519	-15	1	117	154	-5	6	157	253	0	4	1796	1462	6	2	1278	1169
-5	3	1738	1852	-17	3	215	254	-5	8	266	272	-14	1	494	-506	-5	7	389	439	0	6	394	-376	6	3	1059	-1038
-5	4	776	763	-16	2	234	178	-5	10	274	312	-14	2	148	-145	-5	9	812	-819	0	8	1112	1096	6	4	177	-26
-5	5	699	-736	-15	1	356	330	-4	0	183	-67	-14	3	174	-202	-4	1	606	-660	0	10	632	-635	6	5	713	-738
-5	6	630	605	-15	2	133	186	-4	1	145	-177	-14	5	194	-224	-4	2	1062	-1020	0	12	361	-350	6	6	590	601
-5	8	403	425	-14	1	170	162	-4	2	1443	1101	-13	2	389	-456	-4	3	1112	-1005	1	1	3582	3850	6	8	497	465
-5	9	328	-345	-14	2	215	96	-4	3	410	-440	-13	3	293	-333	-4	4	994	-1065	1	2	431	-423	6	9	765	-773
-4	0	241	185	-14	3	356	376	-4	4	376	374	-13	4	231	-296	-4	5	307	359	1	3	888	823	6	10	396	385
-4	1	188	-180	-13	1	379	407	-4	5	1425	1494	-13	5	520	546	-4	6	344	-338	1	5	644	549	6	12	238	34
-4	2	1214	1240	-13	2	154	152	-4	6	1267	-1252	-13	6	199	-279	-4	7	836	853	1	6	905	-893	7	1	784	745
-4	3	925	-893	-13	4	158	250	-4	8	707	-581	-12	1	331	-347	-4	8	239	-274	1	7	359	402	7	2	1455	-1418
-4	5	418	435	-13	6	142	-217	-4	9	471	478	-12	2	97	-154	-4	9	392	438	1	8	329	-345	7	4	112	-116
-4	6	704	-664	-12	2	345	338	-4	12	193	-46	-12	3	431	-441	-4	10	590	-578	1	11	595	-623	7	5	244	-263
-4	7	742	793	-12	3	139	-163	-3	1	1363	1410	-12	4	286	310	-3	1	575	-591	1	13	272	-282	7	7	681	617
-4	8	449	-420	-12	4	342	-198	-3	2	246	-211	-12	5	314	-307	-3	2	126	-187	2	0	2785	2590	7	8	234	-238
-3	1	272	-262	-12	5	721	-722	-3	3	1924	1949	-12	6	642	627	-3	3	470	-493	2	1	808	-819	7	9	494	452

7	10	311	-330	-7	-7	177	-150	4	11	220	294	12	5	305	-260	1	9	186	-225	7	3	575	579	16	2	414	384
7	11	216	243	-8	-7	138	-99	5	0	331	-304	12	6	464	-443	1	11	265	-282	7	4	290	317	17	0	337	-119
8	2	696	215	-6	-8	144	446	5	1	2740	2756	13	0	661	-639	1	12	251	244	7	6	685	-695	17	1	435	367
8	3	292	300	-6	-5	113	102	5	2	356	-380	13	1	340	-305	2	0	2736	1819	7	7	624	636	17	2	139	-127
8	4	937	-912	-5	-4	117	-121	5	3	1659	1636	13	2	1154	-1030	2	1	462	-529	7	9	437	421	17	4	135	-159
8	6	299	243	-3	-7	170	239	5	4	372	-380	13	4	336	-317	2	2	216	-230	7	11	354	402	18	0	503	373
8	9	262	-238	-2	-2	73	101	5	5	1945	1901	13	5	622	-559	2	3	1951	1863	8	0	1103	-1061				
8	10	475	396	-1	-9	147	208	5	6	859	-884	13	7	215	-205	2	4	2068	1930	8	1	362	368		H =	3	
9	1	999	-1006	0	1	3403	-3178	5	7	305	308	14	0	274	-249	2	5	338	356	8	2	847	796	K	L	FO	FC
9	2	223	227	0	3	870	-919	5	8	276	-274	14	1	1007	-870	2	6	735	314	8	3	1707	1746	-12	-8	140	-193
9	3	419	-449	0	5	1361	-1311	5	9	817	756	14	2	322	-309	2	7	275	-348	8	4	708	-401	-9	-9	151	-198
9	4	385	385	0	7	109	193	6	0	432	450	14	3	642	-580	2	8	383	-68	8	5	404	428	-9	-3	96	172
9	5	355	-351	0	11	520	460	6	1	365	-359	14	4	337	-326	2	9	280	-311	8	6	439	437	-2	-11	136	219
9	6	102	139	0	13	215	193	6	2	1122	1169	14	6	437	-458	2	10	503	-499	8	8	313	281	0	1	1342	-1220
10	0	1724	-1549	1	0	4841	-5407	6	3	382	-376	15	0	625	-617	2	11	266	266	8	10	620	491	0	3	2219	-2117
10	2	156	-21	1	1	405	426	6	4	330	327	15	1	469	-433	3	0	1269	-1288	9	0	636	-663	0	5	102	123
10	3	218	245	1	2	2039	-1921	6	5	381	-422	15	2	729	-633	3	1	1183	-1109	9	1	333	-330	0	7	1659	1472
10	4	601	-298	1	3	2476	-2277	6	6	709	639	15	4	167	-200	3	2	611	-623	9	2	1025	1023	0	9	134	155
10	5	461	497	1	4	1665	-1552	6	7	736	-685	15	5	288	-306	3	3	861	851	9	3	221	267	0	11	156	165
10	8	460	-460	1	5	349	-497	6	8	318	307	16	1	330	-457	3	4	178	-171	9	4	1073	1054	1	0	911	-916
11	1	470	-479	1	6	139	170	6	9	330	-369	16	2	126	-143	3	5	1722	1794	9	5	106	151	1	1	367	333
11	3	363	387	1	7	107	124	6	10	363	373	16	3	323	-302	3	6	1316	-1287	9	6	253	235	1	2	1143	-1170
11	4	220	214	1	8	149	-243	6	11	315	-245	17	0	419	-422	3	7	299	300	9	7	772	765	1	3	834	-751
11	5	362	373	1	9	163	176	7	0	329	-356	17	2	242	-260	3	8	333	-360	10	0	776	-750	1	4	2513	-2286
11	6	510	524	1	10	762	686	7	1	1307	1281	17	3	193	185	3	9	185	-224	10	1	220	241	1	6	1235	1146
12	0	426	-127	1	11	303	-299	7	2	1335	-1293	17	4	370	-330	3	11	234	-266	10	2	739	197	1	7	294	-318
12	2	1062	817	1	12	249	226	7	3	681	-668	18	1	335	-327	4	1	2357	-2268	10	3	818	833	1	8	317	352
12	3	195	-234	2	0	477	-434	7	4	454	426	18	2	193	186	4	2	1126	-761	10	5	268	331	1	9	146	221
12	4	665	556	2	1	2329	-2271	7	6	506	-471					4	3	461	-462	10	6	1091	979	1	10	250	237
12	5	678	664	2	3	368	-418	7	8	390	-432		H =	2		4	4	1392	1392	10	8	431	365	2	0	1021	972
12	6	414	382	2	4	289	-313	7	9	307	315	K	L	FO	FC	4	5	2758	-2655	10	10	336	243	2	1	1332	-1378
12	7	390	390	2	5	1124	-1046	7	10	665	-590	-16	-6	142	-4	4	6	1155	1160	11	2	364	408	2	2	512	493
13	1	814	798	2	6	783	716	8	0	132	145	-16	-4	188	215	4	7	890	-899	11	4	266	256	2	3	1356	-1406
13	3	854	811	2	8	582	592	8	1	217	-188	-14	-8	144	-45	4	8	290	322	11	5	189	230	2	4	375	-366
13	4	220	240	2	9	473	464	8	2	328	-286	-14	-6	212	217	4	9	599	-548	11	7	614	578	2	5	1428	-1349
13	5	268	283	2	11	564	570	8	3	171	-201	-13	-9	137	-112	4	10	188	-165	12	0	278	253	2	6	220	196
13	6	301	310	2	12	343	339	8	4	1117	-1110	-10	-10	132	25	5	0	499	-520	12	1	639	585	2	7	280	312
14	0	841	753	3	0	714	-700	8	5	232	331	-9	-9	141	-206	5	1	287	-268	12	2	573	533	2	10	147	165
14	1	253	261	3	1	1329	1481	8	7	338	-406	-9	-8	207	277	5	2	1472	-1562	12	4	222	-60	2	12	223	-208
14	2	724	691	3	2	2313	2330	8	8	135	194	-9	-7	250	-267	5	3	466	444	12	5	318	291	3	0	1486	-1471
14	4	402	268	3	3	829	-791	8	9	476	-436	-6	-8	179	-138	5	4	1562	-1508	12	6	389	420	3	1	991	1026
14	5	399	373	3	4	1309	-1276	9	0	1551	1580	-5	-9	154	-253	5	5	848	884	13	0	528	463	3	2	574	-649
15	1	429	464	3	5	1268	1169	9	3	1356	-1283	-4	-10	154	-220	5	6	1938	-1909	13	1	769	717	3	3	148	136
15	2	191	171	3	6	537	-512	9	4	609	611	-3	-10	240	-258	5	7	562	520	13	2	660	605	3	4	1655	-1665
15	3	276	286	3	7	817	736	9	5	531	-593	0	0	3060	2921	5	8	213	-261	13	3	458	449	3	5	1573	1538
16	0	488	403	3	9	746	723	9	6	417	-404	0	2	2089	1468	5	11	147	109	13	4	317	325	3	6	519	-576
16	1	253	242	3	10	800	760	9	7	189	173	0	4	3230	3073	6	0	713	-746	13	6	435	459	3	7	313	343
16	2	246	251	3	11	264	-228	10	0	584	573	0	6	818	-775	6	1	1063	-1080	14	0	710	695	3	8	596	-597
16	4	298	291	4	0	1279	1301	10	1	864	879	0	8	488	-535	6	2	979	857	14	1	827	778	3	9	319	325
17	1	262	238	4	1	645	664	10	2	296	-307	0	10	607	-445	6	3	281	-315	14	2	986	844	4	2	1183	1229
17	3	356	340	4	2	2241	2298	10	4	782	-747	1	0	176	266	6	4	864	913	14	3	358	351	4	3	487	-516
17	4	169	-219	4	3	101	98	10	7	351	-362	1	1	2347	2388	6	5	1917	-1870	14	4	221	81	4	4	1564	1604
17	5	217	210	4	4	775	851	11	0	777	821	1	2	858	812	6	6	562	524	14	5	585	562	4	5	1223	-1268
18	0	320	245	4	5	1156	-1103	11	2	604	-573	1	3	1746	1548	6	7	262	-291	15	0	191	179	4	6	1802	1750
18	2	302	208	4	6	1376	1357	11	4	229	-203	1	4	725	653	6	8	372	274	15	1	929	837	4	7	473	-494
				4	7	439	-444	11	5	592	-632	1	5	1386	1353	6	10	482	408	15	2	461	413	4	9	446	-387
	H =	1		4	8	627	539	11	6	528	-534	1	6	572	-553	6	12	173	132	15	3	379	369	5	0	404	487
K	L	FO	FC	4	9	459	443	12	1	623	-603	1	7	821	-756	7	0	238	252	15	4	209	239	5	1	630	646
-12	-8	198	-312	4	10	339	369	12	3	802	-780	1	8	132	-122	7	2	753	729	16	0	627	609	5	3	911	880

5 4 576 -557	13 5 369 -365	4 3 1120-1121	12 0 184 -137
5 5 2778 2769	14 0 353 -306	4 4 362 379	12 1 1309 1237
5 6 732 -735	14 1 307 -303	4 5 1706-1710	12 2 364 -246
5 7 308 303	14 2 774 -741	4 6 772 589	12 3 905 448
5 8 342 -354	14 4 367 -314	4 8 1063 960	12 4 216 -170
5 10 281 -287	14 6 317 -317	4 10 388 396	12 5 394 399
6 0 709 -656	15 0 639 -639	5 0 864 967	13 0 645 608
6 1 622 638	15 1 332 -364	5 2 897-1016	13 1 269 -300
6 2 308 306	15 2 422 -387	5 4 1416-1437	13 2 975 907
6 3 399 -391	15 5 444 -413	5 6 1196-1200	13 4 291 310
6 4 1196 1206	16 1 353 -314	5 7 584 592	13 6 247 283
6 6 1329 1335	16 3 185 -222	5 8 246 316	14 1 660 630
6 7 247 -230	17 0 340 -454	5 9 450 493	14 3 275 303
6 8 269 -275		5 11 277 254	14 4 312 256
6 9 292 -265	H = 4	6 0 1954-2024	14 5 387 392
6 11 333 -364	K L FO FC	6 1 498 528	15 1 271 243
7 0 1689 1744	-12 -7 123 143	6 3 486 -444	15 2 313 289
7 2 500 -513	-11-10 181 245	6 4 170 118	16 0 478 420
7 3 629 -634	-10 -9 193 236	6 5 1280-1280	16 4 325 241
7 5 872 838	-7 -7 244 -273	6 6 344 293	
7 6 324 -309	0 0 1179 302	6 10 470 364	H = 3
7 7 241 -249	0 2 802 867	7 0 816 862	K L FO FC
7 10 486 -488	0 4 706 631	7 1 1300-1335	-15 -3 159 232
8 0 822 -824	0 6 1343-1339	7 2 308 -315	-13 -8 195 240
8 1 553 579	0 8 903 -473	7 3 466 451	-13 -4 148 188
8 2 881 -879	0 10 390 -332	7 4 531 -484	-11 -9 154 -212
8 3 706 -728	0 12 150 -86	7 5 117 189	-10 -8 215 -271
8 4 543 -608	1 1 1835 1789	7 7 373 394	-1 -9 179 207
8 5 353 -390	1 2 1106-1021	7 8 281 324	-1 -6 162 225
8 7 886 -811	1 3 661 625	7 9 321 305	0 1 369 -365
8 9 363 -384	1 4 207 187	7 11 476 449	0 3 892 891
8 11 477 -465	1 6 91 100	8 0 1466-1530	0 7 766 760
9 0 676 700	1 7 1142-1084	8 2 679 249	0 9 232 189
9 1 390 -439	1 10 234 -239	8 4 465 436	0 11 438 427
9 2 414 -425	1 11 291 -248	8 6 827 812	1 0 865 -934
9 3 828 -848	2 0 2008 2067	8 7 513 548	1 1 1583 1579
9 5 486 -470	2 1 1807-1866	8 8 479 371	1 2 264 290
9 6 1102-1087	2 2 1444 1165	8 10 744 541	1 3 1325 1312
9 8 594 -576	2 3 1037-1033	9 0 572 560	1 4 140 161
9 10 530 -475	2 4 792 745	9 1 414 -496	1 5 512 459
10 1 249 267	2 5 495 -515	9 3 561 603	1 6 654 626
10 2 618 -589	2 6 636 -462	9 5 782 794	1 9 210 257
10 4 345 -373	2 7 218 229	9 7 1038 1018	1 10 407 338
10 5 405 -370	2 8 489 480	9 9 352 410	2 0 468 441
10 6 130 -177	2 9 393 -386	10 0 256 -274	2 1 1861-1810
10 7 1095-1028	2 10 262 98	10 1 468 442	2 2 2590 2529
10 9 331 -323	3 0 400 444	10 4 343 121	2 3 471 486
11 1 774 -674	3 1 2287 2313	10 5 426 412	2 4 928 903
11 3 289 -277	3 2 1825-1830	10 6 1058 1069	2 5 130 106
11 6 944 -928	3 3 774 794	10 7 333 397	2 6 182 247
11 8 363 -429	3 4 884 -820	10 8 704 620	2 9 336 -367
12 0 464 -444	3 5 312 306	10 10 383 451	2 10 393 399
12 2 896 -896	3 6 810 -719	11 0 635 647	2 11 154 186
12 6 282 -317	3 7 624 610	11 1 363 -320	3 0 1956-1969
12 7 413 -409	3 9 763 775	11 2 776 776	3 1 1964 1937
13 0 257 -242	3 10 272 -298	11 4 328 350	3 2 537 -541
13 1 1260-1155	4 0 1194 1093	11 5 291 277	3 3 1449 1458
13 2 278 -294	4 1 1213-1236	11 6 450 470	3 4 343 330
13 3 452 -436	4 2 860 842	11 7 649 646	3 5 684 643
3 6 168 -187	11 0 380 407	4 2 601 -528	
3 7 104 -118	11 1 956 -891	4 4 599 -603	
3 8 948 -944	11 3 629 -577	4 5 162 -206	
3 9 304 300	11 5 702 -698	4 6 333 -143	
3 10 162 -244	11 7 287 -361	4 7 249 -220	
4 1 1283-1339	12 0 487 -528	4 8 452 438	
4 2 1368 1443	12 1 644 643	4 10 305 200	
4 3 232 278	12 2 1102-1046	4 11 383 384	
4 4 373 385	12 4 380 -360	5 0 542 -514	
4 5 125 110	12 6 442 -501	5 1 835 -847	
4 6 445 472	13 0 533 512	5 2 640 -622	
4 7 761 -783	13 1 837 -777	5 3 469 -478	
4 9 690 -774	13 3 635 -612	5 4 940 937	
5 1 474 566	13 5 465 -456	5 6 358 -339	
5 4 347 394	14 2 485 -472	5 7 603 636	
5 5 646 638	14 3 232 -184	5 9 357 391	
5 6 157 -167	14 5 167 -214	6 0 1417-1367	
5 8 553 -537	15 4 344 -318	6 1 1026-1079	
5 10 273 -330		6 2 675 -669	
5 11 268 -324	H = 6	6 3 485 495	
6 1 1519 1521	K L FO FC	6 4 161 103	
6 2 907 981	-13 -7 156 -178	6 6 590 614	
6 6 400 406	-11 -8 157 230	6 8 563 473	
6 7 522 -521	-11 -7 164 -162	6 10 360 272	
6 9 301 -326	0 0 434 414	6 11 200 268	
6 11 341 -296	0 2 2087-1954	7 0 832 -917	
7 0 2183 2257	0 4 373 -383	7 1 1657-1654	
7 1 728 736	0 6 384 264	7 2 1034-1121	
7 2 447 452	0 8 296 -278	7 4 116 214	
7 3 422 416	0 10 603 -558	7 5 470 455	
7 4 249 -303	1 0 627 -599	7 6 281 -253	
7 6 834 -829	1 1 253 -291	7 7 770 760	
7 8 346 -376	1 2 1898-1838	7 8 187 -240	
7 9 249 212	1 3 1631-1612	8 0 1633-1700	
7 10 331 -374	1 4 1020 -959	8 1 1068-1068	
8 1 1128 1193	1 5 294 276	8 3 330 -339	
8 2 1040 1044	1 6 336 -362	8 4 485 449	
8 3 599 -575	1 7 281 -275	8 6 879 902	
8 5 519 -546	1 9 226 -266	8 8 587 519	
8 6 319 -327	1 10 183 -193	8 10 483 428	
8 7 719 -743	1 11 302 -304	9 0 216 209	
8 9 268 -321	2 0 917 892	9 1 581 -610	
8 10 218 322	2 1 2131-2179	9 2 342 -337	
9 0 867 926	2 2 973 -924	9 3 457 471	
9 1 346 340	2 3 1738-1723	9 4 357 321	
9 2 222 -202	2 4 444 -398	9 6 368 344	
9 3 341 399	2 5 648 -626	9 7 625 675	
9 4 429 -433	2 6 191 25	9 9 342 408	
9 5 618 -586	2 8 557 102	10 0 528 -589	
9 6 853 -868	2 10 131 -183	10 3 466 459	
9 7 377 -427	3 0 173 -211	10 5 652 648	
9 8 536 -562	3 1 1069 1010	10 7 315 345	
9 10 373 -338	3 2 1930-1981	10 8 320 360	
10 0 680 -656	3 3 905 -894	11 0 471 440	
10 3 441 -502	3 4 382 -419	11 2 1029 974	
10 4 391 -392	3 6 537 -529	11 4 910 899	
10 6 764 -748	3 9 276 310	11 5 240 -267	
10 7 716 -718	4 0 859 761	11 6 611 659	
10 9 350 -407	4 1 1534-1545	12 0 550 -514	

12	1	974	881
12	3	984	906
12	5	762	750
13	1	346	-282
13	2	733	719
13	4	419	397
14	0	420	-293
14	3	182	236

H = 7

K	L	FO	FC
-7	-10	212	-235
-6	-6	148	179
-4	-10	201	224
-2	-5	219	236
0	1	1009	1065
0	3	1745	1670
0	5	769	-704
0	7	418	441
0	9	389	406
0	11	193	203
1	0	213	198
1	1	1067	973
1	2	1652	1628
1	3	718	663
1	5	730	705
1	8	439	434
1	10	292	343
2	0	478	530
2	1	383	419
2	2	1366	1369
2	3	1189	1198
2	4	1008	1041
2	6	846	812
2	7	659	607
2	9	176	220
3	1	1422	1441
3	2	956	1008
3	3	667	655
3	4	313	347
3	5	894	883
3	6	560	600
3	8	304	367
3	11	218	-289
4	0	829	854
4	1	525	525
4	2	562	583
4	3	363	329
4	4	689	-703
4	6	370	394
4	7	284	293
4	10	177	-215
4	11	154	-169
5	0	799	866
5	1	800	825
5	2	427	457
5	3	699	-729
5	4	152	180
5	6	218	-232
5	7	310	345
6	0	763	769
6	1	1048	1151
6	2	657	685
6	4	653	-668
6	5	482	-475
6	6	636	655
6	7	641	-636
7	0	1315	1298
7	1	887	986
7	2	535	557
7	4	308	-335
7	6	924	-765
7	7	270	305
7	8	557	-587
7	10	287	-271
8	1	961	933
8	2	353	324
8	6	303	348
8	7	775	-773
8	9	183	-286
9	0	791	848
9	8	314	-374
10	0	441	-434
10	2	927	-890
10	4	574	-607
10	5	324	343
10	6	289	-319
10	7	130	-257
11	0	313	339
11	1	859	-855
11	3	1065	-1038
11	5	585	-588
12	2	856	-813
12	4	658	-635
12	5	147	321
12	6	342	-333
13	1	386	-310
13	3	381	-371
14	2	315	-277
15	4	224	235

H = 8

K	L	FO	FC
-13	-5	142	185
-10	-9	157	131
-7	-11	212	203
-3	-6	239	-216
-3	-7	171	248
0	0	151	-145
0	2	943	-969
0	4	227	146
0	6	404	-386
0	8	407	-377
1	1	325	-348
1	2	321	-331
1	3	806	-701
1	4	675	-700
1	6	578	-628
1	7	890	-885
1	8	237	182
2	0	831	-838
2	1	373	-375
2	2	960	-843
2	3	864	-890
2	4	528	-446
2	5	923	-903
2	6	908	-881
2	8	664	-678
2	9	352	453
3	0	168	-132
3	1	942	-956
3	2	654	-613
3	3	312	-302
3	4	305	-283
3	5	413	-402
3	6	697	-749
3	7	1076	-1071
3	8	347	331
3	9	176	-218
4	0	1333	-1254
4	1	662	-677
4	2	350	-349
4	4	313	-187
4	5	526	-557
4	6	761	-766
4	8	429	-454
4	9	203	292
5	0	548	-599
5	1	588	-565
5	2	631	-699
5	6	395	-374
5	8	255	306
6	0	602	-639
6	1	729	-726
6	2	646	-282
6	4	565	429
6	5	266	-231
6	6	537	532
6	8	400	390
7	0	397	-434
7	5	331	304
7	6	457	-473
7	7	762	741
7	9	216	262
8	0	575	-561
8	4	223	-185
8	5	420	-454
8	6	568	525
8	8	393	454
9	1	722	-742
9	2	687	629
9	7	170	330
9	8	174	198
10	0	526	-565
10	1	879	855
10	4	305	-340
10	8	301	76
11	2	852	793
11	4	364	351
11	5	274	-238
12	0	405	-107
12	1	451	431
12	3	582	533
12	5	448	388
13	2	399	401
13	4	171	209
14	2	389	-286
14	4	345	-338
15	3	453	-452
16	0	241	19

H = 9

K	L	FO	FC
-11	0	150	296
-1	-7	216	203
0	1	477	-374
0	3	823	847
0	5	832	865
0	7	849	828
1	0	152	-203
1	1	239	-213
1	2	230	229
1	3	210	237
1	4	823	806
1	5	387	417
1	6	983	916
1	8	268	304
1	9	238	-301
2	0	258	-280
2	1	104	148
2	2	259	263
2	3	617	642
2	4	269	268
2	5	797	773
2	6	460	503
2	7	1074	1066
2	8	366	-324
2	10	187	-200
3	0	1106	1201
3	1	315	357
3	2	283	344
3	3	534	543
3	4	462	527
3	5	637	625
3	6	1256	1270
3	8	551	570
3	9	295	-394
4	0	314	305
4	1	450	479
4	2	983	968
4	4	530	579
4	5	498	473
4	6	250	292
4	7	582	565
4	8	462	-461
5	0	543	562

H = 10

K	L	FO	FC
-11	-8	149	176
-11	-5	144	154
0	0	934	953
0	4	1471	-1443
0	6	923	-882
0	-10	214	239
1	0	148	186
1	1	726	604
1	2	121	189
1	3	1151	-1096
1	5	1119	-1136
1	7	667	-657
2	0	203	-55
2	2	531	-405
2	4	1047	-1019
2	6	852	-824
2	8	304	-309
2	9	257	328
3	1	108	-133
3	2	790	-746
3	3	671	-655
3	4	317	-345
3	5	636	-667
3	7	513	-505
3	8	261	300
4	0	434	-430
4	1	1048	-1035
4	2	466	-264
4	3	1036	-995
4	4	630	-311
4	6	372	-433
4	7	160	209
4	8	207	-249
5	0	356	-396
5	2	1684	-1619
5	4	457	-462
5	8	235	332
6	0	332	293
6	1	798	-797
6	2	446	112
6	3	935	-921
6	4	127	-95
6	6	284	69
6	7	299	341
6	8	258	271
7	2	544	-557
7	6	152	205
7	7	293	257
7	8	150	233
9	0	399	418
9	1	113	-420
12	2	281	-139
14	0	400	-9

H = 11

K	L	FO	FC
-8	-7	162	119
-4	-5	235	-271
-2	-6	146	167
-1	-5	143	197
0	1	524	-459
0	3	1389	1322
0	5	903	933
0	7	423	459
0	9	215	189
1	0	508	-543
1	2	535	526
1	3	202	-260
1	4	1219	1165
1	6	635	653
1	8	217	299
2	0	226	203
2	2	250	284
2	3	1061	1042
2	4	357	-355
2	5	472	508
2	7	324	381
3	1	678	621
3	2	436	493
3	3	246	237
3	4	396	452
4	0	387	430
4	2	1344	1250
4	3	337	345
5	1	1183	1159
5	3	960	957
6	2	988	994
7	5	302	-326
8	4	249	-316

H = 12

K	L	FO	FC
0	0	160	-92
0	2	653	-646
0	4	963	-821
0	6	552	-561
0	8	603	-551
1	0	373	-388
1	3	846	-806
1	4	289	281
1	5	319	-351
1	7	464	-523
2	0	157	128
2	1	310	-309
2	2	455	-431
2	3	186	233
2	4	495	-337
2	5	159	247
2	6	359	-142
2	8	382	-375
3	0	643	-616
3	1	224	-268
3	2	518	-482
3	3	415	-408
3	4	149	239
4	0	211	130
4	1	833	-781
4	2	562	-317
4	3	417	-426
4	4	190	69
4	6	407	226
5	0	362	-402
5	2	721	-687
6	1	426	-434
6	2	218	67
6	4	374	34
7	3	170	266
8	2	303	378
8	4	222	205
9	3	449	490
9	4	322	311

H = 13

K	L	FO	FC
0	1	193	204
0	3	220	207
0	5	142	238
0	7	729	733
1	0	282	259
1	2	215	247
1	4	221	230
1	6	373	427
2	0	542	541
2	2	275	281
2	3	165	209
2	7	320	342
3	1	402	413
3	4	121	-143
4	0	283	275

4	2	151	174	4	0	271	218
5	4	163	-222	5	1	310	294
6	3	304	-293				
7	2	316	-310				
7	4	243	-247				
8	3	306	-482				
9	0	338	-304				
9	4	336	-283				

H = 14

K	L	FO	FC
0	0	334	-314
0	2	177	50
0	6	543	-465
1	0	247	-270
1	2	247	-253
1	5	197	-222
2	1	339	-323
2	2	199	100
2	4	281	-14
2	6	213	-219
3	0	183	-192
3	1	248	249
3	2	216	-200
4	0	184	224
4	2	307	264
4	4	301	101
5	1	161	242
6	2	463	361
6	4	292	225
7	3	500	505
8	0	350	296
8	2	220	343
9	1	365	290
10	0	496	347

H = 15

K	L	FO	FC
-3	-5	219	-185
1	1	180	180
1	2	142	-146
1	3	147	179
2	1	190	-252
2	2	398	356
3	0	209	-212
3	2	174	-203
4	1	330	-330
5	0	292	-293
5	2	282	-262
6	3	367	-352
7	0	322	-253
7	2	311	-342
8	1	287	-258

H = 16

K	L	FO	FC
2	1	183	-162
3	1	204	198
3	2	216	-209

APPENDIX B: OBSERVED AND CALCULATED STRUCTURE FACTORS FOR THE MONOCLINIC CRYSTAL OF $Mo_2(O_2CC(CH_3)_3)_4$

K = -2

H	L	FO	FC
-15	1	4	1

K = -8

H	L	FO	FC
-14	2	9	9

K = -7

H	L	FO	FC
-14	1	4	6

K = -6

H	L	FO	FC
-14	2	10	10
-14	4	10	13

K = -5

H	L	FO	FC
-14	1	4	3

K = -4

H	L	FO	FC
-14	2	9	10
-14	4	16	17

K = -2

H	L	FO	FC
-14	2	10	11
-14	4	17	18

K = 0

H	L	FO	FC
-14	2	12	14
-14	4	16	17

K =-11

H	L	FO	FC
-13	2	9	9

K = -9

H	L	FO	FC
-13	2	12	12

K = -8

H	L	FO	FC
-13	1	5	6

K = -7

H	L	FO	FC
-13	2	15	16
-13	4	7	8

K = -6

H	L	FO	FC
-13	1	4	4

K = -5

H	L	FO	FC
-13	2	17	18
-13	4	9	10
-13	6	22	23

K = -3

H	L	FO	FC
-13	2	20	19
-13	4	13	13
-13	6	24	25

K = -2

H	L	FO	FC
-13	5	4	5

K = -1

H	L	FO	FC
-13	2	24	24
-13	4	12	13
-13	6	24	24

K = 2

H	L	FO	FC
-13	-5	5	2

K = 10

H	L	FO	FC
-13	-3	8	7

K =-12

H	L	FO	FC
-12	2	9	10

K =-10

H	L	FO	FC
-12	2	14	13

K = -8

H	L	FO	FC
-12	2	21	21
-12	6	22	23

K = -6

H	L	FO	FC
-12	2	22	23
-12	6	26	26

K = -4

H	L	FO	FC
-12	2	22	22
-12	4	6	6
-12	6	30	30
-12	8	28	27

K = -3

H	L	FO	FC
-12	1	4	5

K = -2

H	L	FO	FC
-12	2	20	20
-12	4	4	6
-12	6	35	35
-12	8	30	28

K = -1

H	L	FO	FC
-12	2	24	24
-12	6	36	35
-12	8	28	27

K =-14

H	L	FO	FC
-11	3	9	10

K =-13

H	L	FO	FC
-11	2	14	15
-11	4	5	5

K =-12

H	L	FO	FC
-11	1	4	4
-11	3	7	8

K =-11

H	L	FO	FC
-11	2	17	17
-11	6	19	22

K =-10

H	L	FO	FC
-11	3	9	9
-11	5	5	7

K = -9

H	L	FO	FC
-11	2	23	24
-11	6	26	26

K = -8

H	L	FO	FC
-11	1	5	5
-11	3	12	12

K = -7

H	L	FO	FC
-11	2	27	26
-11	4	8	7
-11	6	30	31
-11	8	30	28

K = -6

H	L	FO	FC
-11	1	5	5
-11	3	7	8
-11	7	4	6

K = -5

H	L	FO	FC
-11	2	26	25
-11	4	8	8
-11	6	34	33
-11	8	32	29

K = -3

H	L	FO	FC
-11	2	22	24
-11	4	6	6
-11	6	38	38
-11	8	34	33

K = -2

H	L	FO	FC
-11	3	3	2
-11	5	9	10
-11	7	4	5

K = -1

H	L	FO	FC
-11	2	27	28
-11	4	8	7
-11	6	41	39
-11	8	37	35

K =-16

H	L	FO	FC
-10	2	19	19

K =-15

H	L	FO	FC
-10	1	6	8
-10	3	9	9

K =-14

H	L	FO	FC
-10	2	25	25

K =-13

H	L	FO	FC
-10	1	5	3
-10	3	6	7

K =-12

H	L	FO	FC
-10	2	29	30
-10	4	7	8
-10	6	16	18

K =-11

H	L	FO	FC
-10	7	4	5

K =-10

H	L	FO	FC
-10	2	36	37
-10	4	11	12
-10	6	25	26
-10	8	22	23

K = -9

H	L	FO	FC
-10	1	7	7
-10	3	12	11
-10	5	7	8

K = -8

H	L	FO	FC
-10	2	46	46
-10	4	20	20
-10	6	30	31
-10	8	27	27

K = -7

H	L	FO	FC
-10	1	12	13
-10	3	13	13

K = -6

H	L	FO	FC
-10	2	49	48
-10	4	22	22
-10	6	34	35
-10	8	31	31

K = -5

H	L	FO	FC
-10	1	5	6
-10	3	4	6

K = -4

H	L	FO	FC
-10	2	57	57
-10	4	23	22
-10	6	34	34
-10	8	35	33
-10	10	15	13

K = -3

H	L	FO	FC
-10	1	3	4
-10	5	7	7
-10	7	7	7

K = -2

H	L	FO	FC
-10	2	66	65
-10	4	15	16
-10	6	38	39
-10	8	42	40
-10	10	15	14

K = -1

H	L	FO	FC
-10	5	6	5
-10	7	6	6

K = 0

H	L	FO	FC
-10	2	80	79
-10	4	21	20
-10	6	35	37
-10	8	43	41
-10	10	15	13

K = 4

H	L	FO	FC
-10	-8	5	4

K =-17

H	L	FO	FC
-9	2	20	21

K =-16

H	L	FO	FC
-9	3	6	7

K =-15

H	L	FO	FC
-9	2	25	25
-9	4	10	11

K =-14

H	L	FO	FC
-9	3	5	7
-9	5	8	9

K =-13

H	L	FO	FC
-9	2	30	31
-9	4	13	13
-9	6	10	10

K =-12

H	L	FO	FC
-9	1	6	6
-9	5	9	9

K =-11

H	L	FO	FC
-9	2	41	41
-9	4	13	13
-9	6	15	16
-9	8	19	20

K =-10

H	L	FO	FC
-9	5	13	13
-9	7	7	9

K = -9

H	L	FO	FC
-9	2	60	60
-9	4	20	19
-9	6	17	17
-9	8	27	26

K = -8

H	L	FO	FC
-9	1	5	6
-9	3	9	9
-9	5	11	12

K = -7

H	L	FO	FC
-9	2	70	69
-9	4	20	20
-9	6	18	18
-9	8	32	31
-9	10	14	14

K = -6

H	L	FO	FC
-9	1	7	6
-9	3	9	9

K = -5

H	L	FO	FC
-9	2	72	73
-9	4	23	22
-9	6	16	16
-9	8	31	29
-9	10	14	14

K = -4

H	L	FO	FC
-9	1	8	8
-9	7	6	6

K = -3

H	L	FO	FC
-9	2	77	78
-9	4	23	24
-9	6	24	24
-9	8	33	31
-9	10	18	16

K = -2

H	L	FO	FC
-9	1	9	9
-9	5	7	7
-9	7	13	13

K = -1

H	L	FO	FC
-9	2	92	90
-9	4	29	30
-9	6	31	30
-9	8	36	34
-9	10	20	19

K = 6

H	L	FO	FC
-9	-1	3	2

K = 16

H	L	FO	FC
-9	-1	3	3

K =-18

H	L	FO	FC
-8	2	16	17

K =-16

H	L	FO	FC
-8	2	21	21
-8	4	14	15

K =-15

H	L	FO	FC
-8	3	6	8
-8	5	7	9

K =-14

H	L	FO	FC
-8	2	25	25
-8	4	17	18

K =-13

H	L	FO	FC
-8	1	8	10
-8	3	6	6
-8	7	3	5

K =-12

H	L	FO	FC
-8	2	34	35
-8	4	19	20
-8	8	18	16

K =-11

H	L	FO	FC
-8	1	16	15
-8	5	6	7
-8	7	8	8

K =-10

H	L	FO	FC
-8	2	54	56
-8	4	25	27
-8	6	5	5
-8	8	24	24

K = -9

H	L	FO	FC
-8	3	9	7
-8	5	11	12
-8	7	6	7

K = -8

H	L	FO	FC
-8	2	69	71
-8	4	35	37
-8	8	29	29
-8	10	25	23

K = -7

H	L	FO	FC
-8	3	11	12
-8	5	7	9
-8	9	5	6

K = -6

H	L	FO	FC
-8	2	68	70
-8	4	33	35
-8	8	30	29
-8	10	26	25

K = -5

H	L	FO	FC
-8	1	4	3
-8	5	5	6
-8	9	4	4
-8	11	7	6

K = -4

H	L	FO	FC
-8	2	72	73
-8	4	45	47
-8	8	28	27
-8	10	29	25

K = -3

H	L	FO	FC
-8	1	12	13
-8	3	8	8
-8	5	4	5
-8	7	7	6

K = -2

H	L	FO	FC
-8	2	76	79
-8	4	50	50
-8	6	11	9
-8	8	35	35
-8	10	32	29

K = -1

H	L	FO	FC
-8	1	3	3
-8	5	6	7
-8	7	9	8
-8	9	5	5

K = 0

H	L	FO	FC
-8	2	91	92
-8	4	68	66
-8	6	9	7
-8	8	37	37
-8	10	33	31

K =-19

H	L	FO	FC
-7	2	11	12

K =-18

H	L	FO	FC
-7	1	7	9

K =-17

H	L	FO	FC
-7	2	20	21
-7	4	15	15

K =-16

H	L	FO	FC
-7	1	7	6
-7	5	6	8

K =-15

H	L	FO	FC
-7	2	23	24
-7	4	15	16

K =-14

H	L	FO	FC
-7	1	5	6
-7	5	9	9

K =-13

H	L	FO	FC
-7	2	29	31
-7	4	17	17
-7	8	15	15

K =-12

H	L	FO	FC
-7	1	19	19
-7	3	11	11
-7	7	5	6

K =-11

H	L	FO	FC
-7	2	43	45
-7	4	26	27
-7	8	21	21
-7	10	24	23

K =-10

H	L	FO	FC
-7	1	13	15
-7	5	7	6
-7	7	11	11

K = -9

H	L	FO	FC
-7	2	62	61
-7	4	46	46
-7	8	28	27
-7	10	34	33

K = -8

H	L	FO	FC
-7	1	10	9
-7	3	3	3
-7	5	5	6
-7	7	5	5

K = -7

H	L	FO	FC
-7	2	59	60
-7	4	47	51
-7	8	30	29
-7	10	42	40

K = -6

H	L	FO	FC
-7	3	7	7
-7	5	4	6
-7	9	6	7
-7	11	4	5

K = -5

H	L	FO	FC
-7	2	63	63
-7	4	46	49
-7	8	28	27
-7	10	42	39

K = -4

H	L	FO	FC
-7	1	16	15
-7	3	15	14
-7	11	5	4

K = -3

H	L	FO	FC
-7	2	83	85
-7	4	47	47
-7	6	4	4
-7	8	37	35
-7	10	43	40
-7	12	6	4

K = -2

H	L	FO	FC
-7	1	5	6
-7	3	11	12
-7	5	4	5
-7	7	10	11
-7	9	8	8

K = -1

H	L	FO	FC
-7	2	116	114
-7	4	56	54
-7	6	5	4
-7	8	51	49
-7	10	48	45
-7	12	6	6

K = 12

H	L	FO	FC
-7	-5	4	1

K =-19

H	L	FO	FC
-6	1	8	9

K =-18

H	L	FO	FC
-6	2	16	16
-6	4	15	15

K =-17

H	L	FO	FC
-6	1	10	11
-6	5	7	7

K =-16

H	L	FO	FC
-6	2	18	18
-6	4	18	20
-6	6	8	9

K =-15

H	L	FO	FC
-6	1	5	7
-6	5	10	12
-6	7	5	7

K =-14

H	L	FO	FC
-6	2	17	17
-6	4	20	19
-6	6	11	10
-6	8	14	14

K =-13

H	L	FO	FC
-6	1	14	15
-6	3	6	6
-6	5	9	8

K =-12

H	L	FO	FC
-6	0	4	5
-6	2	24	24
-6	4	22	24
-6	6	11	11
-6	8	18	19
-6	10	25	25

K =-11

H	L	FO	FC
-6	1	19	20
-6	3	12	13
-6	5	7	8
-6	7	6	7
-6	9	5	4

K =-10

H	L	FO	FC
-6	2	41	43
-6	4	41	41
-6	6	14	16
-6	8	28	29
-6	10	35	33

K = -9

H	L	FO	FC
-6	1	17	17
-6	5	18	17
-6	7	11	9

K = -8

H	L	FO	FC
-6	2	47	47
-6	4	46	48
-6	6	20	22
-6	8	37	37
-6	10	43	42

K = -7

H	L	FO	FC
-6	1	7	9
-6	3	6	7
-6	5	12	14
-6	7	3	3
-6	9	4	4

K = -6

H	L	FO	FC
-6	2	33	36
-6	4	39	38
-6	6	23	24
-6	8	37	37
-6	10	47	45
-6	12	13	12

K = -5

H	L	FO	FC
-6	1	19	22
-6	5	8	8
-6	7	4	4
-6	9	4	5

K = -4

H	L	FO	FC
-6	2	40	42
-6	4	34	38
-6	6	27	30
-6	8	34	33
-6	10	49	45
-6	12	11	10

K = -3

H	L	FO	FC
-6	1	12	11
-6	3	14	14
-6	5	6	6
-6	7	9	9

K = -2

H	L	FO	FC
-6	2	61	60
-6	4	45	49
-6	6	26	26
-6	8	48	45
-6	10	60	56
-6	12	11	10

K = -1

H	L	FO	FC
-6	1	9	11
-6	5	6	6
-6	7	12	11
-6	9	7	6

K = 0

H	L	FO	FC
-6	2	80	77
-6	4	55	63
-6	6	27	26
-6	8	55	50
-6	10	66	62
-6	12	10	11

K =-20

H	L	FO	FC
-5	1	5	6

K =-19

H	L	FO	FC
-5	2	10	9
-5	4	14	14

K =-18

H	L	FO	FC
-5	1	8	9

K =-17

H	L	FO	FC
-5	2	12	12
-5	4	23	25
-5	6	11	11

K =-16

H	L	FO	FC
-5	1	10	10
-5	5	5	7
-5	7	7	7

K =-15

H	L	FO	FC
-5	2	6	7
-5	4	29	29
-5	6	13	13
-5	8	11	11

K =-14

H	L	FO	FC
-5	1	5	6
-5	3	7	6
-5	5	9	9
-5	7	9	9
-5	9	5	6

K =-13

H	L	FO	FC
-5	2	7	6
-5	4	27	31
-5	6	12	13
-5	8	15	16
-5	10	19	19

K =-12

H	L	FO	FC
-5	1	18	17
-5	3	10	9
-5	7	5	7
-5	9	6	7

K =-11

H	L	FO	FC
-5	2	25	25
-5	4	47	49
-5	6	21	23
-5	8	25	25
-5	10	25	25

K =-10

H	L	FO	FC
-5	1	6	7
-5	5	10	10
-5	7	11	13
-5	9	11	11
-5	11	4	2

K = -9

H	L	FO	FC
-5	2	43	45
-5	4	63	65
-5	6	35	34
-5	8	37	38
-5	10	34	35

K = -8

H	L	FO	FC
-5	1	11	11
-5	5	12	12
-5	7	6	7
-5	9	5	6

K = -7

H	L	FO	FC
-5	2	36	37
-5	4	62	64
-5	6	41	42
-5	8	44	43
-5	10	40	39
-5	12	17	17

K = -6

H	L	FO	FC
-5	3	18	17
-5	5	17	17

K = -5

H	L	FO	FC
-5	2	21	27
-5	4	57	59
-5	6	42	41
-5	8	41	41
-5	10	39	37
-5	12	17	16

K = -4

H	L	FO	FC
-5	1	15	15
-5	3	12	12
-5	5	4	3
-5	9	4	5

K = -3

H	L	FO	FC
-5	2	24	25
-5	4	89	89
-5	6	44	43
-5	8	44	42
-5	10	47	43
-5	12	16	16

K = -2

H	L	FO	FC
-5	1	4	3
-5	7	10	9
-5	9	11	12
-5	11	3	3

K = -1

H	L	FO	FC
-5	2	30	28
-5	4	127	122
-5	6	41	39
-5	8	55	55
-5	10	60	57
-5	12	18	18

K =-20

H	L	FO	FC
-4	4	11	13

K =-19

H	L	FO	FC
-4	1	6	7
-4	3	4	4

K =-18

H	L	FO	FC
-4	2	6	8
-4	4	22	23
-4	6	10	11

K =-17

H	L	FO	FC
-4	1	11	10
-4	3	4	5
-4	7	8	9

K =-16

H	L	FO	FC
-4	2	12	11
-4	4	27	29
-4	6	16	18
-4	8	5	5

K =-15

H	L	FO	FC
-4	5	7	8
-4	7	11	12
-4	9	7	9

K =-14

H	L	FO	FC
-4	2	4	7
-4	4	25	27
-4	6	18	18
-4	8	7	8

K =-13

H	L	FO	FC
-4	1	9	9
-4	3	8	7
-4	7	12	12
-4	9	9	9

K =-12

H	L	FO	FC
-4	2	17	17
-4	4	37	40
-4	6	19	21
-4	8	10	10
-4	10	15	15

K =-11

H	L	FO	FC
-4	1	12	12
-4	3	8	10
-4	7	15	16
-4	9	11	11

K =-10

H	L	FO	FC
-4	2	29	31
-4	4	76	76
-4	6	33	33
-4	8	12	13
-4	10	24	24

K = -9

H	L	FO	FC
-4	1	12	13
-4	3	4	3
-4	5	5	5
-4	7	22	21
-4	9	12	11

K = -8

H	L	FO	FC
-4	2	28	27
-4	4	87	91
-4	6	32	34
-4	8	14	14
-4	10	32	33
-4	12	21	21

K = -7

H	L	FO	FC
-4	1	10	11
-4	3	8	5
-4	5	12	12
-4	7	15	15

K = -6

H	L	FO	FC
-4	2	11	13
-4	4	87	91
-4	6	34	34
-4	8	11	10
-4	10	29	30
-4	12	22	22

K = -5

H	L	FO	FC
-4	1	8	9
-4	3	8	6
-4	5	3	5
-4	7	9	8
-4	9	6	6

K = -4

H	L	FO	FC
-4	2	32	31
-4	4	80	81
-4	6	34	36
-4	8	9	9
-4	10	24	23
-4	12	22	22

K = -3

H	L	FO	FC
-4	1	4	2
-4	3	14	17
-4	9	11	11

K = -2

H	L	FO	FC
-4	2	60	56
-4	4	129	123
-4	6	59	59
-4	8	24	23
-4	10	32	30
-4	12	28	28

K = -1

H	L	FO	FC
-4	1	6	7
-4	3	12	7
-4	7	7	6
-4	9	10	9

K = 0

H	L	FO	FC
-4	2	72	64
-4	4	126	116
-4	6	53	57
-4	8	37	35
-4	10	40	38
-4	12	34	33

K = 3

H	L	FO	FC
-4	-5	3	4

K = 11

H	L	FO	FC
-4	-1	3	3

K =-20

H	L	FO	FC
-3	1	8	7
-3	3	5	6

K =-19

H	L	FO	FC
-3	2	4	3
-3	4	16	17
-3	6	10	11

K =-18

H	L	FO	FC
-3	1	9	10
-3	3	8	9
-3	7	8	8

K =-17

H	L	FO	FC
-3	2	5	6
-3	4	22	25
-3	6	18	20

K =-16

H	L	FO	FC
-3	1	13	12
-3	3	11	10
-3	7	8	9

K =-15

H	L	FO	FC
-3	2	6	6
-3	4	27	26
-3	6	23	24

K =-14

H	L	FO	FC
-3	1	4	5
-3	3	6	7
-3	5	5	6
-3	7	9	10
-3	9	5	6

K =-13

H	L	FO	FC
-3	4	24	25
-3	6	22	24
-3	10	13	14

K =-12

H	L	FO	FC
-3	1	17	17
-3	3	20	21
-3	7	3	5
-3	9	5	6

K =-11

H	L	FO	FC
-3	2	17	19
-3	4	59	60
-3	6	39	42
-3	8	4	4
-3	10	19	19

K =-10

H	L	FO	FC
-3	1	6	8
-3	3	11	12
-3	5	5	5
-3	7	13	12
-3	9	9	10

K =-9

H	L	FO	FC
-3	2	14	13
-3	4	82	87
-3	6	54	57
-3	8	5	4
-3	10	29	30
-3	12	27	27

K =-8

H	L	FO	FC
-3	1	30	31
-3	3	13	14
-3	5	4	6
-3	7	12	12
-3	9	3	4

K =-7

H	L	FO	FC
-3	4	94	95
-3	6	60	62
-3	8	9	9
-3	10	31	31
-3	12	32	31

K =-6

H	L	FO	FC
-3	1	8	7
-3	3	7	6
-3	5	12	11
-3	7	13	13

K =-5

H	L	FO	FC
-3	4	73	76
-3	6	57	59
-3	8	15	15
-3	10	27	26
-3	12	31	30

K =-4

H	L	FO	FC
-3	1	24	25
-3	3	15	17
-3	5	10	8
-3	11	3	1

K =-3

H	L	FO	FC
-3	2	34	41
-3	4	102	103

-3	6	84	83
-3	8	17	17
-3	10	28	28
-3	12	33	31

K = -2

H	L	FO	FC
-3	1	11	14
-3	7	7	7
-3	9	6	5
-3	11	5	6

K = -1

H	L	FO	FC
-3	2	48	47
-3	4	121	123
-3	6	107	101
-3	8	5	5
-3	10	44	44
-3	12	40	39

K =-21

H	L	FO	FC
-2	1	5	6
-2	3	5	7

K =-20

H	L	FO	FC
-2	4	8	10

K =-19

H	L	FO	FC
-2	1	12	11
-2	3	10	10
-2	5	5	1

K =-18

H	L	FO	FC
-2	2	4	3
-2	4	18	19
-2	6	18	19

K =-17

H	L	FO	FC
-2	1	16	17
-2	3	13	13

K =-16

H	L	FO	FC
-2	2	3	5
-2	4	28	29
-2	6	22	25
-2	8	7	8

K =-15

H	L	FO	FC
-2	1	17	17
-2	3	10	10
-2	7	5	6

-2	9	6	5

K =-14

H	L	FO	FC
-2	2	17	17
-2	4	23	25
-2	6	20	21
-2	8	7	8
-2	10	13	12

K =-13

H	L	FO	FC
-2	1	15	18
-2	3	14	15
-2	5	8	7

K =-12

H	L	FO	FC
-2	2	8	9
-2	4	39	40
-2	6	31	32
-2	8	7	8
-2	10	15	15

K =-11

H	L	FO	FC
-2	1	24	23
-2	3	22	22
-2	5	6	8
-2	9	7	8

K =-10

H	L	FO	FC
-2	4	63	68
-2	6	61	63
-2	8	9	9
-2	10	21	21

K = -9

H	L	FO	FC
-2	1	17	18
-2	3	29	28
-2	5	5	6
-2	7	4	3
-2	9	11	10

K = -8

H	L	FO	FC
-2	2	5	6
-2	4	71	71
-2	6	76	80
-2	10	26	27
-2	12	36	37

K = -7

H	L	FO	FC
-2	1	33	34
-2	3	18	18
-2	5	6	5

-2	7	3	4
-2	9	5	6

K = -6

H	L	FO	FC
-2	2	5	3
-2	4	54	60
-2	6	72	76
-2	8	8	7
-2	10	23	22
-2	12	37	37

K = -5

H	L	FO	FC
-2	3	22	21
-2	5	11	12
-2	9	3	3

K = -4

H	L	FO	FC
-2	2	5	11
-2	4	76	71
-2	6	69	70
-2	8	12	12
-2	10	23	21
-2	12	36	35

K = -3

H	L	FO	FC
-2	1	31	30
-2	5	7	4

K = -2

H	L	FO	FC
-2	2	6	2
-2	4	147	142
-2	6	93	91
-2	8	22	22
-2	10	36	35
-2	12	39	39

K = -1

H	L	FO	FC
-2	1	35	31
-2	3	14	12
-2	5	15	17
-2	9	4	4
-2	11	4	3

K = 0

H	L	FO	FC
-2	2	96	86
-2	4	176	149
-2	6	94	89
-2	8	13	14
-2	10	50	51
-2	12	46	46

K = 1

H	L	FO	FC
-2	-7	3	2

K = 15

H	L	FO	FC
-2	-7	3	2

K =-21

H	L	FO	FC
-1	2	5	5

K =-20

H	L	FO	FC
-1	1	7	7
-1	3	5	7

K =-19

H	L	FO	FC
-1	2	5	7
-1	4	13	14
-1	6	13	14

K =-18

H	L	FO	FC
-1	1	12	12
-1	3	11	12

K =-17

H	L	FO	FC
-1	2	11	12
-1	4	21	21
-1	6	21	23
-1	8	7	9

K =-16

H	L	FO	FC
-1	1	17	16
-1	3	12	13
-1	5	3	5
-1	9	9	8

K =-15

H	L	FO	FC
-1	2	17	16
-1	4	20	21
-1	6	24	24
-1	8	9	10

K =-14

H	L	FO	FC
-1	1	12	15
-1	3	10	10
-1	5	4	6
-1	9	5	7

K =-13

H	L	FO	FC
-1	2	24	27

-1	4	17	19
-1	6	19	21
-1	8	8	8
-1	10	10	10

K =-12

H	L	FO	FC
-1	1	22	22
-1	3	14	15
-1	5	12	13
-1	9	5	6

K =-11

H	L	FO	FC
-1	2	23	23
-1	4	45	47
-1	6	44	44
-1	8	18	18
-1	10	14	15

K =-10

H	L	FO	FC
-1	1	20	22
-1	3	18	18
-1	5	10	12
-1	7	7	8
-1	9	8	8

K = -9

H	L	FO	FC
-1	2	51	52
-1	4	65	65
-1	6	58	61
-1	8	23	24
-1	10	24	25
-1	12	36	37

K = -8

H	L	FO	FC
-1	1	37	37
-1	3	21	23
-1	5	11	11
-1	7	7	7
-1	9	8	7

K = -7

H	L	FO	FC
-1	2	72	65
-1	4	61	58
-1	6	56	57
-1	8	27	28
-1	10	26	26
-1	12	41	41

K = -6

H	L	FO	FC
-1	1	21	21
-1	3	15	14
-1	7	4	6

-1	9	6	7

K = -5

H	L	FO	FC
-1	2	70	71
-1	4	42	47
-1	6	39	43
-1	8	25	27
-1	10	20	21
-1	12	40	41

K = -4

H	L	FO	FC
-1	1	24	25
-1	3	19	17
-1	5	7	6
-1	9	5	6

K = -3

H	L	FO	FC
-1	2	71	66
-1	4	72	74
-1	6	65	64
-1	8	30	33
-1	10	20	19
-1	12	45	46

K = -2

H	L	FO	FC
-1	3	11	9
-1	9	5	7

K = -1

H	L	FO	FC
-1	2	141	133
-1	4	92	95
-1	6	90	90
-1	8	29	29
-1	10	34	33
-1	12	57	60

K = 2

H	L	FO	FC
-1	-11	3	4

K = 10

H	L	FO	FC
-1	-1	3	0

K =-19

H	L	FO	FC
0	1	4	3

K =-15

H	L	FO	FC
0	-7	3	2

K = -5

H	L	FO	FC
0	7	3	3
0	9	3	2

K = 0

H	L	FO	FC
0	2	143	140
0	4	42	36
0	6	100	100
0	8	43	40
0	10	34	37
0	12	54	54

K = 1

H	L	FO	FC
0	3	5	5
0	5	3	4

K = 2

H	L	FO	FC
0	0	219	227
0	2	7	11
0	4	45	52
0	6	85	86
0	8	50	49
0	10	25	25
0	12	45	44

K = 3

H	L	FO	FC
0	-9	3	3
0	-7	2	3
0	1	8	9
0	5	7	7
0	11	5	6

K = 4

H	L	FO	FC
0	0	278	230
0	2	82	71
0	4	49	42
0	6	39	42
0	8	38	40
0	10	20	22
0	12	34	34

K = 5

H	L	FO	FC
0	1	2	1
0	5	9	8
0	11	6	6

K = 6

H	L	FO	FC
0	0	113	127
0	2	68	64
0	4	43	44
0	6	37	37

H	L	FO	FC
0	8	41	43
0	10	24	24
0	12	34	34

K = 7

H	L	FO	FC
0	1	5	3
0	3	8	8
0	5	13	12
0	7	7	8
0	9	8	8
0	11	8	8

K = 8

H	L	FO	FC
0	0	201	182
0	2	97	91
0	4	57	53
0	6	53	54
0	8	40	42
0	10	25	26
0	12	34	35

K = 9

H	L	FO	FC
0	1	4	4
0	3	15	14
0	5	14	14
0	7	5	5
0	9	11	10
0	11	8	8

K = 10

H	L	FO	FC
0	0	104	108
0	2	35	38
0	4	41	43
0	6	51	51
0	8	36	35
0	10	17	17
0	12	27	27

K = 11

H	L	FO	FC
0	3	15	13
0	5	10	10
0	7	3	3
0	9	10	10
0	11	8	8

K = 12

H	L	FO	FC
0	0	85	76
0	2	21	19
0	4	19	17
0	6	29	30
0	8	19	19
0	10	11	10

K = 13

H	L	FO	FC
0	1	3	3
0	3	8	9
0	5	6	6
0	9	8	8

K = 14

H	L	FO	FC
0	0	59	58
0	2	14	16
0	4	3	3
0	6	19	20
0	8	14	13
0	10	6	7

K = 15

H	L	FO	FC
0	3	13	12
0	5	7	7
0	9	7	8

K = 16

H	L	FO	FC
0	0	47	43
0	2	10	10
0	4	16	13
0	6	26	25
0	8	15	15

K = 17

H	L	FO	FC
0	1	3	2
0	3	11	12
0	5	7	8
0	7	4	3

K = 18

H	L	FO	FC
0	0	33	33
0	2	12	12
0	4	11	11
0	6	17	18

K = 19

H	L	FO	FC
0	3	10	8
0	5	6	6

K = 20

H	L	FO	FC
0	0	17	17
0	2	5	7
0	4	7	7

K = 21

H	L	FO	FC
0	3	5	4

K =-12

H	L	FO	FC
1	-11	4	3

K = -2

H	L	FO	FC
1	-5	3	3

K = 1

H	L	FO	FC
1	0	206	220
1	2	101	97
1	4	19	15
1	6	79	78
1	8	77	76
1	10	11	12
1	12	29	29

K = 2

H	L	FO	FC
1	1	11	11
1	3	7	9
1	5	6	5

K = 3

H	L	FO	FC
1	0	107	103
1	2	14	11
1	4	12	9
1	6	63	62
1	8	62	62
1	12	21	20

K = 4

H	L	FO	FC
1	1	18	19
1	3	5	4
1	5	5	6
1	7	5	5
1	9	7	6
1	11	6	6

K = 5

H	L	FO	FC
1	0	106	110
1	2	6	5
1	4	18	12
1	6	45	50
1	8	45	43
1	12	21	21

K = 6

H	L	FO	FC
1	1	7	7
1	3	15	14
1	5	5	4
1	9	10	10
1	11	8	7

K = 7

H	L	FO	FC
1	0	148	139
1	2	45	45
1	4	15	12
1	6	69	67
1	8	45	44
1	12	28	27

K = 8

H	L	FO	FC
1	1	18	17
1	3	26	23
1	5	9	11
1	7	4	2
1	9	16	15
1	11	9	9

K = 9

H	L	FO	FC
1	0	128	126
1	2	41	45
1	4	2	5
1	6	68	68
1	8	46	44
1	12	25	25

K = 10

H	L	FO	FC
1	3	25	23
1	5	8	8
1	7	3	3
1	9	15	14
1	11	9	9

K = 11

H	L	FO	FC
1	0	64	63
1	2	26	23
1	4	9	9
1	6	46	44
1	8	36	35

K = 12

H	L	FO	FC
1	1	11	9
1	3	12	11
1	5	7	6
1	7	6	4
1	9	11	11
1	11	9	9

K = 13

H	L	FO	FC
1	0	48	47
1	2	22	22
1	6	17	18
1	8	23	22
1	10	3	4

K = 14

H	L	FO	FC
1	3	11	10
1	5	8	8
1	9	8	8

K = 15

H	L	FO	FC
1	0	37	35
1	2	22	18
1	4	5	4
1	6	22	20
1	8	22	21

K = 16

H	L	FO	FC
1	1	3	3
1	3	12	11
1	5	10	9
1	7	5	3
1	9	9	8

K = 17

H	L	FO	FC
1	0	32	32
1	2	17	16
1	4	7	6
1	6	21	21
1	8	19	18

K = 18

H	L	FO	FC
1	3	12	11
1	5	8	7

K = 19

H	L	FO	FC
1	0	21	21
1	2	11	10
1	6	16	14

K = 20

H	L	FO	FC
1	1	3	1
1	3	8	7

K = 21

H	L	FO	FC
1	0	11	12
1	2	7	5

K =-17

H	L	FO	FC
2	-7	5	5

K =-13

H	L	FO	FC
2	-7	3	2

K =-10

H	L	FO	FC
2	-2	3	1

K = -8

H	L	FO	FC
2	-8	3	4

K = -5

H	L	FO	FC
2	-11	3	0

K = -3

H	L	FO	FC
2	-9	3	4

K = -1

H	L	FO	FC
2	-13	3	0

K = 0

H	L	FO	FC
2	0	171	155
2	2	230	210
2	4	27	33
2	6	97	93
2	8	95	93
2	10	15	14
2	12	32	34

K = 1

H	L	FO	FC
2	1	48	44
2	3	5	6
2	5	2	3

K = 2

H	L	FO	FC
2	0	25	39
2	2	100	86
2	6	98	100
2	8	88	88
2	10	17	19
2	12	26	26

K = 3

H	L	FO	FC
2	1	11	11
2	3	13	12
2	5	3	2
2	9	4	6

K = 4

H	L	FO	FC
2	0	67	51
2	2	44	52
2	4	19	23
2	6	65	64
2	8	67	66
2	10	19	19
2	12	19	19

K = 5

H	L	FO	FC
2	1	7	7
2	7	4	2
2	9	6	5

K = 6

H	L	FO	FC
2	0	72	72
2	2	44	42
2	4	22	17
2	6	66	69
2	8	60	60
2	10	14	14
2	12	21	21

K = 7

H	L	FO	FC
2	1	20	19
2	3	11	12
2	5	11	11
2	7	3	2
2	9	7	7
2	11	4	5

K = 8

H	L	FO	FC
2	0	115	106
2	2	83	78
2	4	16	22
2	6	70	70
2	8	64	61
2	10	12	11
2	12	22	23

K = 9

H	L	FO	FC
2	1	6	5
2	3	16	17
2	5	12	12
2	9	7	6
2	11	6	7

K = 10

H	L	FO	FC
2	0	54	58
2	2	50	49
2	4	4	1
2	6	61	59
2	8	55	53
2	10	11	10

K = 11

H	L	FO	FC
2	3	11	11

H	L	FO	FC
2	5	12	10
2	9	6	6
2	11	7	7

K = 12

H	L	FO	FC
2	0	32	28
2	2	34	33
2	6	32	31
2	8	33	33
2	10	8	6

K = 13

H	L	FO	FC
2	3	3	4
2	5	4	6
2	9	4	5

K = 14

H	L	FO	FC
2	0	25	24
2	2	30	29
2	4	9	5
2	6	20	18
2	8	24	23
2	10	5	4

K = 15

H	L	FO	FC
2	3	10	8
2	5	13	10
2	9	5	5

K = 16

H	L	FO	FC
2	0	22	21
2	2	24	22
2	6	23	23
2	8	23	23

K = 17

H	L	FO	FC
2	3	9	9
2	5	8	9

K = 18

H	L	FO	FC
2	0	22	21
2	2	20	18
2	6	18	17

K = 19

H	L	FO	FC
2	3	10	8
2	5	7	6

K = 20

H	L	FO	FC
2	0	12	12

H	L	FO	FC
2	2	10	9

K = -5

H	L	FO	FC
3	-2	2	2

K = -4

H	L	FO	FC
3	-7	3	5

K = -2

H	L	FO	FC
3	-5	2	5

K = 1

H	L	FO	FC
3	0	148	136
3	2	95	101
3	4	63	58
3	6	95	94
3	8	80	79
3	10	23	24
3	12	25	26

K = 2

H	L	FO	FC
3	1	23	25
3	3	23	22
3	5	10	9

K = 3

H	L	FO	FC
3	0	55	48
3	2	46	46
3	4	18	19
3	6	69	69
3	8	71	70
3	10	21	21
3	12	14	15

K = 4

H	L	FO	FC
3	1	8	10
3	3	4	2
3	5	3	5

K = 5

H	L	FO	FC
3	0	12	23
3	2	54	55
3	4	12	11
3	6	43	41
3	8	64	64
3	10	14	14
3	12	12	12

K = 6

H	L	FO	FC
3	1	7	5

APPENDIX C: OBSERVED AND CALCULATED STRUCTURE FACTORS FOR THE ORTHORHOMBIC CRYSTAL OF $Mo_2(O_2CC(CH_3)_3)_4$

H =-14

K	L	FO	FC
-7	1	14	14
-3	5	10	5
-1	1	10	1

H =-13

K	L	FO	FC
-9	1	17	7
-5	3	12	9
-2	3	8	4
0	2	9	8

H =-12

K	L	FO	FC
-12	1	9	6
-9	4	10	14
-5	7	9	9
-4	8	34	40

H =-11

K	L	FO	FC
-13	1	8	8
-11	5	9	10
-8	8	16	18
-7	5	12	11
-6	5	10	10
-6	7	9	7

H =-10

K	L	FO	FC
-14	5	9	10
-9	7	13	12
-5	5	10	6

H = -9

K	L	FO	FC
-17	3	13	14
-13	5	8	9
-10	1	9	10
-9	5	9	9
-8	9	10	9
-4	7	9	9
-3	1	8	10

H = -8

K	L	FO	FC
-16	6	13	13
-12	4	12	6
-11	5	11	14
-9	9	9	7
-3	11	10	4
-2	4	9	6

H = -7

K	L	FO	FC
-13	4	8	7
-11	1	8	3
-7	9	9	12
-3	4	7	4
-2	9	9	8
-2	12	11	14
-1	7	8	7

H = -6

K	L	FO	FC
-14	1	9	5
-10	4	8	5
-8	8	9	7
-3	7	12	11
-3	12	13	12
-1	9	10	5
-1	12	8	10

H = -5

K	L	FO	FC
-17	0	8	13
-13	4	10	10
-5	1	6	5
-3	8	8	10
-3	12	9	12
-2	5	11	12

H = -4

K	L	FO	FC
-20	3	9	9
-18	4	13	12
-8	7	10	4
-4	10	8	7
-3	9	13	12
0	4	11	9

H = -3

K	L	FO	FC
-16	9	10	4
-13	4	9	6
-7	1	10	8
-6	3	11	11
-2	6	7	2
-2	12	10	11

H = -2

K	L	FO	FC
-7	9	7	5
-1	6	7	5

H = -1

K	L	FO	FC
-20	4	10	9
-18	1	10	13
-18	7	8	2
-14	6	8	5
-2	3	7	2
-2	6	6	5
0	6	8	11

H = 0

K	L	FO	FC
-22	0	19	23
-18	1	10	11
-4	1	6	7
0	2	281	289
0	4	89	79
0	6	199	198
0	8	72	68
0	10	63	62
0	12	114	105
2	0	438	454
2	1	6	2
2	2	24	31
2	3	8	9
2	4	85	105
2	5	10	9
2	6	166	166
2	8	83	88
2	10	44	43
2	11	11	10
2	12	90	87
4	0	498	462
4	2	173	152
4	4	103	93
4	5	18	19
4	6	77	82
4	8	70	74
4	10	39	41
4	11	9	9
4	12	68	67
6	0	221	259
6	1	13	14
6	2	145	136
6	3	14	16
6	4	88	92
6	5	13	10
6	6	65	67
6	7	11	13
6	8	79	83
6	9	10	10
6	10	46	46
6	12	65	64
8	0	393	370
8	1	16	16
8	2	197	185
8	3	31	30
8	4	118	116
8	5	27	27
8	6	104	102
8	7	11	10
8	8	72	78
8	9	20	17
8	10	48	51
8	11	17	15
8	12	65	65
10	0	214	222
10	1	14	16
10	2	74	80
10	3	39	38
10	4	89	91
10	5	25	25
10	6	98	98
10	8	64	64
10	9	22	21
10	10	35	33
10	11	18	17
10	12	50	52
12	0	169	159
12	2	47	40
12	3	25	27
12	4	42	39
12	5	21	20
12	6	60	60
12	8	33	33
12	9	14	16
12	10	19	20
12	11	16	13
14	0	120	124
14	2	34	35
14	3	25	24
14	5	15	11
14	6	40	40
14	8	24	22
14	9	14	16
14	10	17	13
16	0	98	93
16	2	21	22
16	3	27	27
16	4	33	32
16	5	16	15
16	6	51	51
16	8	23	27
16	9	15	16
18	0	65	71
18	2	27	26
18	3	26	25
18	4	21	26
18	5	15	17
18	6	31	36
20	0	36	38
20	2	11	16
20	3	11	14
20	4	14	17
20	5	10	12

H = 1

K	L	FO	FC
0	2	33	31
0	4	89	94
0	8	41	42
0	10	15	15
0	12	22	19
1	0	426	442
1	1	5	8
1	2	233	225
1	3	12	15
1	4	117	118
1	5	10	12
1	6	160	158
1	8	88	91
1	10	47	47
1	12	79	76
2	1	10	11
2	2	51	50
2	4	63	70
2	8	34	34
2	10	14	13
2	12	16	19
3	0	211	209
3	1	9	6
3	2	81	75
3	3	19	16
3	4	91	89
3	5	14	11
3	6	123	120
3	8	83	83
3	9	10	12
3	10	24	23
3	12	59	59
4	1	39	40
4	2	67	64
4	3	15	16
4	4	53	59
4	7	10	6
4	8	22	22
4	10	13	12
4	12	14	17
5	0	209	221
5	1	10	12
5	2	65	74
5	3	25	26
5	4	28	40
5	5	9	13
5	6	82	90
5	8	60	60
5	9	13	10
5	10	21	21
5	12	54	56
6	1	23	23
6	2	50	42
6	4	62	56
6	8	20	19
6	10	13	14
6	11	12	8
6	12	14	13
7	0	300	283
7	1	22	22
7	2	113	111
7	3	39	41
7	4	53	49
7	5	12	12
7	6	121	119
7	7	13	12
7	8	62	62
7	9	18	20
7	10	29	27
7	12	61	61
8	1	52	49
8	2	10	5
8	4	70	64
8	8	22	24
8	10	15	16
9	0	264	256
9	1	24	24
9	2	94	96
9	3	46	47
9	4	70	76
9	5	25	24
9	6	124	126
9	8	61	59
9	9	24	24
9	10	26	28
9	12	55	55
10	1	16	20
10	4	50	46
10	8	22	20
10	12	10	9
11	0	135	130
11	1	21	21
11	2	50	46
11	3	41	40
11	4	58	60
11	6	89	86
11	8	48	48
11	9	18	20
11	10	19	18
11	11	17	14
11	12	31	29
12	1	31	29
12	3	9	8
12	4	27	29
12	6	10	3
12	7	7	1
12	8	14	15
13	0	99	98
13	1	10	12
13	2	48	51
13	3	21	22
13	4	19	21
13	5	17	17
13	6	38	39
13	8	24	27
13	9	14	15
13	10	14	16
13	12	53	49
14	2	9	5
14	4	18	19
14	8	11	10
15	0	78	74
15	1	16	14
15	2	38	36
15	3	28	25
15	4	26	28
15	5	11	14
15	6	45	44
15	8	29	30
15	9	12	16
16	1	23	18
16	4	16	17
16	8	13	10
17	0	63	67
17	1	13	14
17	2	28	29
17	3	28	28
17	4	32	30
17	5	12	16
17	6	42	45
17	8	21	25
18	4	13	14
19	0	47	46
19	1	17	11
19	2	19	19
19	3	24	22
19	4	19	18
19	5	16	13
19	6	28	29
21	0	26	28
21	3	12	13

H = 2

K	L	FO	FC
0	0	331	313
0	2	311	293
0	4	142	115
0	6	181	173
0	8	100	103
0	10	37	38
0	12	63	63
1	1	76	76
1	2	128	118
1	3	11	9
1	4	173	161
1	5	13	22
1	8	72	73
1	10	52	53
1	12	16	13
2	0	46	73
2	1	13	12
2	2	101	82
2	3	16	15
2	4	143	156
2	5	12	12
2	6	181	183
2	8	105	105
2	10	20	19
2	12	56	53
3	1	45	46
3	2	69	66
3	3	8	3
3	4	121	114
3	8	56	54
3	10	45	43
3	12	10	15

4	0	130	102	10	3	41	42	17	7	10	8	5	0	26	43	11	5	20	18	21	0	11	13	6	6	69	68
4	1	14	16	10	4	64	66	17	8	14	15	5	1	8	6	11	6	79	78					6	8	27	26
4	2	45	58	10	5	18	21	18	0	44	43	5	2	54	50	11	8	44	45		H =	4		6	10	11	14
4	3	25	24	10	6	124	122	18	1	15	14	5	3	8	10	12	1	27	26	K	L	FO	FC	6	12	23	24
4	4	60	47	10	8	58	57	18	2	26	22	5	4	62	67	12	2	46	47	0	0	139	142	7	1	21	24
4	5	13	14	10	9	16	20	18	3	25	26	5	5	10	12	12	3	14	13	0	2	98	105	7	2	131	128
4	6	136	132	10	10	9	12	18	4	17	18	5	6	97	96	12	4	58	56	0	6	98	94	7	3	14	10
4	8	74	73	10	11	11	11	18	5	11	13	5	8	73	75	12	5	9	8	0	8	29	28	7	4	156	156
4	12	48	45	10	12	39	39	18	6	34	37	5	10	11	10	12	7	12	12	0	10	16	16	7	5	29	28
5	1	9	7	11	1	29	27	19	1	14	13	5	12	36	36	12	8	31	30	0	12	36	35	7	7	24	25
5	2	24	25	11	2	44	39	19	2	16	12	6	1	15	11	12	9	8	6	1	1	18	24	7	8	71	68
5	3	23	20	11	3	14	13	19	4	18	18	6	2	76	75	12	10	25	23	1	2	217	215	7	9	8	8
5	4	83	82	11	4	57	59	20	0	24	26	6	4	102	96	12	11	11	4	1	4	237	229	7	10	47	46
5	5	11	14	11	5	9	5	20	1	9	8	6	5	31	30	13	0	47	54	1	5	13	10	7	12	10	9
5	6	13	12	11	8	33	32	20	3	17	18	6	6	14	13	13	1	8	6	1	7	11	9	8	0	82	77
5	8	46	44	11	9	9	0					6	7	23	21	13	2	22	21	1	8	105	106	8	1	9	11
5	10	37	36	11	10	27	25		H =	3		6	8	49	50	13	3	25	25	1	9	8	11	8	2	69	72
5	12	14	15	12	0	65	55	K	L	FO	FC	6	10	36	37	13	5	9	10	1	10	60	57	8	3	18	18
6	0	142	145	12	1	19	20	0	2	176	185	7	0	121	113	13	6	42	46	1	12	18	13	8	4	28	27
6	1	8	9	12	2	40	41	0	4	191	196	7	2	104	99	13	8	23	23	2	0	108	109	8	5	11	10
6	2	32	36	12	3	30	30	0	8	82	79	7	3	8	9	13	9	9	9	2	1	12	12	8	6	69	69
6	3	18	19	12	4	40	37	0	10	60	59	7	4	82	79	14	2	30	30	2	2	51	50	8	8	27	29
6	4	31	39	12	5	21	20	1	0	296	270	7	5	8	9	14	4	45	41	2	3	31	32	8	9	11	7
6	6	143	144	12	6	64	63	1	1	10	6	7	6	99	99	14	5	19	19	2	4	55	58	8	10	13	14
6	8	60	61	12	7	10	3	1	2	48	52	7	8	74	74	14	7	19	18	2	5	11	11	8	12	21	25
6	10	7	7	12	8	38	40	1	3	23	19	7	10	18	19	14	8	19	20	2	6	103	109	9	1	16	13
6	12	49	51	12	9	12	13	1	4	55	63	7	12	39	38	14	10	19	18	2	7	7	6	9	2	123	127
7	1	55	56	12	10	11	11	1	5	11	13	8	1	44	46	15	0	58	49	2	8	32	32	9	3	9	16
7	2	74	70	13	1	17	17	1	6	184	188	8	2	119	114	15	2	19	16	2	9	10	12	9	4	142	139
7	4	99	100	13	2	12	13	1	8	80	77	8	4	115	118	15	3	17	19	2	12	28	28	9	5	29	29
7	5	19	20	13	3	11	12	1	10	10	11	8	5	28	30	15	4	15	12	3	1	21	11	9	7	36	34
7	6	11	11	13	4	35	35	1	12	61	58	8	6	9	7	15	6	49	46	3	2	137	130	9	8	71	70
7	7	9	8	13	8	14	18	1	13	9	0	8	7	22	22	15	8	20	23	3	4	166	167	9	9	13	13
7	8	48	49	13	10	16	17	2	1	31	36	8	8	61	60	16	1	24	20	3	8	76	78	9	10	44	44
7	10	38	36	14	0	50	50	2	2	112	116	8	10	40	40	16	2	34	34	3	10	46	46	10	0	66	60
7	12	10	13	14	1	16	16	2	3	14	14	8	12	9	10	16	4	39	38	3	12	11	14	10	1	13	14
8	0	229	212	14	2	49	46	2	4	140	139	9	0	87	95	16	5	15	17	4	0	7	4	10	2	39	37
8	1	23	22	14	3	20	19	2	7	9	11	9	1	20	18	16	7	15	17	4	1	12	11	10	3	23	27
8	2	83	82	14	4	16	19	2	8	67	65	9	2	65	68	16	8	20	21	4	2	37	40	10	4	35	38
8	3	45	45	14	5	9	13	2	10	53	51	9	3	34	35	17	0	38	38	4	3	26	27	10	5	16	15
8	4	55	47	14	6	40	39	3	0	107	95	9	4	69	72	17	1	12	10	4	4	23	15	10	6	71	69
8	5	15	16	14	8	31	30	3	1	11	12	9	5	17	20	17	2	10	15	4	5	9	9	10	7	8	7
8	6	138	149	14	9	14	12	3	2	7	4	9	6	96	100	17	3	24	22	4	6	69	65	10	8	26	25
8	8	58	59	15	1	19	19	3	3	20	21	9	8	64	66	17	4	14	17	4	8	28	30	10	9	14	13
8	9	18	18	15	2	19	16	3	4	87	85	9	9	11	12	17	6	37	39	4	12	21	21	10	11	10	8
8	10	17	14	15	4	34	31	3	5	9	11	9	10	17	15	17	8	17	21	5	1	19	15	11	1	16	15
8	12	52	52	15	5	17	12	3	6	152	147	9	12	32	35	18	1	13	15	5	2	96	96	11	2	82	82
9	1	15	13	15	8	13	15	3	8	84	81	10	2	84	84	18	2	25	28	5	3	8	1	11	4	95	93
9	2	60	60	16	0	43	43	3	12	45	42	10	3	8	6	18	4	28	29	5	4	139	137	11	5	12	12
9	3	13	10	16	1	17	16	4	1	32	36	10	4	90	89	18	5	13	13	5	5	17	16	11	7	23	25
9	4	81	86	16	2	32	28	4	2	56	70	10	5	28	27	18	7	17	14	5	7	17	13	11	8	52	50
9	6	9	6	16	3	25	25	4	3	16	16	10	7	24	23	19	0	26	24	5	8	67	63	11	9	11	11
9	7	11	8	16	4	34	29	4	4	98	100	10	8	52	50	19	2	11	14	5	9	11	8	11	10	30	30
9	8	49	48	16	5	15	13	4	6	8	12	10	10	34	34	19	3	17	18	5	10	42	42	12	0	32	35
9	10	33	34	16	6	45	48	4	7	6	8	11	0	65	60	19	4	14	11	5	12	12	13	12	1	13	12
9	12	9	10	16	8	28	30	4	8	50	47	11	1	12	13	19	5	9	10	6	0	85	81	12	2	20	23
10	0	106	116	17	1	21	20	4	9	8	1	11	2	27	23	19	6	23	22	6	2	84	75	12	3	27	24
10	1	25	23	17	2	17	17	4	10	40	39	11	3	31	35	20	2	15	17	6	3	6	4	12	4	11	12
10	2	44	46	17	4	24	26	4	12	13	13	11	4	53	47	20	4	15	17	6	4	33	38	12	5	8	12

12	6	40	41
13	1	14	13
13	2	44	48
13	4	38	38
13	5	11	11
13	7	21	20
13	8	34	32
13	10	17	20
14	0	46	43
14	2	30	27
14	4	9	6
14	5	7	4
14	6	32	31
15	1	13	11
15	2	45	43
15	4	49	49
15	5	23	21
15	7	22	24
15	8	30	28
16	0	28	29
16	2	16	17
16	3	11	10
16	4	15	15
16	6	31	33
16	8	12	13
17	1	15	19
17	2	39	40
17	4	42	42
17	5	16	16
17	7	15	18
18	0	24	22
18	2	15	15
18	5	10	8
18	6	22	23
19	1	13	12
19	2	26	28
19	4	28	29
19	5	10	11
20	4	11	5
21	1	11	7

H = 5

K	L	FO	FC
0	2	255	258
0	4	222	215
0	6	17	19
0	8	108	103
0	10	89	84
1	0	77	72
1	1	17	16
1	2	187	174
1	3	23	22
1	4	36	37
1	5	9	7
1	6	60	57
1	7	7	6
1	10	35	33
1	12	14	15
2	1	24	22
2	2	200	192
2	3	17	14
2	4	176	168
2	6	17	13
2	7	14	15
2	8	95	93
2	10	79	78
2	12	12	13
3	0	56	52
3	1	13	12
3	2	106	101
3	3	16	17
3	4	26	30
3	5	7	7
3	6	71	70
3	10	22	21
4	1	28	26
4	2	131	132
4	3	21	19
4	4	120	124
4	6	14	16
4	7	7	6
4	8	66	66
4	10	65	65
5	0	86	81
5	2	75	68
5	3	9	8
5	6	70	71
5	8	21	22
5	10	11	15
5	12	13	16
6	1	16	16
6	2	133	132
6	3	9	10
6	4	127	126
6	5	25	24
6	6	15	14
6	7	15	18
6	8	66	65
6	10	61	63
6	12	12	11
7	0	111	113
7	1	16	16
7	2	68	67
7	3	20	21
7	4	8	13
7	5	8	8
7	6	70	70
7	7	7	11
7	8	19	22
7	10	12	13
7	11	10	1
7	12	18	19
8	1	35	34
8	2	149	151
8	4	139	137
8	5	23	23
8	7	25	25
8	8	74	71
8	10	64	63
9	0	62	64
9	2	51	44
9	3	6	6
9	6	65	62
9	8	10	9
9	10	10	10
10	1	16	15
10	2	117	119
10	3	12	8
10	4	105	106
10	5	31	29
10	7	29	28
10	8	62	61
10	9	12	11
10	10	52	51
11	0	28	27
11	2	36	38
11	3	11	10
11	4	14	14
11	5	8	7
11	6	37	38
12	1	33	31
12	2	69	69
12	3	20	14
12	4	63	64
12	7	14	15
12	8	42	39
12	10	33	35
13	0	19	18
13	2	42	41
13	6	21	19
14	1	13	13
14	2	35	31
14	4	30	30
14	5	24	21
14	7	18	21
14	8	25	28
15	0	19	18
15	2	31	32
15	4	16	14
15	6	21	19
16	1	23	22
16	2	46	47
16	4	43	44
16	5	14	19
16	7	17	19
16	8	26	27
17	2	16	16
17	4	10	12
17	6	18	20
18	1	20	20
18	2	38	38
18	4	34	35
18	5	14	15
19	2	13	9
20	1	16	13
20	2	21	22

H = 6

K	L	FO	FC
0	0	50	53
0	2	51	43
0	4	31	28
0	6	13	11
0	8	24	23
0	10	11	8
1	2	205	197
1	3	15	15
1	4	126	134
1	5	19	20
1	6	29	30
1	7	13	14
1	8	80	75
1	10	103	101
2	0	37	34
2	1	19	20
2	2	34	33
2	3	27	27
2	4	14	16
2	5	8	9
2	6	12	14
2	7	11	11
2	8	21	19
2	10	10	8
3	1	10	6
3	2	142	135
3	3	8	10
3	4	81	85
3	6	28	31
3	8	61	58
3	10	87	87
4	0	14	16
4	1	8	7
4	2	29	27
4	6	17	16
4	8	16	14
5	1	45	48
5	2	111	117
5	3	12	10
5	4	71	70
5	5	10	12
5	6	30	32
5	7	9	9
5	8	52	52
5	10	74	76
5	12	13	13
6	0	36	31
6	1	15	11
6	2	50	50
6	3	26	25
6	8	15	13
7	1	31	32
7	2	136	137
7	3	10	9
7	4	93	92
7	5	16	17
7	6	32	32
7	7	13	14
7	8	61	59
7	10	72	74
8	0	15	17
8	1	7	8
8	2	38	38
8	3	13	14
9	1	39	40
9	2	129	132
9	4	94	90
9	5	33	34
9	6	21	21
9	7	24	24
9	8	59	60
9	10	65	68
10	1	7	3
10	2	16	18
11	1	37	39
11	2	91	87
11	3	15	16
11	4	63	61
11	5	13	17
11	6	16	15
11	7	14	16
11	8	44	42
11	10	51	53
12	2	12	13
12	3	10	7
13	1	37	34
13	2	39	36
13	3	13	12
13	4	45	42
13	5	12	15
13	7	10	13
13	8	23	26
14	0	21	18
14	2	11	13
15	1	20	22
15	2	52	48
15	4	41	39
15	5	19	20
15	6	10	10
15	7	18	17
15	8	24	23
16	0	10	11
17	1	28	29
17	2	45	43
17	4	35	35
17	5	15	16
17	6	10	6
19	1	22	21
19	2	28	29
19	4	21	23

H = 7

K	L	FO	FC
0	2	189	193
0	4	158	153
0	6	26	28
0	8	87	86
0	10	93	93
0	12	12	13
1	0	25	23
1	1	9	9
1	2	56	55
1	3	18	18
1	4	30	31
1	6	23	23
1	8	9	9
2	2	165	163
2	4	131	124
2	5	18	18
2	6	23	20
2	7	10	14
2	8	80	80
2	10	88	87
3	0	36	36
3	1	7	9
3	2	41	43
3	3	24	24
3	6	18	18
4	1	36	32
4	2	118	118
4	3	19	19
4	4	93	93
4	6	20	23
4	8	63	62
4	10	77	75
5	0	35	34
5	2	17	17
5	3	12	12
5	4	10	11
5	5	8	6
5	6	22	22
5	9	10	7
6	1	17	19
6	2	122	122
6	4	98	97
6	6	24	21
6	8	62	61
6	10	71	72
6	11	11	8
7	0	32	33
7	1	15	14
7	3	24	25
7	5	8	6
7	6	34	32
8	1	32	31
8	2	133	124
8	3	9	6
8	4	103	102
8	5	11	12
8	6	19	19
8	7	15	14
8	8	64	61
8	10	71	68
9	0	35	38
9	2	18	18
9	6	21	21
10	1	30	31
10	2	100	98
10	4	82	79
10	5	15	18
10	6	8	12
10	7	18	21
10	8	52	51
10	10	54	57
11	0	24	20
11	2	20	19
11	6	10	13
12	1	45	42
12	2	60	61
12	3	16	15
12	4	52	51
12	6	9	11
12	7	15	11
12	8	33	34
13	2	12	13
14	1	18	20
14	2	50	48
14	4	44	41
14	5	11	12
14	8	25	25
15	1	12	8
16	1	25	23
16	2	42	42
16	4	37	36
17	1	11	5
17	2	10	7
18	1	22	24
18	2	32	33
18	4	27	28

H = 8

K	L	FO	FC
0	0	118	117
0	2	42	43
0	6	47	46
1	2	137	141
1	3	11	8
1	4	119	117
1	5	16	16
1	6	16	18
1	7	11	13
1	8	69	69
1	10	64	63
2	0	98	103
2	1	11	11
2	2	37	40
2	3	18	18
2	6	40	41
3	1	19	18
3	2	115	109
3	4	94	91
3	5	10	13
3	6	9	12
3	7	12	13

3	8	60	57	12	0	38	38	5	2	63	57	16	2	36	36	9	2	54	54	5	1	9	9	4	4	37	39
3	10	59	57	12	2	21	19	5	3	15	17	16	4	26	27	9	4	50	49	5	2	38	38	4	6	62	62
4	0	73	67	12	6	15	19	5	4	20	20	17	0	17	22	9	5	11	11	5	3	12	14	5	3	9	8
4	2	51	55	13	1	21	21	5	6	52	52	17	2	15	15	9	8	29	30	5	4	29	31	5	4	17	19
4	4	8	6	13	2	50	48	5	8	23	23					10	0	45	45	5	5	9	9	5	5	10	12
4	6	15	13	13	4	41	41	6	2	94	95		H = 10			10	1	14	10	5	6	71	71	6	0	86	83
5	1	18	18	13	5	11	9	6	4	68	64	K	L	FO	FC	10	2	32	33	5	8	41	40	6	2	46	43
5	2	95	94	13	7	14	12	6	8	41	41	0	0	53	52	10	3	16	18	6	2	15	13	6	4	35	39
5	4	83	84	13	8	28	26	6	10	39	38	0	2	81	78	10	4	17	18	6	4	41	42	6	6	54	55
5	6	11	10	14	0	30	28	7	0	68	67	0	4	46	45	10	6	39	60	6	8	20	21	7	4	19	18
5	8	49	48	14	2	11	8	7	1	13	12	0	6	86	87	10	8	17	22	7	0	55	53	7	5	9	10
5	10	55	53	14	3	15	15	7	2	48	48	0	8	45	45	11	1	17	15	7	1	12	11	8	0	78	80
6	0	47	46	14	6	13	16	7	3	25	23	0	10	12	11	11	2	40	39	7	2	43	38	8	2	41	41
6	1	13	15	15	1	14	8	7	4	28	28	1	2	85	82	11	4	35	35	7	3	17	20	8	3	12	13
6	2	47	47	15	2	43	42	7	6	36	36	1	3	8	6	12	0	25	24	7	4	32	33	8	4	34	35
6	3	22	25	15	4	37	36	7	8	23	23	1	4	78	77	12	2	29	29	7	6	66	67	8	6	48	51
6	4	21	21	16	0	23	23	7	9	10	11	1	5	11	13	12	3	17	15	7	8	36	39	10	0	65	66
6	5	13	14	16	2	9	8	7	10	11	12	1	7	8	10	12	4	13	16	8	2	12	13	10	1	11	7
6	6	19	18	16	3	14	15	8	2	95	92	1	8	44	41	12	5	9	10	8	4	43	39	10	2	27	28
6	7	8	10	17	1	14	16	8	3	7	4	1	10	32	34	12	6	39	41	9	0	54	53	10	3	13	15
6	8	9	12	17	2	37	35	8	4	68	65	2	0	38	37	12	7	8	1	9	2	39	38	10	4	24	27
6	9	9	11	17	4	27	30	8	5	12	14	2	2	61	58	13	2	30	31	9	3	19	20	10	5	10	10
7	1	13	9	18	0	18	19	8	6	9	7	2	4	44	41	13	4	28	29	9	4	30	29	11	1	13	12
7	2	102	103					8	7	13	14	2	6	84	87	14	0	16	16	9	6	37	38	11	4	13	9
7	4	94	93		H =	9		8	8	41	40	2	8	40	42	14	2	27	25	10	1	13	14	12	0	49	53
7	6	11	10	K	L	FO	FC	9	0	76	74	3	1	11	12	14	3	17	18	10	4	30	29	12	2	19	19
7	7	12	10	0	2	133	127	9	2	47	47	3	2	75	72	14	4	11	12	11	0	40	38	12	3	13	16
7	8	48	49	0	4	87	92	9	3	12	14	3	4	68	64	15	2	26	28	11	2	28	26				
7	10	52	53	0	6	13	10	9	4	21	21	3	5	15	17	15	4	25	25	11	3	18	19		H = 13		
8	0	57	51	0	8	52	47	9	6	52	50	3	7	13	12	16	0	16	16	11	4	24	23	K	L	FO	FC
8	1	13	13	0	10	52	50	9	7	8	3	3	8	37	41	16	2	19	19	11	6	47	48	1	0	89	93
8	2	50	50	1	0	114	117	9	8	18	16	3	10	29	30					12	1	16	17	1	2	57	56
8	3	21	22	1	2	71	66	10	2	73	71	4	0	47	45		H = 11			12	4	19	23	1	4	33	32
8	4	20	20	1	3	7	5	10	4	51	49	4	2	49	47	K	L	FO	FC	13	0	30	31	1	6	46	49
8	5	11	11	1	4	30	33	10	5	19	22	4	3	8	9	0	2	13	14	13	2	18	20	3	0	83	87
8	6	17	19	1	6	79	82	10	7	14	19	4	4	16	17	0	4	49	47	13	3	17	19	3	2	46	45
8	7	9	9	1	8	27	26	10	8	33	34	4	6	76	78	0	8	26	25	13	4	11	13	3	4	28	30
8	8	14	10	1	10	19	18	11	0	54	53	4	8	32	31	1	0	82	81	14	2	10	10	3	6	47	50
8	9	9	11	2	1	10	7	11	2	28	29	5	2	72	67	1	2	42	42	15	0	28	26	5	0	86	88
8	10	13	14	2	2	117	113	11	4	18	16	5	4	61	59	1	4	37	38	15	1	12	9	5	2	41	39
9	1	17	18	2	3	9	11	11	5	10	8	5	8	39	38	1	6	91	93					5	4	21	22
9	2	93	92	2	4	74	76	11	6	41	41	6	0	48	47	1	7	9	0		H = 12			5	6	48	49
9	3	9	4	2	5	15	22	12	1	21	18	6	1	16	14	1	8	45	45	K	L	FO	FC	6	5	12	12
9	4	81	82	2	7	19	20	12	2	31	32	6	2	32	30	2	1	10	11	0	0	131	129	7	0	85	86
9	5	22	20	2	8	48	46	12	4	37	36	6	3	22	25	2	2	10	9	0	2	48	46	7	2	34	35
9	7	20	22	2	10	48	48	12	5	13	13	6	4	13	15	2	4	43	42	0	4	36	35	7	4	17	19
9	8	46	47	3	0	94	91	12	7	11	12	6	6	80	81	2	5	15	19	0	6	75	78	8	1	10	12
9	10	46	48	3	2	64	61	12	8	23	24	6	8	25	27	2	7	15	12	0	8	41	40	9	0	72	73
10	0	57	56	3	4	22	24	13	0	37	36	7	1	12	12	2	8	24	25	1	4	20	21	9	2	28	30
10	2	42	40	3	6	64	64	13	2	21	20	7	2	68	66	3	0	62	63	1	8	11	13	9	3	10	13
10	4	16	16	3	8	22	24	13	3	10	12	7	4	59	58	3	2	36	36	2	0	114	111	9	4	16	19
10	6	21	22	3	10	12	15	13	6	29	28	7	8	34	36	3	4	33	34	2	2	41	39	11	0	53	55
11	1	32	31	4	1	15	15	14	2	42	43	8	0	60	58	3	6	80	82	2	4	36	39				
11	2	66	66	4	2	101	97	14	4	32	32	8	1	13	14	3	8	42	43	2	6	73	75		H = 14		
11	3	11	5	4	3	8	3	15	0	25	24	8	2	38	34	4	1	13	13	2	8	40	42	K	L	FO	FC
11	4	58	56	4	4	66	64	15	1	9	8	8	3	26	26	4	2	12	11	3	4	17	18	0	0	88	89
11	6	8	5	4	8	41	41	15	2	15	14	8	4	14	15	4	4	44	41	3	8	15	14	0	2	45	48
11	7	16	18	4	10	43	41	15	3	20	17	8	6	76	76	4	8	24	23	4	0	99	96	0	4	27	25
11	8	35	37	5	0	74	72	15	5	10	9	8	8	20	23	5	0	59	55	4	2	44	43	1	2	21	21

1	4	13	17
2	0	82	83
2	2	41	41
2	4	26	28
3	2	19	19
3	4	12	16
4	0	77	79
4	1	11	5
4	2	36	36
4	4	22	26
5	2	16	16
5	4	16	13
6	0	74	76
6	2	32	35
7	2	14	14
8	0	63	66

H = 15

K	L	FO	FC
0	2	13	17
1	0	63	64
1	2	14	17
3	0	55	55

APPENDIX D

In the monoclinic crystal of $Mo_2(piv)_4$, with two crystallographically equivalent molecules in the primitive lattice cell, $\Phi_1'(k)$ and $\Phi_2'(k)$ designate Frenkel exciton bands of states for the two symmetry equivalent molecular transitions, where $\hat{k}$ is the wave vector.

The two Davydov bands may be represented by

$$\Phi_I'(k) = (\Phi_1'(k) + \Phi_2'(k))/\sqrt{2}$$

and

$$\Phi_{II}'(k) = (\Phi_1'(k) + \Phi_2'(k))/\sqrt{2}.$$

Transitions are allowed only to the two Davydov states $\Phi_I'(0)$ and $\Phi_{II}'(0)$. If μ_1 and μ_2 represent electric dipole operators for the symmetry related molecules, the corresponding transition moment vectors $\hat{\mu}_1$ and $\hat{\mu}_2$ are given by $\hat{\mu}_1 = \langle\phi_1'|\mu_1|\phi_1^0\rangle$ and $\hat{\mu}_2 = \langle\phi_2'|\mu_2|\phi_2^0\rangle$. Here, ϕ_1' and ϕ_1^0 are the excited- and ground-state molecular wavefunctions for molecule 1, and ϕ_2' and ϕ_2^0 represent the corresponding molecule 2 wavefunctions. The vector $\hat{\mu}_1$ may be expressed by $\hat{\mu}_1 = x\hat{a} + y\hat{b} + z\hat{c}$, where $\hat{a}$, $\hat{b}$, and $\hat{c}$ are the crystallographic unit vectors. The glide operation in I2/c transform the vector $\hat{\mu}_1$ into $\hat{\mu}_2$ for molecule 2, expressed as $\hat{\mu}_2 = x\hat{a} - y\hat{b} + z\hat{c}$. The transition moments from the ground state ϕ^0 to the Davydov states $\Phi_I'(0)$ and $\Phi_{II}'(0)$ are found by

$$\hat{\mu}_I = \langle\Phi_I'(0)|(\mu_1 + \mu_2)|\Phi^0\rangle = \sqrt{N/2}\,(\hat{\mu}_1 + \hat{\mu}_2)$$

$$= \sqrt{2N}\,(x\hat{a} + z\hat{c}) = \sqrt{2N}\,(-0.4690\hat{i} + 0.8952\hat{k})$$

$$\hat{\mu}_{II} = \langle \Phi_{II}'(0) | (\mu_1 + \mu_2) | \Phi^0 \rangle = (\mu_1 - \mu_2)/\sqrt{N/2}$$

$$= \sqrt{2N}\,(y\hat{b}) = \sqrt{2N}\,y\hat{j} = \sqrt{2N}\,(0.0708)\hat{j}$$

N is the number of unit cells in the crystal, and the $\sqrt{N}$ factor results from the normalization of the exciton wavefunction.

The intensities for transition moments μ_I and μ_{II} in the extinctions are proportional to:

$$I_1 \simeq (\mu_I \cdot E\hat{x}_1)^2 = 0.5922$$

$$I_2 \simeq (\mu_I \cdot E\hat{x}_2 = 0.2826$$

$$I_1 \simeq (\mu_{II} \cdot E\hat{x}_1)^2 = 0.0003$$

$$I_2 \simeq (\mu_{II} \cdot E\hat{x}_2)^2 = 0.0030$$

The orthorhombic crystal of $Mo_2(piv)_4$ has four molecules in the primitive lattice cell. The electric dipole-allowed transition to the four Davydov states are:

$$\Phi_I'(0) = (\Phi_1'(0) + \Phi_2'(0) + \Phi_3'(0) + \Phi_4'(0))/2$$

$$\Phi_{II}'(0) = (\Phi_1'(0) + \Phi_2'(0) - \Phi_3'(0) - \Phi_4'(0))/2$$

$$\Phi_{III}'(0) = (\Phi_1'(0) - \Phi_2'(0) + \Phi_3'(0) - \Phi_4'(0))/2$$

$$\Phi_{IV}'(0) = (\Phi_1'(0) - \Phi_2'(0) - \Phi_3'(0) + \Phi_4'(0))/2$$

The four symmetry-related molecular transition moments are:

$$\hat{\mu}_1 = x\hat{a} + y\hat{b} + z\hat{c}$$

$$\hat{\mu}_2 = -x\hat{a} - y\hat{b} + z\hat{c}$$

$$\hat{\mu}_3 = x\hat{a} - y\hat{b} - z\hat{c}$$

$$\hat{\mu}_4 = -x\hat{a} + y\hat{b} - z\hat{c}$$

As before, $\hat{\mu}_1 = \langle \phi_1' | \mu_1 | \phi_1^0 \rangle$, and so on. The transition

moments from the ground state to the Davydov states are found by:

$$\hat{\mu}_I = \langle \Phi_I'(0) | (\mu_1 + \mu_2 + \mu_3 + \mu_4) | \Phi^o \rangle$$
$$= (1/2)\sqrt{N}\,(\hat{\mu}_1 + \hat{\mu}_2 + \hat{\mu}_3 + \hat{\mu}_4) = 0$$

$$\hat{\mu}_{II} = \langle \Phi_{II}'(0) | (\mu_1 + \mu_2 + \mu_3 + \mu_4) | \Phi^o \rangle$$
$$= (1/2)\sqrt{N}\,(\hat{\mu}_1 + \hat{\mu}_2 - \hat{\mu}_3 - \hat{\mu}_4 = 2\sqrt{N}\, z\hat{c}$$
$$= 2\sqrt{N}\,(0.8746)\hat{k}$$

$$\hat{\mu}_{III} = \langle \Phi_{III}'(0) | (\mu_1 + \mu_2 + \mu_3 + \mu_4) | \Phi^o \rangle$$
$$= (1/2)\sqrt{N}\,(\hat{\mu}_1 - \hat{\mu}_2 + \hat{\mu}_3 - \hat{\mu}_4) = 2\sqrt{N}\, x\hat{a}$$
$$= 2\sqrt{N}\,(0.4787)\hat{i}$$

$$\hat{\mu}_{IV} = \langle \Phi_{IV}'(0) | (\mu_1 + \mu_2 + \mu_3 + \mu_4 | \Phi^o \rangle$$
$$= (1/2)\sqrt{N}\,(\hat{\mu}_1 - \hat{\mu}_2 - \hat{\mu}_3 + \hat{\mu}_4) = 2\sqrt{N}\, y\hat{b}$$
$$= 2\sqrt{N}\,(-0.07712)\hat{j}$$

For the spectroscopic face 110, the transition to the Davydov state $\Phi_I'(0)$ is forbidden in the extinctions, whereas $\Phi_{II}'(0)$ is allowed in c-polarization only, and the transition to the Davydov states $\Phi_{III}'(0)$ and $\Phi_{IV}'(0)$ are allowed in $\perp$c polarization only. The intensities for the transition momemts $\hat{\mu}_{II}$, $\hat{\mu}_{III}$ and $\hat{\mu}_{IV}$ in the extinctions are proportional to:

$$I_c \simeq (\mu_{II} \cdot \hat{Ex}_1)^2 = 0.7649$$
$$I_{\perp c} \simeq (\mu_{II} \cdot \hat{Ex}_2)^2 = 0$$
$$I_c \simeq (\mu_{III} \cdot \hat{Ex}_1)^2 = 0$$
$$I_{\perp c} \simeq (\mu_{III} \cdot \hat{Ex}_2)^2 = 0.0743$$

$$I_c \simeq (\mu_{IV} \cdot \hat{Ex}_1)^2 = 0$$

$$I_{\perp c} \simeq (\mu_{IV} \cdot \hat{Ex}2)^2 = 0.0040$$